PROTEOMICS AND KINETIC MODELING ANALYSIS OF A 4-CHLOROSALICYLATE DEGRADING BACTERIAL COMMUNITY

Von der Fakultät für Lebenswissenschaften

der Technischen Universität Carolo-Wilhelmina

zu Braunschweig

zur Erlangung des Grades eines

Doktors der Naturwissenschaften

(Dr. rer. nat.)

genehmigte

D i s s e r t a t i o n

von Roberto Andrés Bobadilla Fazzini

aus Santiago de Chile, Chile

1. Referent: Prof. Dr. Kenneth N. Timmis

2. Referent: Prof. Dr. Dieter Jahn

eingereicht am: 25.09.2006

mundliche Prufung (Disputation) am: 07.11.2006

Druckjahr 2006

A mi esposa Alejandra

A mis hijos Emilia, Andrés y Benjamín

AKNOWLEDGEMENTS

During the development of my work there are several persons who collaborated in one way or another to accomplished it. Special thanks to my direct supervisor Dr. Dipl-Ing. Vitor Martins dos Santos who provide guidance and gave me the chance to perform this study and to PD Dr. Dietmar Pieper, Prof. Dr. Burkhard Tümmler, Dr. Volker Hecht and Dr. Max Schobert for fruitful discussions.

Thanks to all the Environmental Microbiology Department leaded by Prof. Dr. Kenneth N. Timmis and most specially to my group mates, Amit, Filip, Jacek, Massimo, Miguel and Piotr.

AGRADECIMIENTOS

No quisiera dejar pasar la oportunidad de agradecer a los amigos que han generado un ambiente grato y de mucho compañerismo, haciendo mas fáciles aquellos momentos de nostalgia y soledad en tierras tan lejanas. Agata, Alexandre, Andrew, Bea, Christiane, Faiza, Felipe, Gonçalo, Howard, Magally, Marcelo, Mariela, Melissa, Nacho, Pablo, Peter, Popi, Rosalila, Silvana, Tom, u Pedro y Victoria, muchas gracias a todos.

Finalmente, quiero agradecer el apoyo incondicional de mi esposa Alejandra, por su amor y comprensión y especialmente, por su sonrisa ¡te amo!

ABSTRACT

The high complexity of natural occurring bacterial communities is the major drawback limiting the study of these important biological systems, where intricate interactions are taking place among its members. In this study, a comparison between pure cultures of *Pseudomonas* sp. strain MT1 and stable community cultures composed by the former one plus addition of *Achromobacter xylosoxidans* strain MT3 (in a proportion 90:10), both members of a real community isolated from a polluted sediment by enrichment in 4-chlorosalicyllate (4CS) as single source of carbon and energy, were used as a model system to study the bacterial interactions that take place under severe environmental states. The analysis of steady and dynamic states in continuous and batch cultures, respectively, was carried out at the proteome, metabolic profile and population dynamic level. A proteome reference map for *Pseudomonas* sp. MT1 was created consisting of 118 different proteins from several functional groups, including aromatic degradation pathways and outer membrane proteins, whose differential expression was evaluated at 4CS limiting conditions and under exposure to 4CS shock loads and high concentrations of toxic intermediates (4-chlorocatechol (4CC) and protoanemonin).

Carbon-limiting studies showed a higher metabolic versatility in the community, since upregulation of parallel catabolic enzymes was observed, indicating a possible alternative carbon routing in the upper degradation pathway. A significant change in the outer membrane composition of *Pseudomonas* sp. MT1 was observed in the presence of *A. xylosoxidans* MT3 as well as under different culture conditions, demonstrating the importance of the outer membrane as a sensing/response protection barrier with high selective permeability, and highlighting the role of the major outer membrane proteins OprF and porin D in *Pseudomonas* sp. MT1 under the culture conditions tested. Remarkably, 4CS shock loads generated a stress response in the pure culture and a 'metabolic response' in the community, where *A. xylosoxidans* MT3 helped to prevent 4CC and protoanemonin toxic accumulation, providing a more robust biodegradative capacity and showing a coordinated metabolic response at the community level. Finally, in order to establish a possible mechanistic explanation to such difference, a kinetic metabolic model was initially developed for pure strain MT1 and community cultures. Both models showed predictive capacity, provided accurate data for initial conditions were available, attributing the robustness of the community to the enhanced biodegradative potential of toxic intermediates.

I. INTRODUCTION

Bacterial communities constitute an important biological complement of the environment, performing essential functions for the equilibrium of natural systems. The analysis of bacterial communities is therefore necessary in order to understand the critical aspects that affect its function. However, the high complexity of natural occurring bacterial communities is perhaps the major obstacle that restrain the advances in this important field. For this reason, simplified approaches are required in parallel to the development of more appropriate tools to study such complexity.

The increased amount of information given by entire organism sequencing projects, have open a new era in the Life Sciences. Large quantities of data are now available, and recent fields of research have emerged to analyze this vast dataset. A major advantage of genome driven research resides in the fact that the genomic complement of a cell is almost constant and therefore, its analysis can produce 'permanent statements' about cellular properties. The study of metagenomes recovered from the environment has been an important step towards the functional prediction of bacterial communities. However, if it is true that genetic information contains the code for cell functioning, it is also true that it lays under complex regulatory networks that govern the transcriptional and to some extent the traductional processes, and finally the function will be carried out by the ultimate product: the proteome. Single cell identity is provided by the spectrum of proteins expressed on it. While the genome offers total cell potential, the proteome shows the real one. A major challenge in modern life sciences today comprises the understanding of the dynamic expression, function and regulation of the entire set of proteins of a cell (Zhu et al., 2003).

Initially *in vivo* and later *in vitro* analysis have permitted the observation of environmental phenomena, giving rise to all sorts of theories and conclusions. However, those conjectures are mainly limited by the possibility to develop such analysis at lab-scale. The amount of information gathered so far, together with the boost in computational capacity, have raised the possibility of performing virtual or '*in silico*' experiments. Modeling and simulation is becoming an extensive practice in many laboratories and multidisciplinary research groups with combined experience in life sciences and computational research are leading this area. Metabolic modeling can be used as a strategic tool in order to improve experimental design, enhance data interpretation of complex protein expression patterns and give rise to mechanistic interpretations of the system's behavior.

II. PROJECT RATIONALE

A bacterial community previously isolated from the upper zone of the sediment from a polluted stream (Bitterfeld, Sachsen-Anhalt, Germany), obtained by continuous culture enrichment based on its ability to grow on 4-chlorosalicylate (4CS) as sole carbon source, constitutes the model system used in this work (herein termed MT community). Initial studies, showed that the MT community is composed by four strains and most recently, biochemical studies performed on one of its members, *Pseudomonas* sp. MT1, indicated the presence of novel catabolic pathways (Nikodem et al., 2003).

The model MT consortium corresponds to a real and stable community. It is a system able to metabolize key intermediates ((chloro)-salicylates) in the biodegradation route of very toxic compounds ((chloro)-dibenzofurans and (chloro)-dibezo-*p*-dioxins) (Boening, 1998). It works aerobically, and it has a simple composition with only four members: *Empedobacter brevis* MT2, *Achromobacter xylosoxidans* MT3 and *Pseudomonas veronii* MT4, and *Pseudomonas* sp. MT1, the dominant member and the only one able to transform and grow with 4CS as the sole source of carbon and energy (Pelz et al., 1999).

Table 1. Composition of the 4-chlorosalicylate degrading MT consortium

CONDITION/ STRAIN	%			
	Pseudomonas sp. MT1	*E. brevis* MT2	*A. xylosoxidans* MT3	*P. veronii* MT4
12°C *	84 ± 3	1	8 ± 4	8 ± 4
25°C ¥	80.6 ± 6.9	1.7 ± 0.7	16.8 ± 0.7	0.9 ± 0.4

*Pelz et al.,1999
¥ Tillmann, 2004

Studies concerning carbon sharing within the community showed elaborated metabolic interactions, where especially toxic intermediates – 4-chlorocatechol and protoanemonin – are "transferred" among its members for complete mineralization of the carbon source (Figure 1). A study of stable isotope incorporation into strain specific fatty acids, has shown that labeled 4-chlorocatechol is partially taken by strain MT3 and further degraded. In the case of labeled protoanemonin, a dead-end product of MT1 metabolism (Nikodem et al., 2003) and a critical intermediate due to its inherent antibiotic activity (Blasco et al., 1995), it has been shown that strain MT4 has a preferential incorporation of the label into its biomass, indicating that it may play a detoxification role within the consortia, allowing higher 4CS loads to continuous community cultures. Furthermore, protoanemonin reaches toxic levels for pure continuous cultures of strain MT1 at dilution rates over 0.8 d^{-1} which is not the case for analogous consortia cultures (Pelz et al., 1999).

From the data shown by Pelz and co-workers, a typical metabiosis cooperation type is observed in this community with the members forming an 'assembly line', where the later partners in the line profits from the intermediates synthesized by the former one, giving rise to a more stable culture avoiding the accumulation of toxic intermediates.

Moreover, the biochemical studies performed on strain MT1 show that a new inducible degradation pathway for 4- and 5-chlorosalicylate via 4-chlorocatechol, where a mixture of enzymes from the classical 3-oxoadipate pathway (catechol 1,2-dioxygenase and muconate cycloisomerase) and the chlorocatechol pathway (maleylacetate reductase) join, implying novel catabolic qualities inside the community (Nikodem et al., 2003). In the same study, the purification and characterization of muconate cycloisomerase and *trans*-dienelactone hydrolase responsible for the transformation of 3-chloromuconate to

unstable 4-chloromuconolactone and maleylacetate, respectively, was proposed showing also the presence of a second muconate cycloisomerase responsible for the

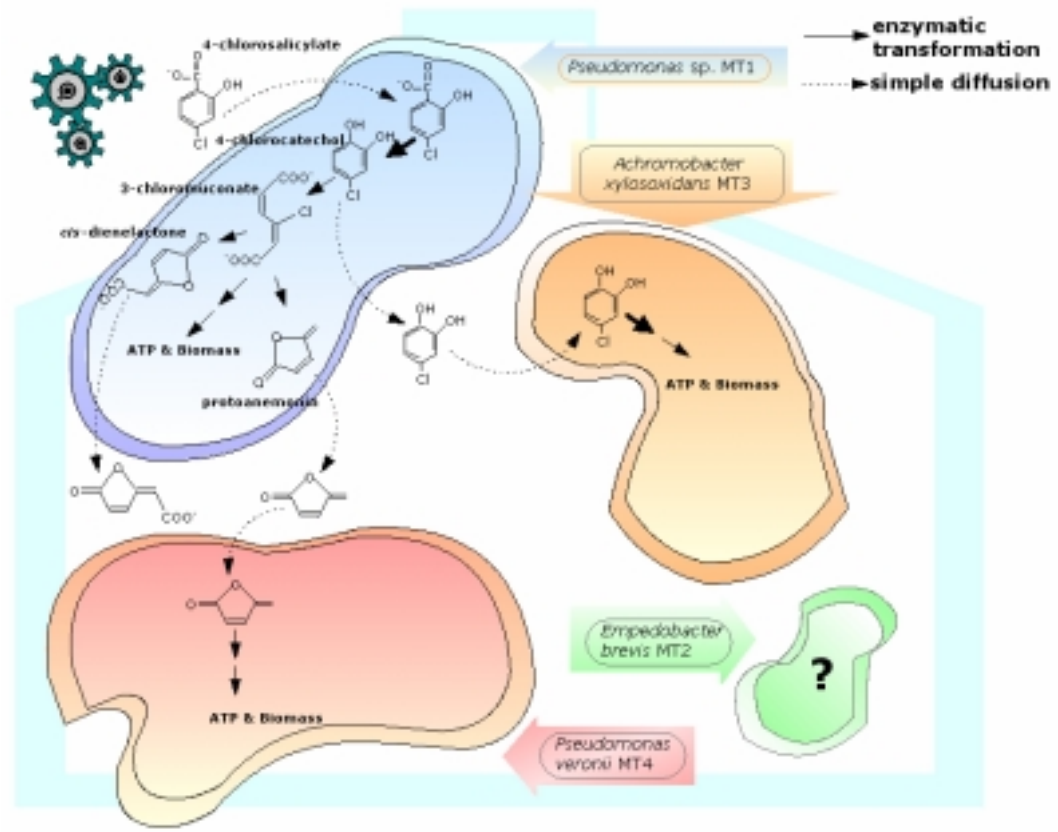

Figure 1. Scheme of MT community 4-chlorosalicylate upper degradation pathway.

major accumulation of *cis*-dienelactone, which cannot be further degraded by strain MT1. Moreover, protoanemonin formation is proposed to be a spontaneous reaction competing with an enzyme catalyzed transformation by *trans*-dienelactone hydrolase, assumption supported by kinetic model simulations (Nikodem, 2004).

However, the knowledge acquired so far does not provide enough information about the behavior of the community as an entity. There are still questions concerning the bacterial

interactions that lead to concerted gene and protein expression in the consortium, driving the metabolite and population dynamics via, for instance, the expression of parallel catabolic pathways and sensing mechanisms, which are seeking for an answer.

This work aims to understand the bacterial interactions that take place within the MT community. Specifically (i) to develop a mechanistic explanation of these interactions, focusing on the well described upper degradation pathway, where the community members interact establishing a carbon sharing network and, (ii) to evaluate the key aspects that confer stability and robustness to the MT community under poorly degradable substrate and toxic intermediate formation. To achieve these aims, an integrated approximation combining different analytical techniques namely, proteomics, population dynamics and metabolite profiling were used and integrated into a kinetic metabolic model.

III. LITERATURE REVIEW

3.1 Bacterial Communities

The environmental behavior of microorganisms at the metabolic level depends on interactions among members of complex communities at different trophic levels. A major component of environmental communities is composed by bacteria, driving the biogeochemical cycles that account for the elemental steadiness of the biosphere (Pace, 1997). The complexity of natural occurring bacterial communities is vast, and a good example of such convolution can be represented in a recent study of the Sargasso Sea, where "whole-genome shotgun sequencing" was applied to collected microbial populations from seawater samples, showing the presence of 1,800 species (based on multiple phylogenetic markers) including 148 previously unknown, demonstrating the oceanic microbial diversity and the significant presence of anonymous microorganisms (Venter et al., 2004). The habitat-wide presence of bacteria is well represented at the communities in the rhizosphere, the environmental compartment defined as: "*the soil surrounding the roots that is influenced by living roots*", showing a tight interaction between plants and bacteria, including the development of bacterial communities in the plant nodules producing nitrogen fixation and the plant disease suppression exerted by *Pseudomonas* species (Kent & Triplett, 2002). Furthermore the presence of bacterial consortia in almost every known environment can be reflected on the knowledge concerning extremophiles, microorganisms able to survive under 'extreme' conditions exceeding by far optimal or standard conditions for growth and reproduction. Bacteria have been identified in severe environments such as deep sediments and mid-ocean ridge hot springs (Kerr, 1997) and permanent ice layer of lakes in the Antarctic (Priscu et al., 1998). The broad presence of bacterial communities is a reflection of their

importance, since they have an enormous influence in the natural equilibrium and environmental homeostasis playing a key role to keep biosphere's balance.

3.1.1 Characterization of bacterial communities

The classical ecological approach for describing an ecosystem, goes first through the characterization of the community structure by identification and enumeration of the species present and later, via assignment of the roles in the ecosystem functioning to species or groups. Traditional microbiological approaches require the generation of pure cultures, allowing the characterization of the different community members. These strategies, typically employed by microbial ecosystem and population ecologists, although successful at single cultivable strains, have not been practical for the study of microbial consortia. Analysis of bacterial communities from different environments have found that the proportion of cells that may be cultured is not representative of the diversity of the microbial community present, and it is often reported that direct microscopic counts exceed viable cell counts by several orders of magnitude (Holben & Harris, 1995). In addition, most microorganisms that thrive on ecosystems are uncultivable and, even if the pure culture physiology of a particular strain is well understood, it is still not possible to infer its ecophysiology as a member of a microbial community (Wagner et al., 2006).

The fast development of molecular biology tools, particularly the enormous advances in genomics have tackled the issue in terms of species identification in complex mixtures by 16S rDNA extraction-separation and sequencing (Orita et al., 1989; Fischer & Lerman, 1983) and more recently, allowing the collection of different organism genomes, producing genomic libraries from microbial communities and other multi-species arrays

in the field called Metagenomics (Handelsman, 2004), permitting the prediction of function and isolation of novel genes. Development of large capacity vectors such as fosmids and bacterial artificial chromosomes (BACs) together with the increasing sequencing capacity, has set the consent to apply genomic analysis to a large environmental scale such as Venter et al. (2004) study of the Sargasso Sea, where detailed analysis of soil dominating bacterial divisions (Wieland et al., 2001) and molecular phylogenetic views of microbial diversity in alpine and artic soils (Nemergut et al., 2005). However, while the first step on 'the classical ecological approach' has been at least partially fulfilled, i.e., the identification of the species composing environmental communities (considering that only the most abundant can be detected), the step of 'role assignment' is yet to be understood.

Microbial consortia are a central element in life maintenance. Therefore, it is necessary to understand the ecophysiology of the different microbial associates that encompass them. Metabolic diversity within bacteria is large, and also a basis for bacterial classification. Properties such as nutrients and energy sources are used to classify different types of microbes, provided they can be independently cultivated. Hence, culture-independent techniques have been developed in order to assess and link community composition with function. There are several methods that combine species identification with substrate uptake, thus connecting community structure with metabolic function. Stable-isotope probing (SIP), involving the determination of the incorporation of stable-isotope-labeled elements (e.g., ^{13}C stable isotope) in recovered cell specific biomarkers such as fatty acids and/or nucleic acids, offer the possibility to distinguish functional specificity. For example, SIP has been used (i) to investigate methanol-utilizing microorganisms in soil (Radajewski et al., 2000), (ii) to identified a species from the genus *Thaurea* as the main responsible for phenol degradation in a bioreactor

community (Manefield et al., 2002), and (iii) to unravel the carbon sharing within an aromatic biodegradation bacterial community working with 4-chlorosalicylate (Pelz et al., 1999). Fluorescent *in situ* hybridization (FISH), a technique based on the specificity of bacterial 16S rRNA sequence coupled to fluorescence labeling (De Long et al., 1989) is able to differentiate close related bacteria on many environmental samples and, when coupled to microautoradiography (MAR), after incubation with radioactively labeled substrate, can provide simultaneous information of the different species-function sets at single cell/cell cluster level. Widely applied nowadays, FISH-MAR is only low-throughput method and limited to a reduced number of simultaneous bacterial populations due to restrictions on fluorophore application and hampered by environmental sample 'suitability' (e.g., a major fraction of bulk soil bacteria is not amenable to FISH-MAR) (Wagner et al., 2006). Recently isotope arrays, rRNA-targeted DNA microarrays designed to measure the incorporation of radioactive substrate into the target rRNA, can generate in principle, simultaneous information about thousands of probes (organisms), being a high-throughput method already applied in the analysis of the diversity and radioactive bicarbonate incorporation of ammonia-oxidizing bacteria in a nitrifying activated sludge as a model system (Adamczyk et al., 2003). Isotope arrays though simple, are strongly dependent on the availability and performance of suitable rRNA-targeted oligonucleotide microarrays which are still under optimization.

3.1.2 Bacterial communities and communication

Bacterial metabolism includes the production of a series of secondary metabolites and response to an ample range of chemicals in their environment, where microorganisms generally subsist in habitats that present low initial nutrient availability or total depletion, caused by their own consumption and/or by the build up of competing microbes. Nutrient availability rapidly changes, as new carbon and energy sources enter the cell's environment. Thus, microorganisms in nature experience a "feast or famine" cycle of nutrient deficiency disturbed by pulses of increased nutrient levels. To deal with this deficiency, many microorganisms and particularly bacterial communities have developed competent nutrient uptake and sensing mechanisms that are induced, for example, by starvation conditions (Lazazzera, 2000). Cell-to-cell communication play an important role in the 'environmental sensing' and response of bacteria to their surroundings. Quorum sensing, described as the mechanism for the coordinated regulation of the behavior at the cell population level, triggered by the accumulation of a signal molecule above a threshold, has raised a productive and competitive area of current research (Taga & Bassler, 2003;Keller & Surette, 2006). Production of oligopeptides (e.g., *Staphylococcus* species), *N*-acyl homoserine lactones (e.g., Pseudomonad) and autoinducer-2 (e.g., *Vibrio* and *Salmonella* species) are well documented ways that bacteria use to communicate and generate a population response in order to improve fitness.

Syntrophic interactions in bacterial communities are also an interesting example of 'fitness support', for example, in the biodegradation of aromatic compounds where the biochemical steps are shared among community members in order to completely mineralize recalcitrant and/or toxic substrates (Wittich et al., 1999; Shim et al., 2005).

A well described example of chemical signaling within microbial communities has been observed at the biofilm structure in the human oral cavity, one of the better-characterized spatially and temporally complex bacterial organizations. In this particular case, the interaction of two early colonizing members of the dental plaque biofilm has been characterized. A signal event generated by *Velionella atypica* triggers an increment in the expression of alpha-amylase encoding gene (*amy*B) in *Streptococcus gordonii*, enhancing carbohydrate fermentation and therefore lactic acid production, the preferred carbon source of *V. atypica* (Egland et al., 2004). This bacterial interaction has been recognized as 'chemical manipulation' since the chemical sender strain alters the behavior of the recipient with a negative effect on the fitness of the last one (Keller & Surette, 2006).

3.1.3 Bacterial Communities and Biodegradation

The essential role that microbial communities undertake in the environment as well as its ubiquity is mainly due to their metabolic versatility and rapid evolution. Many works have analyzed the metabolic pathways that allow bacteria to transform and mineralize different carbon sources. Extensive studies have been carried out in the description of the biochemistry related to the elimination of environmental pollutants. Metabolite sharing networks describing syntrophic interactions among bacterial community members, for example, the cooperation of methanotrophic and methanol oxidizing bacteria (Wilkinson et al., 1974) and bacterial consortia reductive dehalogenation of tetrachloroethylene (Chen, 2004), a common sediment and groundwater pollutant, are nice examples of how biodegradation can reduce the toxicity of contaminants, and in the best case totally eliminate their noxious effect. Microbial degradation of aromatic compounds and particularly of the halogenated derivatives, due to their extensive use in industry and xenobiotic nature, has received important attention. The basic aromatic unit,

the benzene ring, is one of the most widely spread chemical structure units in nature, and its thermodynamic stability grants its persistence in the environment. Several structural variants, e.g., the phenolic derivatives and the chlorinated dioxins (chloro-dibezo-*p*-dioxins) are universally toxic, limiting its biological degradation (Sparling et al., 1981). However, microbial metabolic versatility has the capacity to 'activate' aromatic compounds by the hydroxylation of the benzene ring, making it suitable for subsequent biodegradation steps. This activation step is carried out by multi-component oxygenases that usually introduce two hydroxyl groups at the *ortho*- or *para*-position to each other. Aerobic degradation of aromatic compounds occurs predominantly via three branches represented by the activated benzene ring metabolites: protocatechuate (3,4-dihydroxybenzoic acid), gentisate (2,5,-dihydroxybenzoic acid) and catechol (1,2-dihydroxybenzene) (Harwood & Parales, 1996).

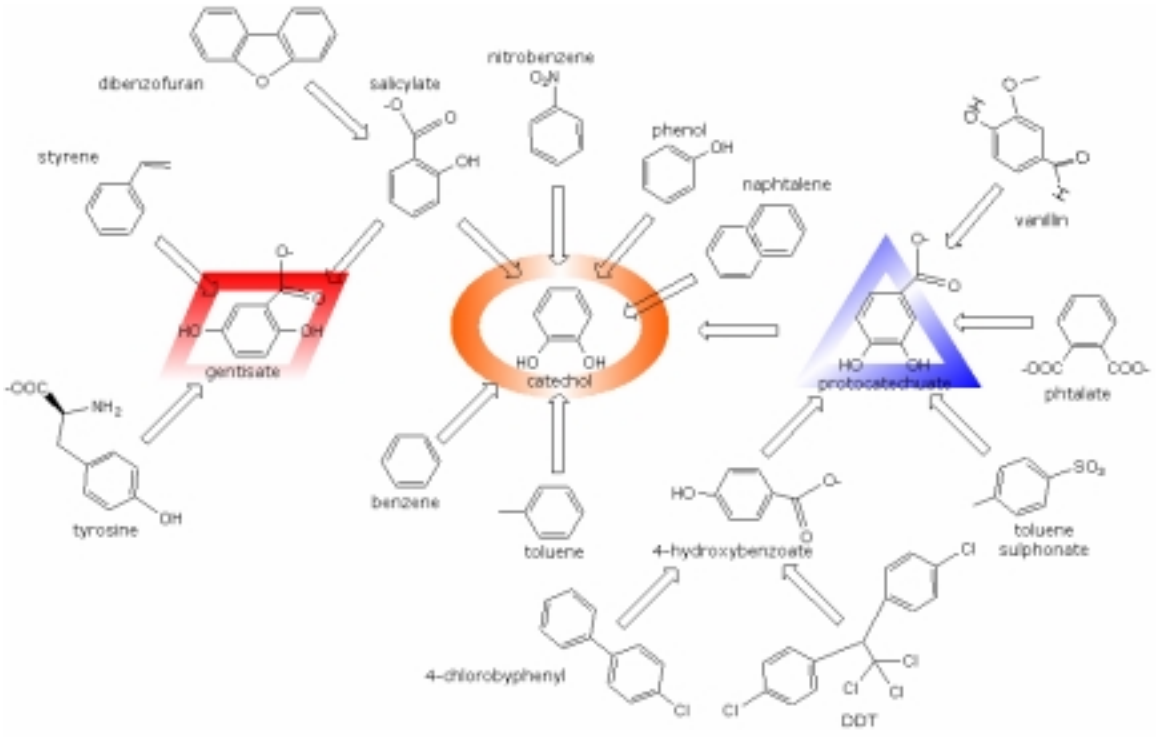

Figure 2. Funneling intermediates in the biodegradation of aromatic compounds: gentisate, catechol and protocatechuate.

Many aromatic degradative pathways converge on at least one of these three intermediates (Figure 2). Later steps of biodegradation involve ring cleavage and further oxidation, with oxygen being the most common final electron acceptor for microbial respiration, since aerobic biodegradation provides higher amount of energy to the cells.

In the case of highly chlorinated aromatic compounds, initially degradation occurs via reductive dehalogenation, where the chlorine is enzymatically replaced by hydrogen (Reineke & Knackmuss, 1988). Bioremediation treatments have shown that a combination of sequential anaerobic and aerobic treatment is more effective than anaerobic conditions alone, showing that degradation tasks are shared among microbial community members that thrive within oxygen gradient environments, such as ground waters and activated sludge (Master et al. 2002). The description of isolated bacterial communities able to degrade chlorinated aromatic compounds goes back to the early 80's. The work of Shelton & Tiedje showed a methanogenic consortium composed of seven bacterial species with a series of dechlorinating, benzoate-oxidizing and methane forming members that together utilize 3-chlorobenzoate as unique source of carbon and energy (Shelton & Tiedje, 1984). More recently, the metabolic interactions taking place in a two species microbial consortium, composed of *Pseudomonas putida* strain R1 and *Acinetobacter* sp. strain C6, which depending on growth conditions presented a different population dynamics. Under limiting concentrations of benzyl alcohol, a substrate that can be used by both strains as single source of carbon and energy, and when the cells were grown on planktonic culture, *Acinetobacter* strain C6 prevailed whereas under similar substrate feeding, but changing to surface attached biofilm growth, the opposite situation occurred. In the planktonic case, strains directly compete for the substrate, while in the biofilm different stages of development were observed, highlighting the importance of temporal and spatial organization of consortia (Christensen et al., 2002).

From the previous, it is important to stress that biofilms are the most common structure for stable bacterial communities in the environment (Branda et al., 2005).

In summary, environmental consortia are intricate organizations of microorganisms presenting complex interactions among its members. The extent to which these communication systems are described in terms of chemical interactions, competition, environmental limitations and niche partitioning, the more advances can be achieved in all the potential involved areas from biotechnological products to infectious diseases.

3.2 Proteomics

3.2.1 Protein identification techniques

A series of techniques are now widely available to analyze the proteome. Great development of Mass Spectrometry (MS) and particularly the nondestructive ionization (soft ionization) of peptides namely, electrospray ionization (ESI) (Fenn et al., 1989) and matrix-assisted laser desorption ionization (MALDI) (Karas & Hillenkamp, 1988) coupled to quadrupole mass analyzers that generate fragment ion spectra from selected precursor ions, and most commonly to time-of-flight (ToF) mass analyzers that measure the mass of intact peptides, constitutes powerful high throughput tools for proteomic research. ToF is based on the fact that ions of different mass and equally charged require different amounts of time to travel the same distance when accelerated by an electrical field. The developments in MS technology have made possible the fast analysis and identification of peptides and proteins. Usually MALDI-ToF is preferred due to its inherent high throughput and simplicity, where typically a MS spectrum of a tryptic digested protein generates a series of peptide masses, that can be enough to develop a peptide mass fingerprint (PMF) analysis against a calculated list of all the expected peptide masses for each entry in a protein database. Algorithms generate a probability-based score in order to reject random matches (low scored), setting a confidence level for protein identification (e.g., $p < 0.05$) (Perkins et al., 1999; Kapp et al., 2005). The increasing number of entries available in protein databases (NCBInr, Uniprot, Swissprot, etc.) allows the identification of proteins based on previously sequenced genes. Therefore, PMF searches of new proteins that may only partially share their sequence with 'known proteins' is somehow restricted. It is also possible to apply Tandem MS (MS/MS) to purified digested proteins, in order to obtain sequenced fragments by *ab initio* sequencing. Those fragments are compared for sequence similarity against protein

databases and probability-based scored in a similar way to the PMF analysis, discarding random matches. Although, standard N-terminal or internal fragment Edman sequencing can be also applied, being restricted only by the amount of protein available (Edman, 1950).

3.2.2 Protein separation techniques

Prior to protein identification, it is necessary to extract and separate the proteome from the cell. Protein extraction and purification techniques have been previously developed in the area of biochemistry, particularly in the analysis of enzymatic activity and protein structure. However, standard protein extraction-purification methods isolate mostly the water soluble proteins or so-called cytosolic protein fraction, that in the best case includes proteins only partially embedded in membranes, but excludes most of the integral membrane proteins. Different cell fractionation-protein-solubilization techniques are available to partially overcome this issue (Bunai & Yamane, 2005). With respect to complex protein mixture separation, the initial approach was performed in the mid 70's with the development of two-dimensional gel electrophoresis (2-DE) (O'Farrell et al., 1975), a powerful technique that separates proteins first based on their isoelectric point, where the complex mixture is subject to migration within an pH gradient while an electrical field is applied (isoelectric focusing (IEF)), followed by standard sodium dodecyl sulfate polyacrylamide gel electrophoresis (SDS-PAGE), where denatured proteins are separated based on their molecular weight. This technique presents a high resolution capacity, being able to resolve thousands of proteins in a single gel, including post-translational modified proteins and moreover, provides a way to determine differential expression through comparative pattern analysis (Righetti et al., 2004). Major

disadvantages refer to difficulties in reproducibility, poor dynamic range and the biased of the method towards abundant and soluble proteins. More sophisticated difference in-gel electrophoresis (DIGE) uses sensitive fluorescent labeling prior to separation, allowing the load of two samples in a single gel slab in order to eliminate gel-to-gel variations and increasing the range of quantitation (Unlu et al., 1997). 2-DE by itself cannot provide the identity of the resolved protein spots and needs to be coupled to protein identification methods such as MALDI-ToF or ESI-Q-ToF (Figure 3).

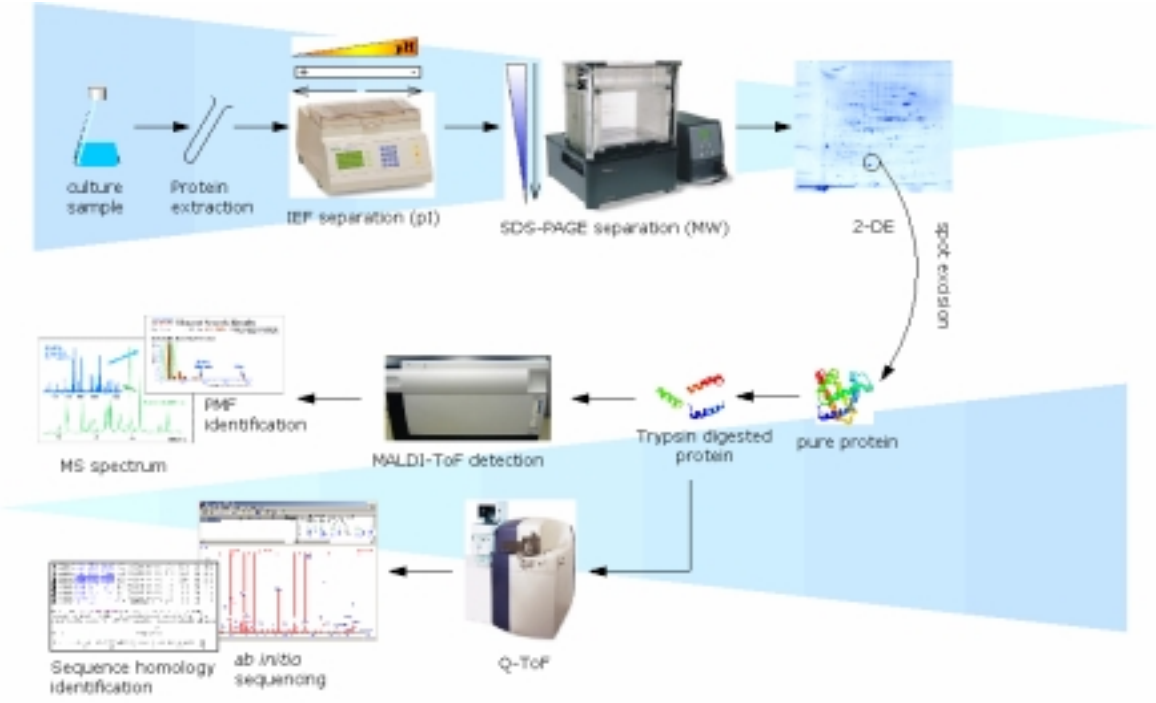

Figure 3. Standard proteomic procedure: from culture to protein identification.

Later, the coupling of liquid chromatography (LC) with MS has had a great impact on proteomic development and become an alternative method to 2-DE (Fligge et al., 1998) . Ionic or reverse phase column chromatography is usually used to separate complex mixture of typically tryptic digested protein extracts, detected mainly by ESI-Q-ToF. First study of LC-MS – also called shot-gun proteomics – identified 1500 proteins from yeast

lysate, including low abundant and hydrophobic proteins (Washburn et al., 2001). However, as initially developed, shot-gun proteomics assesses only the presence of proteins and requires additional technology to infer expression profiling. Stable isotope labeling has been used to tackle this problem by differential incorporation of stable isotope in the samples to be compared and, from the ratio of light and heavy isotopes into peptides, assessing the initial protein amount (Oda et al., 1999). Alternatively, isotope-coded affinity tags (ICAT), where specific aminoacid residues are labeled, separated and later purified by affinity can increase the recovery of low-abundance proteins (Yu et al., 2002). Disadvantages of shot-gun proteomics arise when observing that not all peptides are suitable for analysis. Also ICAT is restricted to the presence frequency of possible residues to be labeled (e.g., usually cysteine residues are labeled in ICAT but 8% of yeast proteins does not contain such residue). The most successful case of shot-gun proteomics identified 2000 protein species, a number within the possibilities of 2-DE (Kubota et al., 2005).

3.2.3 Proteomics and stress response

If there is a particular field where proteomics have had an enormous impact, this is the analysis of stress response. Numerous publications refer to the analysis of the differential expression patterns of a control (normal growth conditions) versus a stress culture, being mainly the classical 2-DE the method chosen. Stress, defined as the sum of the biological reactions to any adverse stimulus (stressor) that tends to disturb the organisms homeostasis, is a general effect caused by many agents. Within bacterial communities, the stressors are mainly physical (e.g., temperature, pressure, shearing force) or chemical (e.g., limited nutrients, pH, osmolarity, reactive oxidative species

(ROS) and toxic compounds such as antibiotics, secondary metabolites and xenobiotics).

Oxidative stress perhaps has been the most studied, probably due that it is a general form of stress generated by many stressors. Many chemicals do not exert stress by themselves but by the generation of ROS. Aromatic compound stress is mainly due to the formation of toxic intermediates. Catechol and its derivatives are toxic towards many microorganisms. High concentrations of 3- substituted catechols cause uncoupling of NADH conversion, leading to the formation of hydrogen peroxide and raising Fenton's reaction, where hydrogen peroxide couples to iron ions forming free radicals that can react against biomolecules such as DNA, proteins and membranes, ultimately leading to irreversible damage (Schweigert et al., 2001a).

In the field of aromatic stress response, despite a wide diversity of microorganisms are able to aerobically degrade aromatic compounds, the genus *Pseudomonas* has received most of the attention, due to the wide spectrum of contaminants that this genus is able to degrade (Wackett, 2003). Additionally, Pseudomonad constitute one of the most ubiquitous and versatile group of bacteria (Widmer et al., 1998), from opportunistic pathogens such as *Pseudomonas aeruginosa* (Gilligan, 1991) to innocuous saprophytic species like *Pseudomonas putida* (Wackett, 2003), being considered as an archetype of gram negative bacteria.

Proteomic studies carried out after the publication of *P. putida* strain KT2440 sequence (Nelson et al., 2002), have investigated different sorts of stress. Strain KT2440 subject to iron deprivation provoked as expected, up regulation of iron uptake systems such as ferripyoverdine receptor A, and related outer membrane proteins, while some proteins that require iron as a cofactor such as catalase and superoxide dismutase (SOD) where

down regulated. Interestingly, when compared to the same conditions at *P. aeruginosa* strain PAO1, a second form of iron-independent SOD was detected and allocated as one of the crucial factors that allow *P. aeruginosa* to colonize eukaryotic surfaces (Heim et al., 2003). Proteomic analysis of phenol-induced stress performed on strain KT2440 have shown upregulation of alkyl hydroperoxide reductase, subunit C (AhpC), SOD and ferredoxin-NADP reductase (Fpr), all involved in oxidative stress response. At the same time, a series of enzymes involved in aminoacid biosynthesis were also upregulated, suggesting a possible aminoacid limitation under phenol stress (Santos et al., 2004). It is important to note that AhpC belongs to the piroxiredoxin group, one of the most important proteins in antioxidant defense in bacteria and yeast (Hoffman et al., 2002). In contrast to phenol-induced stress, a more recent work on protein differential expression performed on the same strain using chlorophenoxy herbicides as stressors, showed downregulation of biosynthetic pathways (including tryptophan synthase) and a mild oxidative stress response depending on the chemical tested, while the major functional group of proteins upregulated was the one including transporters and outer membrane proteins, where outer membrane protein OmpA was associated to potential efflux mechanism of detoxification (Benndorf et al., 2006).

Solvent tolerance is one the most striking properties found in *Pseudomonas* strains (Inoue & Horikoshi, 1989). Solvent tolerance mechanisms include cell membrane modifications altering its permeability and active solvent export by means of efflux pumps (Ramos et al.,2002). Proteomic analysis over *P. putida* DOT-T1E, a toluene tolerant strain, revealed the importance of chaperon GroES and CspA2 proteins as well as translational elongation factor EF-Tu, acting on protein refolding in the cytosol as well as in the periplasm, highlighting the role of enhanced metabolite uptake and glucose as

well as central metabolism enzymes, due to the high energetic requirements of toluene extrusion (Segura et al., 2005).

Proteomics of strain KT2440 have also included the analysis of the parallel biodegradation pathways of aromatic compounds, showing a relatively relaxed pathway regulation. A recent study reported that a benzoate induced culture expressed not only the expected β–ketoadipate set of enzymes (catechol 1,2-dioxygenase, muconate cycloisomerase, 3-oxoadipate enol-lactone hydrolase and 3-oxoadipate CoA-transferase) but in addition, enzymes of the protocatechuate pathway (4-hydroxy-benzoate hydroxylase and 3,4-protocatechuate dioxygenase) (Kim et al., 2006).

As a consequence of the diverse proteomic studies performed over the last decade, general and specific stress responses have been evaluated, giving a good insight into the tolerance and adaptation processes that prevail in microorganisms in order to survive and persist in the environment. Although still scarce compared to genomic databases, 2-DE databases are increasing giving the possibility to observe and compare between proteomic studies (SWISS-2DPAGE at http://ca.expasy.org/ch2d/).

3.2.4 Proteomics and Bacterial Communities

Many stress studies have analyzed carefully the variation of the proteome in a single strain showing interesting responses, where intricate protein toolkits synchronized by sophisticated regulatory networks, have evolved to allow bacterial survival under stress conditions such as, extreme temperatures, nutrient availability or antibiotics produced by other microorganisms. However, a major question arises with respect to the extrapolation from these studies to real environmental conditions, where the stress response needs to be coordinated at the community level. An extremely challenging new

area of research, aligned within the proteomics field, has emerged to deal with protein expression in mixed cultures: Metaproteomics. The term 'metaproteome' initially coined in the context of environmental metagenomics (Rodriguez-Varela, 2004) was later extended as a new 'omics' in the study of Wilmes & Bond, where 2-DE was applied for the first time to a β–Proteobacteria dominated bacterial community in a sequential batch reactor designed for enhanced biological phosphorous removal (Wilmes & Bond, 2004). A more comprehensive study, combining both high throughput genomics and proteomics, in the reconstruction of a natural acidophilic biofilm consortia from a mine drainage by shot-gun sequencing (Tyson et al., 2004), was used to create a database of 12,148 proteins and later, using shot-gun proteomics (nano-LC coupled to MS/MS), detecting the presence of predicted proteins. The biofilm was dominated by bacteria of the genus *Leptospirillum* and archea form the *Ferroplasma* group. Relative abundance of individual proteins showed the predominance of 'hypothetical proteins' (42%), followed by ribosomal proteins (13%) and chaperons (11%). Again, piroxiredoxins appeared as abundant proteins, revealing that under the acidic environment, detoxification from ROS is an important issue (Ram et al., 2005). The two briefly described studies, together with a third study performed on an aquatic community (Kan et al., 2005) constitute the studies published in the field of metaproteomics up to date.

Proteomic data can provide a close view into the essential functions that are accomplished and allocated among members of natural communities. "Investigations that focus on limited numbers of highly expressed proteins can have immediate impacts on developments in the field" (Wilmes & Bond, 2006).

3.3 Metabolic Modeling

The starting point of mathematical modeling of bacterial metabolism goes together with the initial Michaelis-Menten approach to kinetics of enzymatically catalyzed reactions (Michaelis & Menten, 1913) and the empirical Monod equation for growth kinetics (Monod et al., 1949), being the first a particular case of the more general Law of Mass Action first expressed by Waage and Guldberg in 1864, that relates the rate of a chemical reaction to the product of the effective concentrations of each participating molecule (Waage & Guldberg, 1864).

Metabolic modeling can be divided into two main categories based on model structure: kinetic and stoichiometric models. In the case of the stoichiometric models, metabolic flux analysis (MFA) has been widely used for the quantitation of the intracellular fluxes in the metabolism of bacteria and yeast (Gombert & Nielsen, 2000). The principles of stoichiometric models are based on linear algebra. First, a reconstruction of the metabolic network based on available information about the biochemistry of the cell metabolism is created. Then, metabolites are classified as internal or external according to the model boundaries, and the dynamics of the integrated metabolic network is described in the form of mass balances, stating that the change in metabolite concentration as a function of time (flux), corresponds to the difference between formation and consumption rates. The set of equations generated at the mass balance are used to build a stoichiometric matrix. The assumption of a steady state, where the net fluxes are equal to zero, and a series of 'constrains' imposed by thermodynamics (mainly reaction reversibility) and enzyme or transporter capacities, are typically considered and incorporated into the model, bounding the 'solution space', a multidimensional space containing all steady state flux distributions that are mathematically possible through the metabolic network. The next step is to determine

meaningful steady states as possible solutions. To do so, mathematical programming is used to identify metabolic network states that maximize a particular network objective function. The most used approach corresponds to flux balance analysis (FBA) that uses linear optimization to calculate optimal flux distributions (Varma & Palsson, 1994). Stoichiometric models present the unique capacity to simulate at the genome-scale level, and have been used to study fairly complete organism metabolic networks like that of *Escherichia coli* (Varma & Palsson, 1993), *Saccharomyces cerevisiae* (Famili et al., 2003) and *Helicobacter pylori* (Schilling et al., 2002).

Integration of stoichiometric models with proteomics was performed for *Haemophilus influenzae* strain Rd KW20, employing a combination of proteomic and intermediary metabolism modeling (Raghunathan et al., 2004). In this study, 353 proteins (only 38% identified with statistical significance) from both, microaerobically and anaerobically grown cells, from a previous proteomic study of *H. influenzae* (Kolker et al., 2003) were associated with reactions in a stoichiometric model of *H. influenzae* metabolic network (Edwards and Palsson, 1999), based on the reactions catalyzed by each protein. Forty-one genes to be 'deleted' *in silico* where selected based on their absence in the microaerobic proteome study. The gene-protein-reaction associated relations were individually deleted from the model, calculating each time the optimal growth solution (objective function) in the absence of the protein. Sixteen proteins were classified as 'essential' since biomass production was totally impaired by the deletion of any in this group, suggesting that alternative pathways not currently included in the metabolic reconstruction may exist, provided this gene products are absent on *H. influenzae* proteome.

After the stoichiometric matrix is constructed and constrained, a parallel pathway structure assessment of the metabolic network under study can be carried out by means

of convex analysis, to determine the so-called 'elementary flux modes', which corresponds to the minimal set of enzymes that operate under steady state (Schuster et al., 2000). A subset of the elementary modes named 'extreme pathways', correspond to the edge flux distributions of the convex space (Papin et al., 2003). Both sets can be extremely useful to analyze the redundancy of the metabolic network (Price et al., 2004).

Stoichiometric models are powerful tools but have a very restricted predictive power (Gombert & Nielsen, 2000). The incorporation of new constrains could reduce the possible solution space and can increase the predictive capacity of this kind of model (Price et al., 2004). Neither flux balance analysis nor pathway analysis incorporates information on reaction kinetics and regulation, limiting their insight into dynamic responses (Schilling et al., 2001).

At the other end of the metabolic modeling area resides the more traditional kinetic modeling approaches. When complete information is accessible about the kinetics of a particular cellular process, it is possible to describe the dynamics of these events by following the stoichiometry of the metabolic pathway and combining it with kinetic expressions. The general strategy to build kinetic models, provided there is sufficient information, goes through the definition of the system boundaries (definition of the variables that control, influence or regulate the system but are assumed to remain constant, for example, temperature and pH in continuous cultures), determination of mass balance equations for the state variables (basically state variables represent the quantities whose values will change in time and must follow mass conservation), formulation of the rate laws or kinetic expressions (algebraic expressions to be evaluated in order to generate a 'flux' or mass per unit time of the given chemical species through a given process) and finally correlate the state variables to experimental data to assess the predictive capacity. Figure 4 shows the stages of kinetic modeling development.

Kinetic modeling has been used for a long time as a process designing tool in bioreaction engineering, since enzymes are being used in a multitude of industrial processes (Nielsen et al., 2003). The basic enzyme kinetics derived from mechanistic modeling by Briggs and Haldane (Briggs & Haldane, 1925) who supported the derivation previously achieved by Michaelis and Menten, marked the start point of quantitative enzymology. Briefly, they considered that the enzyme could exist as free enzyme (*E*) and forming an enzyme complex with the substrate (*ES*), and the conversion of substrate (*S*) to product (*P*) proceeds in two steps:

$$E + S \underset{k_{-1}}{\overset{k_1}{\rightleftarrows}} ES \xrightarrow{k_2} E + P \tag{1}$$

The reaction set, expressed by mass action kinetics assuming homogeneous reactions in a three dimensional space (Voit & Savageau, 1987) with a first reversible second order and a second irreversible first order reactions, assuming that the complex concentration is constant in time (i.e., *ES* is in a *pseudo* steady-state) gives the mass balance:

$$\frac{d[ES]}{dt} = k_1[E][S] - k_{-1}[ES] - k_2[ES] = 0 \tag{2}$$

The total enzyme E_0 is assumed constant:

$$E_0 = E + ES \tag{3}$$

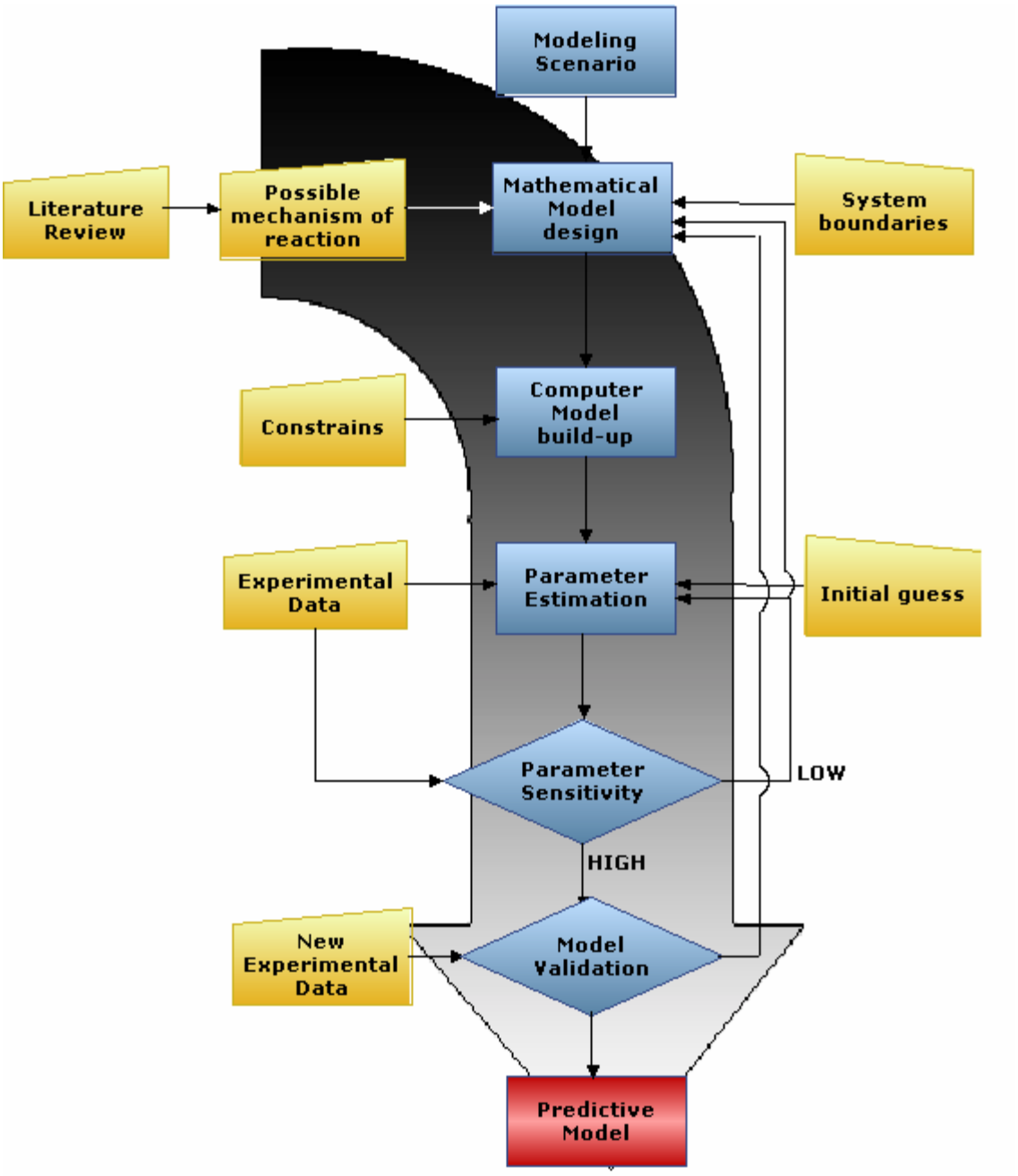

Figure 4. Modeling research and development flow chart towards a predictive model.

Combining (2) and (3) and solving for [*ES*]:

$$[ES] = \frac{k_1[E_0][S]}{k_1[S] + (k_{-1} + k_2)} = \frac{[E_0][S]}{[S] + \frac{k_{-1} + k_2}{k_1}} \quad (4)$$

The first step is considered infinitely fast with respect to the second and therefore the rate of the reaction *v* is determined by decomposition of *ES* by a first order reaction:

$$v = k_2[ES] = \frac{k_2[E_0][S]}{[S] + \frac{k_{-1} + k_2}{k_1}} = \frac{k_2[E_0][S]}{[S] + K_M} = \frac{V_{\max}[S]}{[S] + K_M} \quad (5)$$

A main requisite for the validity of the *pseudo*-steady state approximation (also called *quasi-steady-state*) is the requirement of an excess in substrate with respect to enzyme concentrations (Laidler et al., 1955). An extra advantage beyond the simplicity of the approach, is the time independent relation of the initial rate with initial substrate concentration that leads to a linear correspondence between the reciprocal plot (*1/[S]* vs. *1/v*) from which the reaction parameters can be determined (Burk & Lineweaver, 1930). Whole chapters on enzymology in biochemistry books deal with Michaelis-Menten approach, particularly describing reactions with two substrates or one inhibitor, recounting variants of the Michaelis-Menten approximation based on the proposed mechanism of reaction, such as ternary complex or bi-bi mechanisms for mixed substrates and competitive, uncompetitive or non-competitive inhibition. However, the rate form as shown on (5) requires several experiments run at different initial substrate concentrations to estimate the parameters V_{max} and K_M. The double reciprocal graphical representations present the advantage to visually differentiate the mechanism of reaction, having an important educational value. Nonetheless, their parameter estimation

can be very inaccurate due that a linear transformation of a non-linear equation distorts the error in the measured variables and subsequently impact the obtained parameters (Cornish-Bowden, 1975). Moreover, experimental results of kinetic research of enzyme-catalyzed reactions are usually obtained as progress curves, i.e. registration of substrate depletion or product formation as a function of time. Therefore, the integral form of the Michaelis-Menten equation has been used to determine V_{max} and K_M from a single experiment using progress curve analysis (Robinson & Characklis, 1984).

Equation (5) corresponds to the rate of variation of substrate concentration with time:

$$v = -\frac{V_{\max}[S]}{[S]+K_M} = \frac{d[S]}{dt} \tag{6}$$

Expression (6) correspond to a non-linear implicit differential equation, since the independent variable *S* cannot be isolated. The lack of a close form solution presents computational difficulties associated with progress curve analysis.

Integration of (6) between time zero and time *t* gives:

$$V_{\max} t = [S_0] - [S] + K_M \ln\left(\frac{[S_0]}{[S]}\right) \tag{7}$$

being S_0 the initial concentration of substrate (concentration at time zero).

Parameter estimation of V_{max} and K_M requires non-linear regression. Fitting the data directly to nonlinear models requires an initial estimate of the parameters ('initial guess') (Robinson & Characklis, 1984), which are improved stepwise until the established 'cost function' reaches a minimum. Usually, the cost function corresponds to the sum of the squared deviations of the difference between simulated values for the state variables

and experimental or observed values. Initial guess of the parameters is a very important step that can be done using the linearized forms of the integrated Michaelis-Menten expression (7), such as:

$$\frac{t}{\ln(S_0/S)} = \frac{1}{V_{\max}}\frac{(S_0 - S)}{\ln(S_0/S)} + \frac{K_M}{V_{\max}} \tag{8}$$

$$\frac{(S_0 - S)}{\ln(S_0/S)} = \frac{t}{\ln(S_0/S)}V_{\max} - K_M \tag{9}$$

$$\frac{t}{(S_0/S)} = \frac{K_M}{V_{\max}}\frac{\ln(S_0/S)}{(S_0 - S)} + \frac{1}{V_{\max}} \tag{10}$$

Evaluation of these linearized forms with simulated data containing simple errors in S_0 – since initial substrate concentration is not error-free – showed that expression (10) produced on average the best estimates of K_M and V_{max} (Robinson & Characklis, 1984).

Kinetic parameter estimation is a crucial step in model development in order to be able not only to fit a set of experimental data, but to predict possible kinetic behavior (Shiraishi & Savageau, 1992) and a series of software packages are available to perform progress curve analysis (Mendes, 1997; Straathof, 2001.; Goudar et al., 2004). Since parameter estimation is a crucial step, the determination of the parameter sensitivity is important as well. Parametric sensitivity can be defined as: “the sensitivity of the system behavior with respect to changes in parameters” (Varma et al., 1999). Sensitivity equations, defined as the first derivative of the state variable with respect to a particular parameter of a nonlinear model, predicts whether unique estimates of the parameters in a given model can be determined, and evaluate if there are linearities among parameters in the model expression (Robinson & Characklis, 1984). Sensitivity analysis can also be

directly evaluated by multiparameter variation, evaluating the variation in model prediction with respect to observed values. Such approach has been recently accomplished after the derivation of the explicit form of the integrated Michaelis-Menten equation (7) using the Lambert W function (Schnell & Mendoza, 1997) by means of three-dimensional visualization of the error in the K_M and V_{max} space, allowing the observation of local minima and evaluating the determination of the true global minimum during the parameter estimation iterative process (Goudar et al., 2004).

Finally, it is important to highlight that parameter estimation has been a common practice in the determination of enzyme kinetics *in vitro*, being extremely useful in the assessment of the mechanism of isolated reactions. However, the extent of *in vitro* estimated parameter's use to *in vivo* situations is often highly inappropriate, since substrate concentration and enzyme activity together with protein-protein interactions, among other factors, play an important role in the cell biochemical processes (Wright, 1960; Shiraishi & Savageau, 1992).

Overall, a unique feature of kinetic models, is the possibility to describe the dynamic behavior of a system from a global perspective, becoming an extremely fundamental tool for qualitative and quantitative analysis of different culture conditions such as stationary state occurrence and oscillations.

IV. MATERIALS AND METHODS

4.1 Strains

Pseudomonas sp. MT1 and *Achromobacter xylosoxidans* strain MT3 were previously isolated by continuous culture enrichment from a polluted stream in Bitterfeld, Sachsen-Anhalt, Germany as previously described (Pelz et al., 1999).

4.2 Chemicals

Chemicals were purchased from Amersham Biosciences (Pittsburgh, PA, USA), AppliChem (Darmstadt, Germany), Baker (Philipsburg, NJ, USA), BioRad (Hercules, CA, USA), Fluka AG (St. Gallen, Switzerland), Merck AG (Darmstadt, Germany), Pharmacia Biotech AB (Upsala, Sweden), Riedel de Haen (Seelze, Germany), Roche (Basel, Switzerland), Roth (Karlsruhe, Germany), Serva (Heidelberg, Germany) and Sigma-Aldrich (St. Louis, MO, USA). 4-chlrosalicylate (4CS) and 4-chlorocatechol (4CC) were obtained from TCI Europe nv (Zwijndrecht, Belgium). Protoanemonin was synthesized as previously described (Crey et al., 2003). 3-chloromuconate standards for HPLC were freshly prepared from 4-chlorocatechol as described in Nikodem et al. (2003). Standards for HPLC of muconate, *cis*- and *trans*-dienelactone were kindly provided by Dietmar Pieper (Helmholtz-Zentrum für Infektionsforschung, Braunschweig, Germany).

4.3 Culture Conditions

Pseudomonas sp. MT1 was grown aerobically in 5L BIOSTAT B bioreactors (Sartorius BBI Systems GmbH, Melsungen, Germany) at a working volume of 4L in minimal medium

consisting of phosphate buffer ($Na_2HPO_4.2H_2O$ 17.5 g/L; KH_2PO_4 6 g/L; $(NH_4)_2SO_4$ 2.5 g/L (pH 7.2)), supplemented with 0.165 g/L of $MgSO_4.H_2O$ and 7.5 mg/L of $FeCl_3$, and trace elements in milligrams per liter (mg/L): MgO, 14.30; $FeSO_4.7H_2O$, 6.0; $CaCO_3$, 2.7; $ZnSO_4.H_2O$, 2.0; $MnSO_4.2H_2O$, 1.16; $CoSO_4.7H_2O$, 0.37; $CuSO_4.5H_2O$, 0.33; H_3BO_3, 0.08). 4-chorosalicylate (98% purity, TCI Europe) 10 mM feeding solution was used as single carbon source at the dilution rates of 0.1, 0.2 and 0.4 d^{-1}, 30º C, pH 7.2 ensuring >50% dissolved oxygen concentration. A minimum of five residence times were given for steady state attainment.

Bioreactor containing sterile minimal media with 4-chlorosalicylate 1 mM as single source of carbon was inoculated 5% (v/v) with a minimal media supplemented with acetate 5 mM overnight culture of *Pseudomonas* sp. MT1, run in batch mode until significant turbidity increment ($OD_{650} \geq 0.15$) and switched to continuous mode at a specific dilution rate. In the case of mixed cultures, after steady state achievement of *Pseudomonas* sp. MT1 pure culture, a 5% (v/v) inoculum coming from minimal media supplemented with acetate 5 mM overnight culture of *A. xylosoxidans* MT3 was added.

A major pre-requisite is the achievement of the steady state, a culture state where the cells are subjected to constant conditions and thus growing at a constant growth rate, defined by the dilution rate (*D*):

$$D = \frac{F}{V} \tag{11}$$

where *F* corresponds to the flow rate and *V* to the working volume.

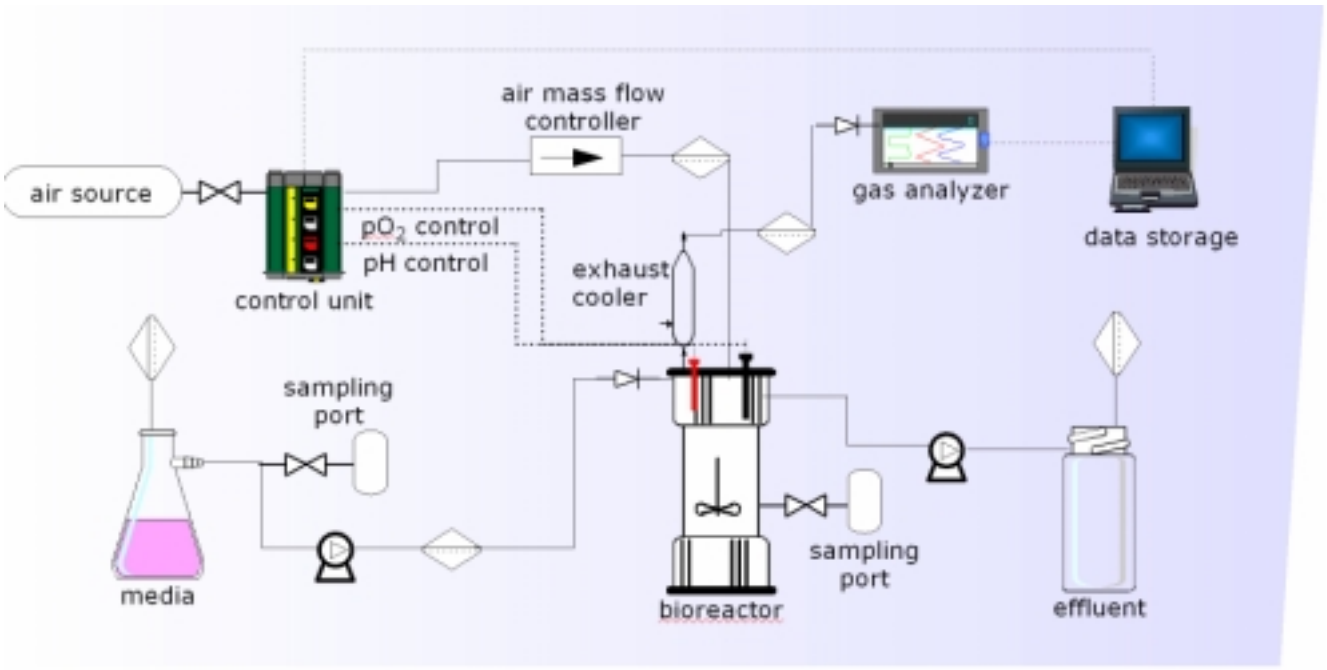

Figure 5. Scheme of bioreactor operation

The change in biomass concentration (X) as a function of time is given by:

$$\frac{dX}{dt} = \mu X - DX \tag{12}$$

At steady state, the biomass concentration is constant, therefore:

$$\frac{dX}{dt} = 0 \Rightarrow \mu = D \tag{13}$$

The growth rate μ can be stage-managed since it is a function of D.

It is important to stress that steady state achievement depends on the culture conditions but also on the cultured organism. As a general rule a minimum culture stabilization residence times (working volume change time or hydraulic residence time) is necessary before assuming steady state and therefore, culture monitoring until constant conditions achievement is required.

4.4 Dynamic State: Substrate Shock Load

After steady state achievement, continuous cultures were switched to batch conditions under different concentrations of 4CS or 4CC to force a dynamic condition. To do so, culture feeding was stopped and sterile 4CS or 4CC was added at a specific final concentration. Metabolite concentrations were monitored until total degradation. Between 2 and 6 replicates for each concentration were tested.

4.5 Enumeration Of Bacteria And Quantification Of Biomass

Colony forming units (CFU) were determined by plating a dilution series on Luria – Bertani (LB) plates, after incubation at 30 ºC for 48 h. Optical density of cell suspensions were measured at 650 nm (model Ultraspec.2000 UV/VIS, Hitachi, Tokyo, Japan).

4.6 Metabolic Profile: High Performance Liquid Chromatography

High Performance Liquid Chromatography (HPLC) using a separation-module, (Waters Alliance TM 2690, Waters Corporation, Milford, MA, USA) equipped with a reverse phase column (C60, 125-3 mm, Macherey-Nagel, Düren, Germany), operated under a solvent mixture gradient of Methanol-H_2O, each containing H_3PO_4 0.1% (v/v) as mobile phase at a flow rate of 0.25 mL/min was used. Detection was conducted using a Photodiode array detector (Waters TM 996-UV/Vis, Waters Corporation, Milford, MA, USA).

Typical retention times (RT) under the solvent gradient used were : 3-chloromuconate (RT = 7 min), 4-chlorocatechol (RT = 15 min), 4-chlorosalicylate (RT = 26 min), catechol (RT= 3 min), *cis*-acetylacrylate (RT= 2 min), *cis*-dienelactone (RT = 5 min), gentisate (RT= 6

min), muconate (RT= 5.6 min).protoanemonin (RT = 4 min), protocatechuate (RT= 3.7 min), salicylate (RT= 18 min) and *trans*-dienelactone (RT= 3 min).

Culture samples were centrifuged for 5 min at 13.000 rpm and 4° C to remove biomass and any suspended solids. Supernatant was transferred to a glass vial, closed with a teflon septum screw cap, and stored at -20° C in the dark until measurement.

4.7 Flow Cytometry Analysis

Flow cytometry measurements were carried out using a Fluorescence-Activated Cell Sorter FACSCalibur flow cytometer (BD Biosciences, San Jose, CA, USA) equipped with a 488-nm excitation argon-ion laser at 15mW. Low aspiration speed was used (~12 µL/min).

4.7.1 Cell viability determination

Live and dead cell discrimination was carried out using a standardized commercial kit (Cell viability kit, BD Biosciences, San Jose, CA, USA). Basically the method distinguish between cells with intact and compromised membranes, based on its differential permeability to Propidium iodide (PI). Live cells are impermeable, while dead and/or injured cells allow penetration of PI to varying degrees.

Culture samples were diluted in filtered PBS + Tween (0.01% w/v) buffer, aliquoted and incubated for 15 min at room temperature in the dark with Thiazole Orange (0.84 µM final concentration) for total cell measurement. Afterwards, sample was stained with PI (17.2 µM final concentration), homogenised and measured immediately for dead and alive determination. Count cell events per mL were calculated assuming a constant flow of 12 µL/min.

4.7.2 Fluorescence *in situ* hybridization (FISH)

Culture samples were fixed with formaldehyde 4% for 2h at 4°C. Cells were collected by centrifugation and washed twice with PBS pH 7.4, and stored in PBS/Ethanol solution (50:50) at -20°C. Hybridization was performed in a buffer solution made of NaCl 2 M, Tris-HCl 0.02M pH 8.0, 0.01% w/v SDS and 30% v/v formamide at 46°C for 2h in the dark with gentle agitation, in the presence of specific fluorescent oligonucleotide probes (IBA GmbH Göttingen, Germany), at a final concentration of 100 ng/µL (Kaminski et al., 2006). After incubation, samples were collected by centrifugation and washed twice with buffer solution (NaCl 0.1M, Tris-HCl 0.02M pH 8.0, 0.01% w/v SDS and EDTA 0.005M) pre-heated at 48°C, and finally resuspended in cold PBS pH 7.4 and immediately measured.

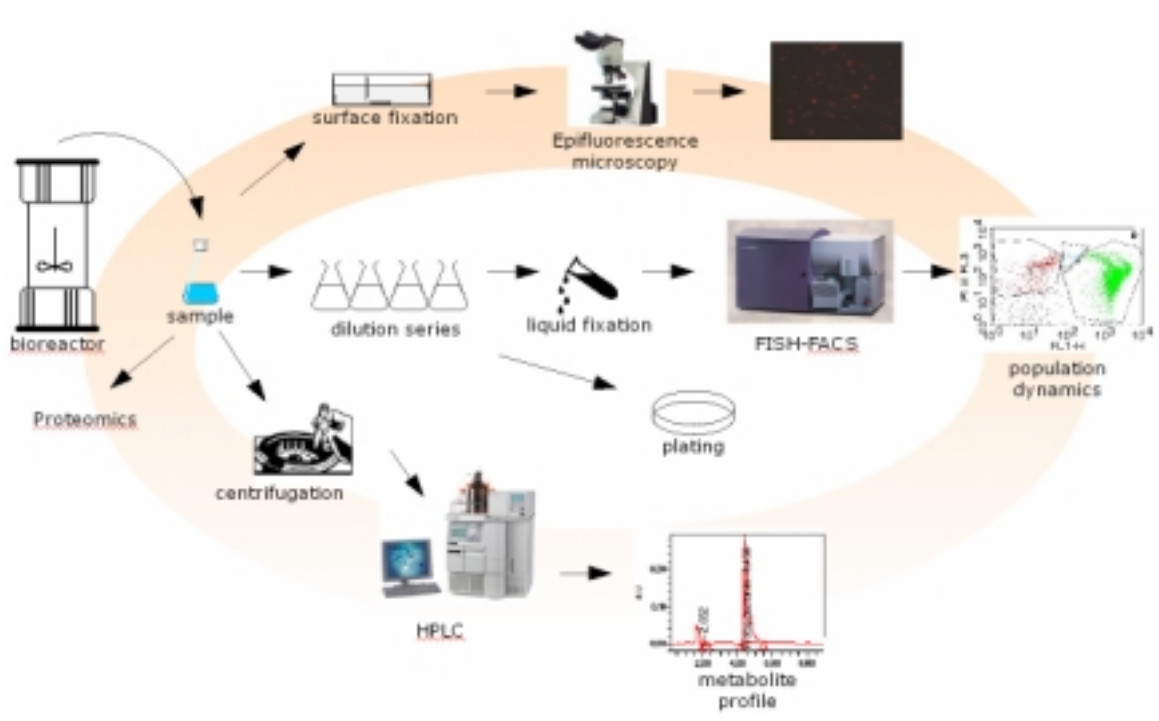

Figure 6. Sampling procedure.

4.8 Proteomics

Protein expression patterns in pure as well as mixed cultures were analyzed by standard proteomics 2-DE techniques as follows:

4.8.1 Cell collection and Protein extraction

Continuous culture samples were collected at different time intervals after steady state achievement, or before and during the shock load (2, 5 and 7 h after the shock load) for dynamic conditions. Samples were centrifuged at 8000 rpm for 15 min (RC5C-Sorvall Instruments, Thermo Electron, Langenselbold, Germany). Pellet cells were washed twice with PBS solution pH 7.4, and resuspended in protein extraction solution (Urea 7 M, Thio-urea 2 M, CHAPS 4% w/v, Tris base 20 mM and 1,4-dithiothreitol (DTT) 30 mM, including protease inhibitor cocktail (Complete™ Mini Protease inhibitor cocktail tablets, Roche Diagnostics GmbH, Mannheim, Germany). The suspension was sonicated (Labsonic U, B. Braun, Melsungen, Germany) and ultracentrifuged at 30,000 rpm for 30 min (Sorvall Ultracentrifuge OTD-Combi, Thermo Electron, Langenselbold, Germany). Supernatant was aliquoted for precipitation of proteins using the 2-D Clean-Up Kit (Amersham Biosciences, Pittsburgh, PA, USA).

4.8.2 First dimension: isoelectric focusing

Analytical determinations were carried out with 100 µg of protein mixture determined by Bradford (Bio-Rad protein assay, Bio-Rad, Hercules, CA, USA) , diluted up to 300 µL with rehydration solution (7 M Urea; Serdolit; 2 M Thio-urea; 4% w/v CHAPS; 20 mM

Trizma base) in the presence of ampholytes and under reducing conditions, on ReadyStrip IPG strips, 17 cm, pH 3-10 (Bio-Rad, Hercules, CA, USA). Passive rehydration was carried out for 2h at 20ºC on the focusing tray. Samples were covered with silicon oil to avoid dehydration. Active rehydration was performed at 50V for 12h. Isoelectric focusing was done at a final voltage of 10,000 V on Protean®IEF cell (Bio-Rad, Hercules, CA, USA) until reaching 75 kVh. Focused samples were stored at –70°C until the second dimension step.

4.8.3 Second dimension: Equilibration and SDS-PAGE

Focused ReadyStrip IPG strips were equilibrated first in equilibration buffer containing Urea 6 M, Trizma Base 0.375 M, pH 8.6, Glycerin 30% v/v, SDS 2% w/v and DTT 2% w/v and later in the same buffer replacing DTT with iodoacetamide 2.5% w/v. After equilibration, second-dimension separation was performed on 12-15% gradient SDS-polyacrylamide 20x20 cm gels with the focused sample embedded in 0.5% IEF agarose in a Protean Plus Dodeca Cell (Bio-Rad, Hercules, CA, USA) at 100 V overnight.

The gels were fixed in 10% trichloroacetic acid solution for a minimum of 3 h, stained with 0.1% w/v Coomassie™ Brilliant Blue G-250 solution overnight, and finally de-stained with distilled water.

Images of the 2-DE gels were captured with a molecular imager GS-800 calibrated densitometer (Bio-Rad, Hercules, CA, USA) and processed using Z3 image analysis software (Compugen, San Jose, CA, USA) for protein differential expression analysis.

4.8.4 Protein Identification

Protein spots were excised manually from the gels. Spots were de-stained, and digested overnight using sequence grade modified trypsin (Promega, Madison, WI, USA). The peptides were eluted and desalted with ZipTip® (Millipore, Bedford, MA, USA). For MALDI-ToF analysis, the samples were loaded along with α-cyano-4-hydroxycinnamic acid matrix. The target was then analyzed using a Ultraflex II ToF (Bruker Daltonics Inc. Billerica, MA, USA) and resulting spectra were used for Peptide Mass Fingerprint (PMF), analyzed using FlexAnalysis 2.0 and Biotools 2.2 software (Bruker Daltonics Inc. Billerica, MA, USA). Database search was carried out on NCBInr database using Profound version 4.10.5 (Proteometrics, New York, NY, USA). For ESI Q-ToF analysis, 3 µL of sample were directly analyzed after Zip-Tip elution in a Micromass Q-ToF micro™ mass spectrometer (Waters Corporation, Milford, MA, USA). *Ab initio* sequencing analysis was carried out using MassLynx Mass Spectrometry Software 4.0 (Waters Corporation, Milford, MA, USA). Sequence similarity searching against protein databases was performed using FASTA (European Bioinformatics Institute, Cambridge, UK at http://www.ebi.ac.uk/fasta33/).

4.8.5 Protein differential expression analysis

Differential expression (DE) analysis was done using Z3 image analysis software version 3.0.7 (Compugen, San Jose, CA, USA). Basically, scanned gel images were saved in grayscale, 300 dpi with no adjustments. Images were first subject to automatic spot detection, with automatic minimum spot contrast and manually adjusted minimum spot area (usually 100 (arbitrary units)). Detected spots were edited manually in order to obtain a better pattern. A minimum of three independent replicates for each reference

condition were analyzed and combined using the Raw Master Gel (RMG) algorithm. Comparison of the RMG reference gel was performed in triplicate, that were independently wrapped and matched to the reference RMG to obtained at least three independent DE sets. DE was defined as the ratio of spot expression in a comparative image to the expression of a corresponding spot in a reference image. Upregulation corresponds to a two-fold or higher DE values and downregulation to 0.5-fold or lower DE values. Average DE values from the replicates are shown in DE tables (appendix). Error corresponds to the standard deviation.

V. RESULTS AND DISCUSSION

5.1 Steady State Cultures

The study of global trends in complex systems, such as bacterial communities, requires reproducible and reliable homogeneous conditions in order to avoid any bias in the analysis due to secondary effects caused by physico-chemical variations. Therefore, this present study was conducted in continuous culture, a system that provides a constant environment and helps to reveal relevant biological tendencies, and at the same time, can be consider more close to real environmental conditions compared to simple batch culture techniques (Hoskisson & Hobbs, 2005).

5.1.1 *Pseudomonas* sp. MT1 steady state continuous cultures

Pseudomonas sp. strain MT1 constitutes the most important member of the MT community composing over 80% of the population and being the only strain able to perform the first metabolic step of degradation from 4CS to 4CC (Nikodem et al., 2003). Therefore, initial studies were carried out on strain MT1 in order to perform a combined analysis of metabolic profile and proteome pattern.

First, following previous studies (Pelz et al., 1999), strain MT1 was cultured continuously at a D of 0.2 d^{-1} as described in materials and methods (section 2.3). This conditions of growth were used as the reference for further culture variation. A proteome reference map was created including 128 spots, corresponding to 118 different proteins in a broad molecular weight range (10-100 kDa) and isoelectric point (3-10 pI). Identified proteins are shown in Figure 7 and described in Table 2, including important enzymes directly involved in the upper degradation pathway of 4CS like salicylate hydroxylase (SalA,

spot 25), catechol 1,2-dioxygenase (CatA1 and CatA2, two different isoenzymes identified, spots 28 and 134, respectively) and 3-oxoadipate:succinyl-CoA transferase α and β subunits (CatJ, spots 24 and 37, respectively). Particularly interesting was the presence of aromatic degradation enzymes apparently not directly involved in the degradation of 4CS, but to close related pathways, in Figure 7, catechol 2,3-dioxygenase (spot 87), protocatechuate 3,4-dioxygenase α and β subunits (3,4-PCD spots 46 and 57, respectively), 4-hydroxyphenylpiruvate dioxygenase (4-HPPD spot 72) and 3-carboxymuconate cycloisomerase (spot 9). To this respect, expression of 3,4-PCD has been reported under non-induced culture conditions (Heim et al., 2003; Kim et al., 2006). Moreover, more distantly related aromatic degradation enzymes were detected as well, including 2,3-dihydroxybiphenyl 1,2-dioxygenase (BphC spot 23), 2-oxohepta-3-ene-1,7-dioic acid hydratase

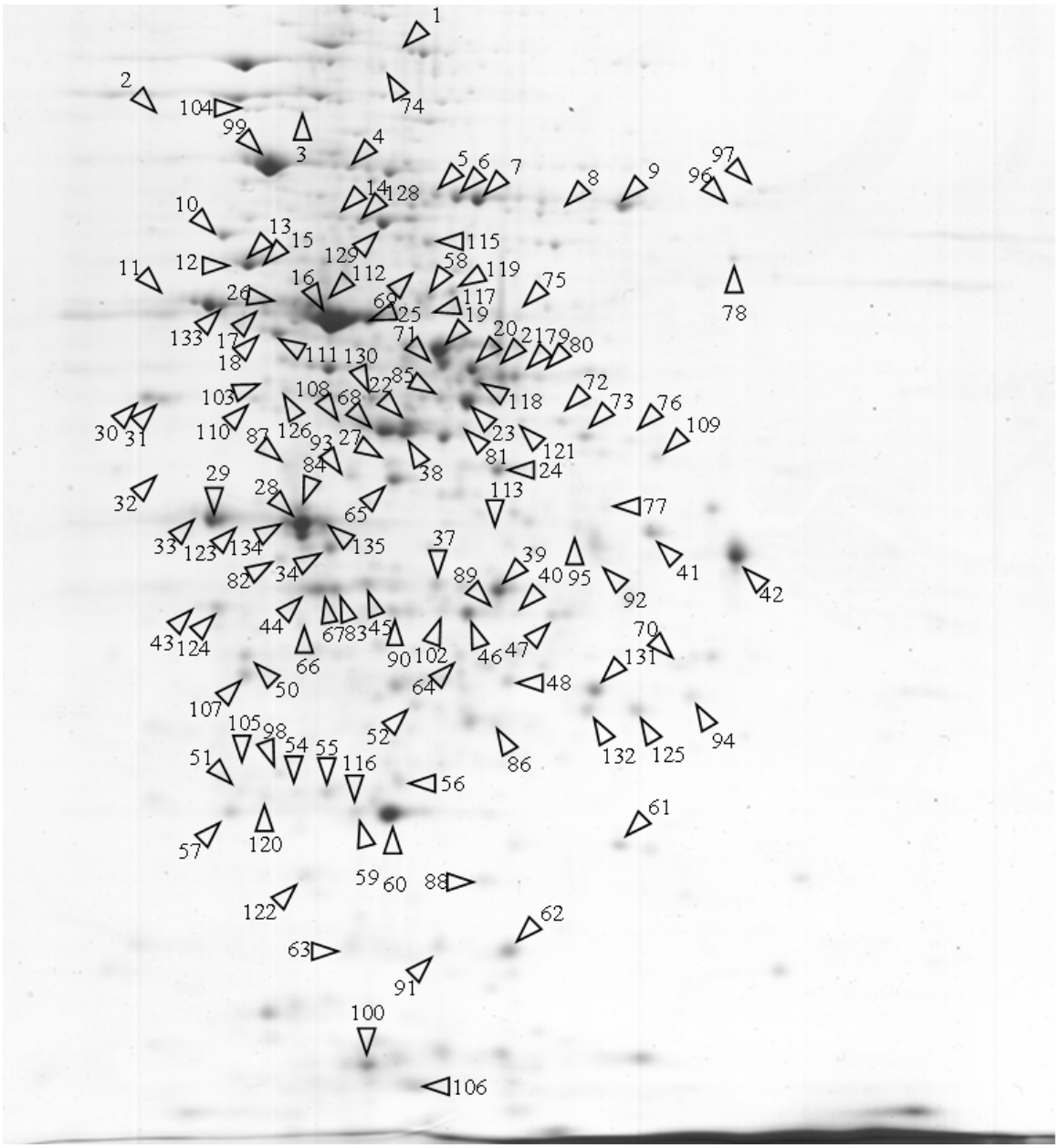

Figure 7. Reference proteome map of *Pseudomonas* sp. MT1 in 4CS continuous culture (D = 0.2 d^{-1}, 30°C, pH 7.2, pO_2 >50%, minimal media M9, feeding solution 4CS 10 mM).

Table 2. Proteome reference map list of proteins identified in *Pseudomonas* sp. strain MT1 with statistical significance.

Spot No.[¥]	Protein Description	Theoretical MW [kDa]	Theoretical pI	NCBInr accession No.
	Aromatic degradation enzymes			
9	3-carboxy-cis,cis-muconate cycloisomerase	48.87	6.1	gi|26988113
23	2,3-dihydroxybiphenyl 1,2-dioxygenase (BphC)	34.97	5.0	gi|3059192
24	3-oxoadipate:succinyl-CoA transferase, α subunit (CatJ α)	31.24	5.9	gi|48732882
25	salicylate hydroxylase (SalA)	48.40	5.9	gi|15809677
28	catechol 1,2-dioxygenase (CatA2)	33.57	4.9	gi|400768
29	putative oxygenase	30.54	5.4	gi|33573503
37	3-oxoadipate:succinyl-CoA transferase, β subunit (CatJ β)	27.39	5.2	gi|77381498
46	protocatechuate 3,4-dioxygenase, β subunit (3,4-PCD β)	26.29	6.2	gi|70728700
57	protocatechuate 3,4-dioxygenase α subunit (3,4-PCD α)	20.72	4.8	gi|48732886
72	4-hydroxyphenylpyruvate dioxygenase (4-HPPD)	40.63	5.1	gi|15596062
81	biphenyl dioxygenase	44.30	5.0	gi|510288
82	2-keto-4-pentenoate hydratase/2-oxohepta-3-ene-1,7-dioic acid hydratase (HpaG)	27.41	5.6	gi|23015330
84	reductase component of salicylate 5-hydroxylase (Sal5)	36.00	6.2	gi|27372222
87	catechol 2,3-dioxygenase	35.12	5.4	gi|14715448
90	acyl CoA:acetate/3-ketoacid CoA transferase, β subunit	27.39	5.2	gi|48732883
114	3-oxoadipate:succinyl-CoA transferase, α subunit	25.76	5.5	gi|48732993
130	xenobiotic reductase B (XenB)	37.90	5.3	gi|24982339
134	catechol 1,2-dioxygenase (CatA2)	33.57	4.9	gi|77458554
	Periplasmic, outer membrane proteins and transporters			
19	branched-chain amino acid ABC transporter, periplasmic amino acid-binding protein	39.66	6.4	gi|70728680
27	uncharacterized protein conserved in bacteria (hypothetical membrane associated protein)	38.87	9.3	gi|48859490
30	outer membrane porin F precursor (OprF)	37.42	4.7	gi|4530365
31	outer membrane protein and related peptidoglycan-associated (lipo)proteins (OprF)	37.67	4.8	gi|48731955|
42	ABC-type amino acid transport/signal transduction systems, periplasmic component/domain (extracellular solute-binding protein, family 3)	34.19	6.4	gi|77384759

Spot No.[¥]	Protein Description	Theoretical MW [kDa]	Theoretical pI	NCBInr accession No.
47	membrane protease subunits, stomatin/prohibitin homologs (HflC-like protein)	34.26	7.8	gi|46311920
48	ABC-type amino acid transport/signal transduction systems, periplasmic component/domain	27.56	5.5	gi|48732828
52	ABC-type amino acid transport/signal transduction systems, periplasmic component/domain (extracellular solute-binding protein, family 3)	27.68	5.5	gi|48732828
61	YceI precursor	22.39	7.8	gi|77385508
62	outer membrane protein H1 [Precursor]	21.26	7.9	gi|77460462
63	yojA (periplasmic ferredoxin-type protein, subunit of nitrate reductase)	15.40	10.9	gi|405930
65	extracellular solute-binding protein, family 3	36.64	6.5	gi|77381203
88	starvation-inducible outer membrane lipoprotein	21.60	5.9	gi|42629847
93	ABC-type amino acid transport/signal transduction systems, periplasmic component/domain	36.90	6.5	gi|48732598
103, 126	ABC-type amino acid transport/signal transduction systems, periplasmic component/domain (extracellular solute-binding protein, family 3)	37.80	6.5	gi|48732598
109	ABC-type Fe3+-hydroxamate transport system, periplasmic component	37.88	5.6	gi|66046323
111	outer membrane porin (OprD homolog)	46.46	5.7	gi|48729184
133	porin D	48.46	5.5	gi|70732098
	Cell envelope biogenesis			
5,6,7	dihydrolipoamide dehydrogenase (E3 component of 2-oxoglutarate dehydrogenase complex) (LPD-GLC)	51.31	5.9	gi|1706442
8	UDP-N-acetylmuramoylalanine-D-glutamate ligase	49.89	5.5	gi|21204233
43	NmrA-like	26.81	5.1	gi|77458502
45	enoyl-[acyl-carrier-protein] reductase (NADH)	28.81	5.3	gi|48731665
68	UDP-N-acetylenolpyruvoylglucosamine reductase	38.47	5.2	gi|77458502
95	glycosyltransferases involved in cell wall biogenesis	34.4	9.3	gi|71899363
105	UDP-N-acetylglucosamine enolpyruvyl transferase	23.22	10.5	gi|23006264
122	(3R)-hydroxymyristoyl-[acyl carrier protein] dehydratase ((3R)-hydroxymyristoyl ACP dehydrase)	17.00	6.1	gi|47605657
	Stress Response			
1	penicillin acylase	98.14	7.3	gi|46310114
2	transcription termination factor NusA	55.29	4.5	gi|23470955

Spot No.[¥]	Protein Description	Theoretical MW [kDa]	Theoretical pI	NCBInr accession No.
11	D-alanyl-D-alanine carboxypeptidase, fraction A; penicillin-binding protein 5	45.66	8.5	gi|24050895
16	translation elongation factor TU (EF-Tu)	44.32	5.2	gi|48728524
34	translation elongation factor Ts (EF-Ts)	29.90	5.2	gi|48732722
54	Alkyl hydroperoxide reductase, subunit C (AhpC1)	20.43	4.9	gi|26989162
55	Alkyl hydroperoxide reductase, subunit C (AhpC2)	20.39	5.0	gi|48733206
59	Superoxide dismutase [Fe] (SOD1)	22.12	5.6	gi|2511749
60	Superoxide dismutase [Fe] (SOD2)	21.81	5.6	gi|24982333
66	BpoC (high homology with arylesterase, possible non-haem peroxidase)	30.16	6.6	gi|41409635
77	CagA (cytotoxin associated protein A)	38.11	9.1	gi|22335887
92	universal stress protein (UspA)	31.39	5.9	gi|46164823
94	NTP pyrophosphohydrolases including oxidative damage repair enzymes	23.01	4.9	gi|48834691
99	chaperonin GroEL	58.50	5.00	gi|77384725
101	beta-lactamase	33.10	9.5	gi|76583829
106	chaperonin Cpn10	10.55	5.7	gi|77384726
121	hydrogen peroxide-inducible genes activator	36.13	6.9	gi|17989239
	Central Metabolism			
4	glutamine synthetase, type I	53.03	5.2	gi|24986826
10	FKBP-type peptidyl-prolyl cis-trans isomerase (trigger factor)	48.11	4.8	gi|77383923
12, 13	F0F1-type ATP synthase, beta subunit	50.32	4.9	gi|23469339
14, 128	ATP synthase F1, alpha subunit	56.44	5.5	gi|28855956
129	F0F1-type ATP synthase, alpha subunit	55.50	5.4	gi|48731319
15	FKBP-type peptidyl-prolyl cis-trans isomerase (trigger factor)	48.11	4.8	gi|82739287
17	enolase	46.75	4.9	gi|48732741
20	succinyl-CoA synthase, beta subunit	41.50	5.8	gi|48729501
32	fructose-1,6-bisphosphate aldolase	39.29	5.3	gi|22995491
39	succinyl-CoA synthetase, alpha subunit	30.85	6.1	gi|68343411
89	succinyl-CoA synthase, alpha subunit	30.96	5.9	gi|70729112
56	acetoacetyl-CoA reductase protein	26.00	6.2	gi|15967014
71	succinyl-CoA synthetase, beta subunit	41.53	5.8	gi|48729501
73	glyceraldehyde 3-phosphate dehydrogenase	36.49	6.1	gi|9949314
75	citrate synthase	48.00	6.2	gi|77457992

Spot No.[¥]	Protein Description	Theoretical MW [kDa]	Theoretical pI	NCBInr accession No.
113	ATPase associated with various cellular activities, AAA_5	33.34	5.9	gi|48729699
117	isocitrate dehydrogenase, NADP-dependent, prokaryotic type	46.11	5.4	gi|48729767
132	succinate dehydrogenase, iron-sulfur protein	26.14	6.6	gi|28852641
	Amino acid Metabolism			
22	ketol-acid reductoisomerase	37.19	5.5	gi|48728466
38	histidinol-phosphate aminotransferase HisH	39.99	4.9	gi|13475919
58	arginine deiminase	46.69	5.6	gi|48730780
74	aspartyl-tRNA synthetase	66.20	5.3	gi|68346391
104	2-isopropylmalate synthase (Alpha-isopropylmalate synthase)	62.76	5.2	gi|38257977
118	ornithine carbamoyltransferase	38.24	6.1	gi|48730781
119	argininosuccinate synthase	45.50	5.4	gi|48730315
	Cell division and replication			
3	chromosomal replication initiator protein DnaA	54.24	8.3	gi|28262837
18	DNA-directed RNA polymerase, alpha subunit	37.33	4.9	gi|28851115
21	DNA polymerase III, delta prime subunit	36.95	6.3	gi|42735025
26	cell division protein FtsA	44.70	5.2	gi|68346679
69	RNA-directed DNA polymerase	51.40	11.2	gi|7271418
	Transcriptional regulators			
44	transcriptional Regulator, LysR family	33.64	7.2	gi|78696079
49	response regulator (CorR)	22.11	6.5	gi|15282020
76	putative transcriptional regulator	36.1	5.4	
86	cyclic nucleotide-binding:Bacterial regulatory protein (Crp)	26.62	9.8	gi|77691852
124	transcriptional regulator (OmpR)	27.78	5.8	gi|28896928
	Non- clasified proteins			
33	porphobilinogen deaminase (HemC)	34.34	6.1	gi|19714161
40	L0015-like protein (Transposase IS66 family)	31.30	9.5	gi|18265862
41	conserved hypothetical protein	34.31	10.5	gi|33592722
51	isochorismatase hydrolase	22.84	5.2	gi|77459786
64	probable electron transfer flavoprotein	26.58	7.6	gi|17427935
67	senescence marker protein-30 (SMP-30)	34.30	5.5	gi|91786097
70	electron transfer flavoprotein beta-subunit	27.73	5.8	gi|33592118
78	hypothetical protein Pflu02003553 (putative signal peptide)	50.74	8.9	gi|48730134

Spot No.[¥]	Protein Description	Theoretical MW [kDa]	Theoretical pI	NCBInr accession No.
79	hypothetical protein (putative phage integrase)	36.61	9.5	gi|24985122
80	hypothetical protein (high homology with Phage integrase [Pseudomonas fluorescens PfO-1] GI:77456973)	36.61	9.5	gi|24985122
83	hypothetical protein HP1454	35.20	9.3	gi|15646063
85	uncharacterized conserved protein	39.41	8.8	gi|23467370
91	repressor of phase I flagellin	20.01	7.9	gi|46395288
96	transposase	47.37	10.1	gi|21554219
97	hypothetical protein Pflu02003553	52.00	8.9	gi|48730134
98	Transposase	20.95	9.6	gi|29896025
100	flagellar protein (FliS)	15.22	4.8	gi|24113301
102	septum formation inhibitor-activating ATPase	30.46	5.5	gi|48731998
108	twitching motility protein (PilT)	38.98	6.3	gi|53757925
110	delta-aminolevulinic acid dehydratase	37.00	5.4	gi|21110452
112	TraN-like (conserved hypothetical TraN-like protein found in conjugate transposon)	42.52	5.9	gi|29611516
115	conserved hypothetical protein (predicted kinase)	48.35	5.6	gi|16265283
116	protease subunit of ATP-dependent Clp proteases	23.95	5.4	gi|38257977
120	signal recognition particle GTPase	23.34	8.9	gi|23008862
123	repeat protein K	31.21	6.2	gi|34369789
125	putative transaldolase-like protein	25.02	5.5	gi|19746931
131	hypothetical protein	28.00	6.1	gi|49658854

[¥] Spot numbers are referred to Figure 7

(spot 82) and xenobiotic reductase B (XenB, spot 130). XenB has been described in the process of reduction of 2,4,6-trinitrotoluene (TNT) by *P. fluorescens* I-C (Pak et al., 2000), and its physiological role has been associated to detoxification mechanism in bacteria (Blehert et al., 1999).

Protein identified as 2-oxohepta-3-ene-1,7-dioic acid hydratase designated HpaG, presents 43.5% aminoacid sequence identity to 4-hydroxyphenylacetate degradation isomerase (gi|83717800), close related to homoprotocatechuate and homogentisate catabolic pathways (Barbour & Bayly, 1981).

The presence of general stress response proteins, like the universal stress protein UspA (spot 92) and chaperon proteins GroEL (spot 99) and Cpn10 (spot 106) and elongation factors EF-Tu and EF-Ts (spots 16 and 34, respectively), and oxidative stress response proteins such as superoxide dismutase (SOD1 and SOD2 two isoforms, spot 59 and 60, respectively), alkylhydroperoxide reductase C (AhpC1 and AhpC2 two isoforms, spots 54 and 55) and NTP pyrophosphohydrolase (spot 94), indicate that culturing conditions may represent a stress to bacterial culture to some extent.

Under these conditions, metabolite profile was determined by HPLC. Constant concentration of *cis*-dienelactone (5.18 ± 0.57 µM) and protoanemonin (12.35 ± 1.63 µM) were observed with no other metabolite present under the analytical conditions tested. Total absence of substrate indicate nutrient limiting conditions. Biomass reached a constant concentration of 7.24e08 ± 1.29e08 CFU/mL equivalent to an observed OD_{650} of 0.197 ± 0.066. Figure 8 shows an example of the metabolite profile as well as the biomass monitoring observed under these conditions.

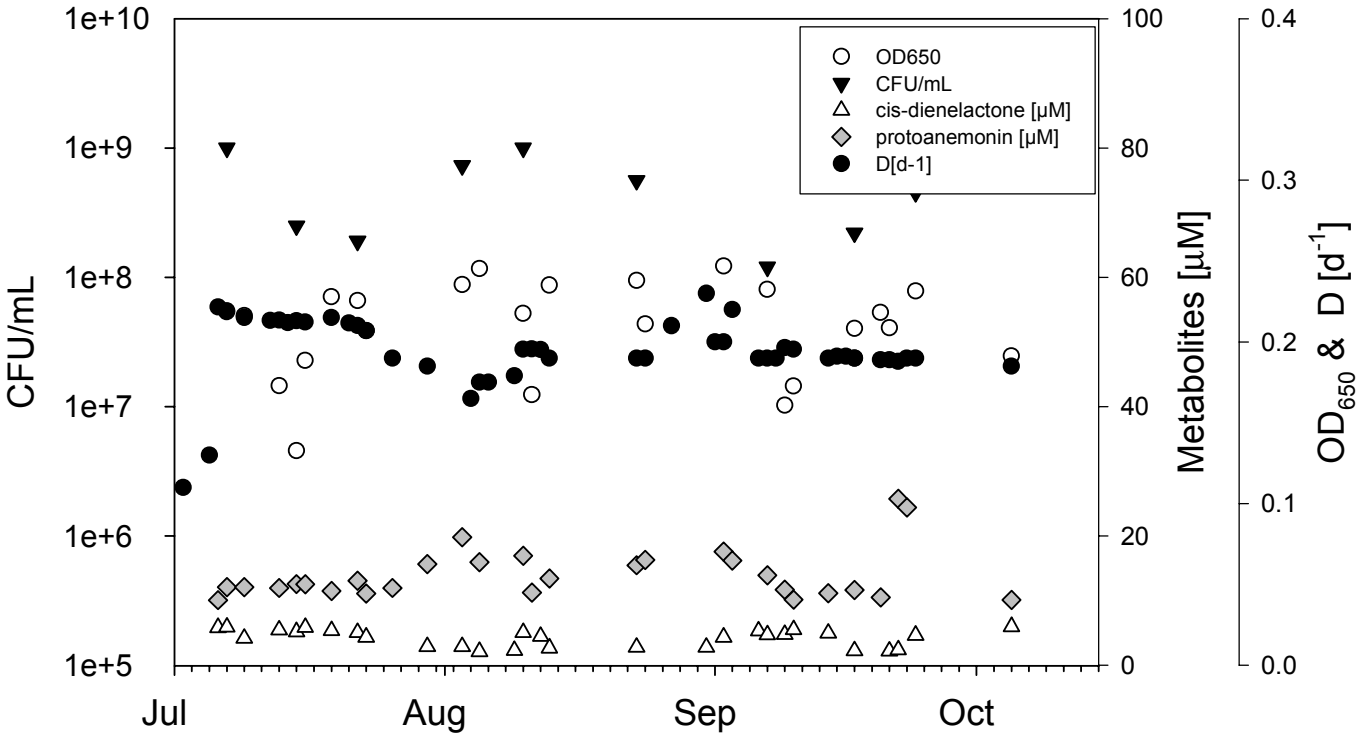

Figure 8. *Pseudomonas* sp. MT1 continuous culture monitoring (D = 0.2 d^{-1}, 30°C, pH 7.2, pO_2 >50%, minimal media M9, feeding solution 4CS 10 mM).

5.1.1.1 Low dilution rate steady state continuous cultures of *Pseudomonas* sp. MT1

In order to observe the effect of more severe nutrient limiting conditions, the dilution rate was set at 0.1 d^{-1}, allowing stabilization of the culture and monitoring the metabolite profile as well as the biomass concentration. As expected, lower concentrations of *cis*-dienelactone (2.07 ± 1.32 µM) as well as lower biomass content with 2.36e08 ± 8.29e07 CFU/mL and OD_{650} corresponding values of 0.183 ± 0.051 were observed. However, protoanemonin concentrations raised significantly up to 24.36 ± 3.27 µM, indicating major variations in dead-end metabolite production.

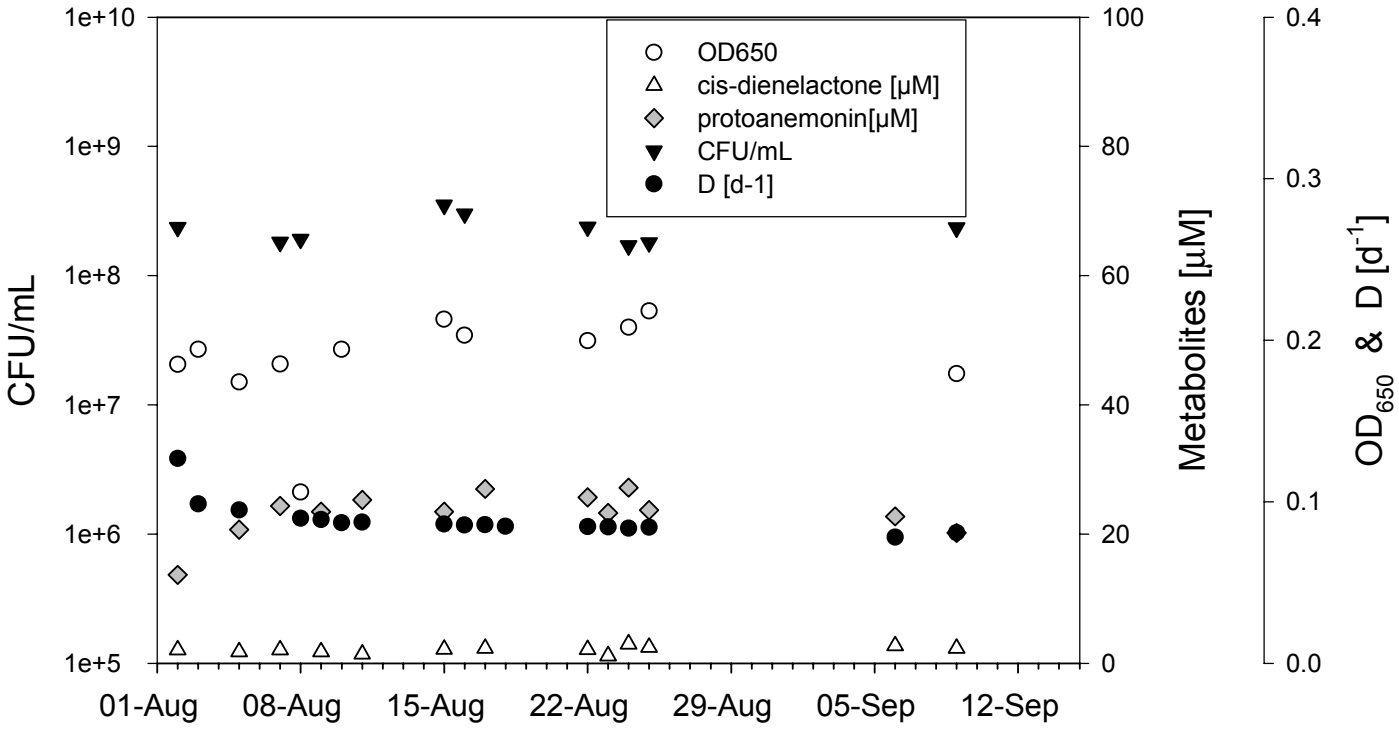

Figure 9. *Pseudomonas* sp. MT1 continuous culture monitoring (D = 0.1 d^{-1}, 30°C, pH 7.2, pO_2 >50%, minimal media M9, feeding solution 4CS 10 mM).

Compared to the proteome at the reference condition of 0.2 d^{-1}, the identified enzymes involved in the upper degradation pathway of 4CS, SalA and CatA1 showed downregulation (DE 0.22 ± 0.09 and 0.09 ± 0.02, respectively) (Figure 10, panels A and C). Highly expressed parallel aromatic pathway enzymes such as BphC (DE 0.30 ± 0.07, Figure 10, panel D) and 3-carboxymuconate cycloisomerase were repressed as well (DE 0.35 ± 0.01). However, low expressed enzymes belonging to parallel aromatic catabolic pathways showed no differential expression, e.g., catechol 2,3-dioxygenase (DE 1.10 ± 0.26).

Most identified enzymes of the central metabolism such as succynil-CoA synthase β subunit (DE 0.04 ± 0.01) and succinate dehydrogenase (DE 0.38 ± 0.02) were

downregulated, indicating a lower carbon flux at the current dilution rate. Unexpectedly enolase (phosphopyruvate hydratase), an enzyme involved in the reversible transformation of the central metabolism metabolite, phosphoenolpyruvate, was overexpressed at low dilution rate (DE 3.75 ± 0.49, Figure 10, panel C) together with fructose 1,6-bisphosphate aldolase (DE 5.96 ± 1.63), indicating a possible central metabolism adaptation to improve *Pseudomonas* MT1 fitness to low substrate loads. Enolase participates also in aromatic aminoacid metabolism, catalyzing the oxidation of 3-dehydroquinate, and members of the enolase superfamily MLE subgroup are able to transform muconate to muconolactone (Gerlt & Babbitt, 2001), so it is possible to relate its overexpression to 4CS upper degradation, rather than to glycolisis or gluconeogensis pathways.

Proteins associated to general stress response showed lower expression levels at the lower dilution rate of 0.1 d^{-1}. EF-Ts showed a DE of 0.40 ± 0.09 and UspA was absent (Figure 10, panels A and B, respectively). Identified oxidative stress proteins presented a divergent behavior, being SOD1 overexpressed (DE 3.84 ± 0.88) and AhpC2 downregulated (DE 0.30 ± 0.06) together with a senescence marker protein-30 (SMP-30) that presented a DE of 0.06 ± 0.01. SMP-30, initially characterized as a mammal protein, is present in several bacterial genus including *Pseudomonas*, and although its function in bacteria has not been elucidated, it is related to oxidative stress protection in mice (Sato et al., 2006).

Interestingly, a series of transporters and outer membrane proteins showed higher expression levels under these conditions. Major outer membrane protein OprF and different ABC-type aminoacid transport/signal transduction system transporters, belonging to the extracellular solute-binding protein family 3 were upregulated (Figure 10, panel B, Table 2, spots 48, 93 and 103). Moreover, a permease of the major

facilitator superfamily (MFS) was *de novo* synthesized at low dilution rate (Figure 10, panel C red circled). Previous studies have shown the role in chemotaxis and transport of 4-hydroxybenzoate in *Pseudomonas putida* by PcaK, a MFS transporter that belongs to the aromatic acid/H^+ symporters family (Ditty & Harwood, 1999).

OprF presented a differential expression of 11.10 ± 3.29 fold (Figure 10, panel A), allocating an important role to this outer membrane protein under severe nutrient limiting conditions. OprF, an homolog of *E. coli* OmpA (Sugawara et al., 1996), has been related as an important virulence factor in *P. aeruginosa* and its resistance to a series of antibiotics (Peng et al., 2005). In addition, its loss caused a significant decrease in outer membrane permeability in *P. aeruginosa* mutants (Nicas & Hancock, 1983). The outer membrane constitutes a selective permeation barrier, and porins were initially identified as nonspecific diffusion channels (Nakae, 1976). OprF among several porins, are required to facilitate substrate diffusion in nutrient-limited environments (Harder & Dijkhuizen, 1983). OprF has been classified as part of the 'slow porins', being present in the outer membrane mainly as a closed pore with a minority containing the open channel (Sugawara et al., 2006), contributing to the intrinsically high resistance levels of Pseudomonad to toxic agents (Nikaido, 2003).

In the work done by Chevalier and co-workers, the deletion of the *oprF* gene in *P. fluorescens* was followed by upregulation of OprD family channel proteins (Chevalier et al., 2000). To this respect, strain MT1 showed higher protein expression levels of porin D at lower dilution rates (Figure 10, panel C), indicating that simultaneous and complex diffusion events are concomitantly regulated. Porin D belongs to the OprD porin family, recently characterized in *P. aeruginosa* (Tamber et al., 2006), that has been previously linked to aromatic substrate uptake mechanisms, such as vanillate transport by porin VanP in *Acinetobacter* species (Metzgar et al., 2004) and OpdK in *P. aeruginosa*. In

addition, a benzoate putative porin gene *benF* is situated in the middle of a degradative operon in *P. putida* (Nelson et al. 2002).

Downregulation of ketol-acid reductoisomerase (KARI) and arginine deiminase (ADE) (DE 0.43 ± 0.04 and 0.25 ± 0.01, respectively), together with the upregulation of ABC-type aminoacid transport/signal transduction system transporters (appendix Table ap-2a, spots 48, 93 and 103) indicates an altered aminoacid metabolism. On one hand, a possible limitation entailing enhanced aminoacid uptake and, on the other hand different aminoacid requirements, downregulating branched-chain amino acids biosynthesis catalysed in part by KARI (Tyagi et al., 2005). Alteration of aminoacid metabolism has been reported before in *P. putida* KT2440 proteome in response to aromatic compounds like phenol (Santos et al., 2004) and chlorophenoxy herbicides (Benndorf et al., 2006).
Another protein upregulated at low dilution rate was Porphobilinogen deaminase (HemC, DE 3.41 ± 1.71, Figure 10, panel A) essential for the synthesis of *heme* precursors. Former work carried out in *P. aeruginosa* homolog genes *hemC* and *hemD*, affected *algD* promoter activity during growth on nitrate. The *algD* gene encodes NAD-linked GDPmannose dehydrogenase, essential for the mucoid phenotype, an important virulence factor expressed by *P. aeruginosa* that may protect bacterial cells in harsh environments (Mohr et al., 1994).

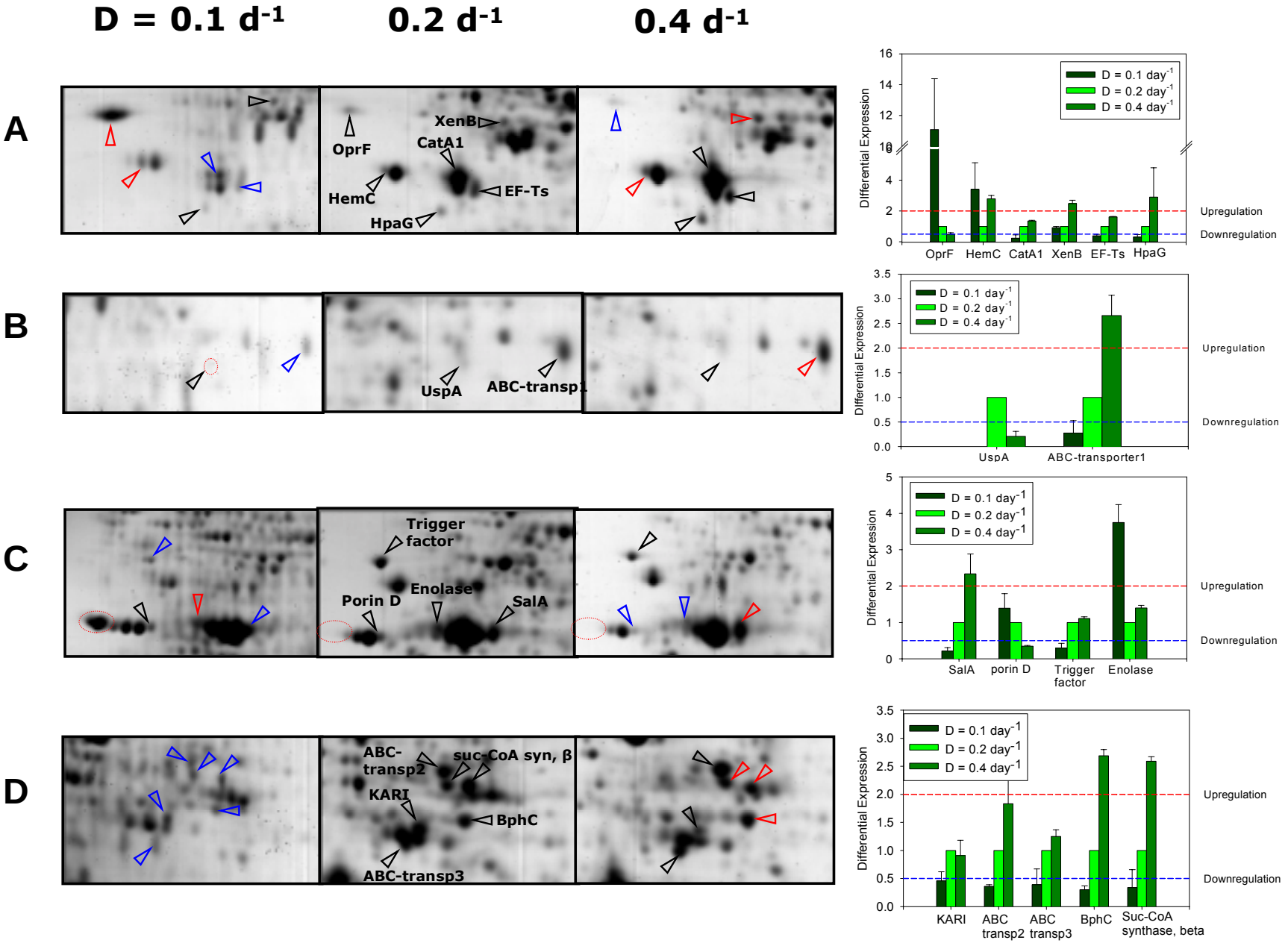

Figure 10. Selected proteome comparative views of *Pseudomonas* sp. MT1 continuous cultures at different dilution rates (*D*).

5.1.1.2 High dilution rate steady state continuous cultures of *Pseudomonas* sp. MT1

Nutrient insufficiency is perhaps the most common stress faced by microorganism in the environment (Harder & Dijkhuizen, 1983), where cells experience nutrient deficiency cycles disturbed by pulses of increased nutrient levels. Consequently, feast and famine cycles are and interesting way to analyze bacterial proteomic response. It is important to highlight that growth conditions though certainly improved from the original environmental situation, are in this case not comparable to traditional cultures with easy degradable carbon sources. Former studies on MT community have shown low growth rates for all consortia members (Rabenau, 2004) probably due to the intrinsic toxic xenobiotic nature of 4CS and particularly of the first degradative steps that involve toxic intermediates.

In order to compare the response of *Pseudomonas* sp. MT1 to higher substrate loads, continuous cultures were subject to a dilution rate of 0.4 d^{-1}. At this dilution rate, a significant increase in biomass was observed based on a substantial rise in turbidity values (0.320 ± 0.022 OD_{650}). However biomass, determined by plate counting did not show a proportional increase (5.62e08 ± 4.03e07 CFU/mL), indicating that alternative biomass determination methods should be included in order to accurately quantify the biomass concentration.

Under these conditions, a different metabolite profile was observed with higher levels of *cis*-dienelactone (22.81 ± 6.68 µM), four times higher than the concentration observed at a *D* of 0.2 d^{-1}, and slightly higher concentration of protoanemonin (17.69 ± 8.07 µM). Interestingly, a switch in concentrations was observed under current *D*, since *cis*-

dienelactone concentration was higher than protoanemonin, being the opposite at the reference (0.2 d^{-1}) and low (0.1 d^{-1}) *D* tested before.

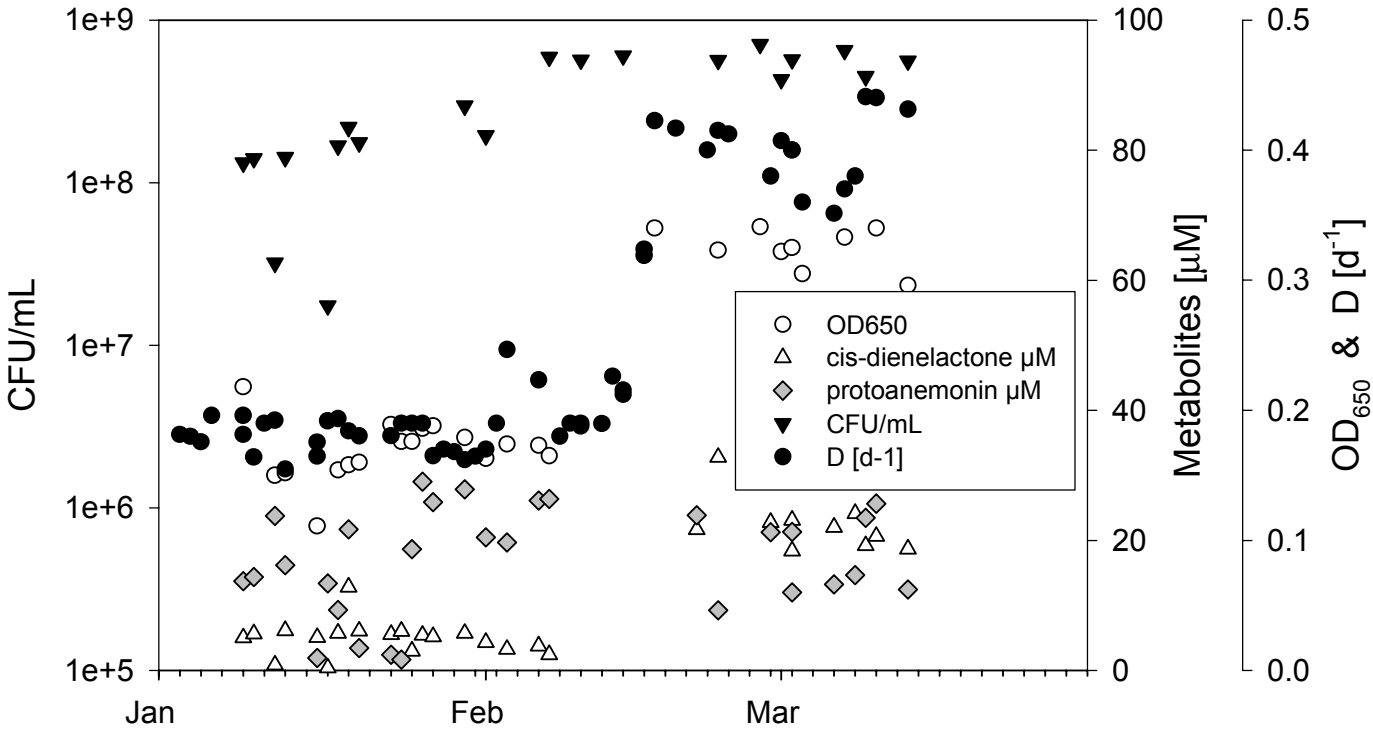

Figure 11. *Pseudomonas* sp. MT1 continuous culture monitoring (*D* = 0.2 and 0.4 d^{-1}, 30°C, pH 7.2, pO_2 >50%, minimal media M9, feeding solution 4CS 10 mM).

Under these conditions, higher expression levels were observed for the enzymes of the main catabolic pathway with upregulation of SalA (DE 2.34 ± 0.54) as well as parallel aromatic degradative routes (e.g., XenB DE 2.47 ± 0.23 and BphC DE 2.69 ± 0.11), as shown in Figure 10, panels A, C and D). Central metabolism identified enzymes, showed higher expression levels as expected, and upregulation was observed for succinyl-CoA synthase β subunit (DE 2.59 ± 0.08 Figure 10, panel D) and glyceraldehyde 3-phosphate dehydrogenase (DE 8.29 ± 0.06). Comparative proteome pattern analysis, showed upregulation of chaperonin GroEL and Cpn10 (appendix Table ap-2a, spots 99 and 106) while oxidative stress proteins were non-differentially

expressed. The chaperonin GroES, the cpn10 from *E. coli*, interacts with GroEL (cpn60) assisting the folding of cytosolic proteins, an essential function for bacterial growth (Fayet et al., 1989).

Particularly interesting was the upregulation of a different set of extracellular solute-binding proteins (appendix Table ap-2a, spots 42, 47 and 52, Figure 10 panels B and D) compared to low dilution rate experiences, indicating different transport requirements under the current culture condition. Moreover, outer membrane proteins OprF and porin D were downregulated (DE 0.49 ± 0.10 and 0.35 ± 0.02, respectively. Figure 10, panels A and C), supporting the hypothesis of facilitated diffusion of 4CS mediated by outer membrane porins as an important mechanism for substrate uptake in *Pseudomonas* sp. MT1 under low substrate feeding rates.

5.1.2 *Pseudomonas* sp. MT1 and *Achromobacter xylosoxidans* strain MT3 steady state cultures

While analyzing the proteome of strain MT1 under different dilution rates, a parallel analysis was carried out at mixed continuous cultures of strains MT1 and MT3. To do so, a pure continuous culture of *Pseudomonas* sp. MT1 was inoculated with strain MT3 after steady state achievement. Mixed culture monitoring at the reference dilution rate of 0.2 d^{-1} showed an apparent higher biomass content with similar CFU counts (1.39e08 ± 9.11e07 CFU/mL) but higher turbidity (0.326 ± 0.073 OD_{650}) with respect to pure MT1 cultures. Quantification of specific CFU for MT1 and MT3 showed a proportion of 90% strain MT1 and 10% strain MT3 but required a confirmation by culture independent techniques. Metabolite profile did not show variations in the metabolites detected, with similar concentration levels of *cis*-dienelactone (5.94 ± 0.63 µM) and protoanemonin

(13.84 ± 1.90 µM) compared to those observed in single MT1 cultures under equivalent conditions. For mixed cultures only low dilution rate of 0.1 d^{-1} was compared to the reference condition, analyzing biomass content, metabolic profile as well as the proteomic pattern. Differential expression (DE) was evaluated from at least three independent protein extracts, analyzed after 2-DE and comparative proteome pattern against a reference condition was performed as described in section 4.8.5.

5.1.2.1 Low dilution rate steady state continuous community cultures of *Pseudomonas* sp. MT1 and *Achromobacter xylosoxidans* strain MT3

Mixed continuous cultures of strains MT1 and MT3 at a dilution rate of 0.1 d^{-1} presented lower biomass content determined by plate counting (1.19e08 ± 4.13e07 CFU/mL) and turbidity measurements (0.254 ± 0.050 OD_{650}), compared to the reference community culture at a *D* of 0.2 d^{-1}. Dead-end metabolites protoanemonin and *cis*-dienelactone also showed reduced concentrations (11.36 ± 2.34 and 3.61 ± 0.30 µM, respectively).

Proteome analysis showed downregulation of some of the upper degradation enzymes of the main degradative pathway (SalA DE 0.37 ± 0.03 and CatA2 DE 0.23 ± 0.05, Figure 12, panel A and B). However, CatA1 showed non-differential expression (DE 0.86 ± 0.01) showing a different expression pattern compared to analog MT1 pure culture. Parallel aromatic catabolic pathways were not differentially expressed with the sole exception of 3-carboxymuconate cycloisomerase that was downregulated (DE 0.20 ± 0.11) and remarkably HpaG, that was highly upregulated (DE 17.93 ± 2.76, Figure 12, panel A). Interestingly, an upregulation of a reductase component of salicylate 5-hydroxylase was observed in mixed cultures, indicating that the presence of strain MT3

modifies the protein expression pattern of strain MT1, enhancing the role of parallel pathways in mixed cultures at the low dilution rate of 0.1 d^{-1}.

Identified proteins involved in central metabolism showed downregulation (e.g., ATP synthase α and β subunits DE 0.16 ± 0.10 and 0.47 ± 0.15, respectively). Enolase was downregulated, with a DE of 0.44 ± 0.22, suggesting that central metabolism fluxes are possibly reduced due to lower carbon load.

Changes in the expression levels of proteins of the general stress response group, namely bacterial elongation factor EF-Tu and EF-Ts were observed. EF-Tu was upregulated (DE 2.47 ± 0.36) while EF-Ts was downregulated (DE 0.48 ± 0.05). These elongation factors are interacting proteins involved in polypeptide chain elongation in protein biosynthesis. EF-Tu may be implicated in protein folding and protection from stress, showing chaperone activity *in vitro* (Caldas, et al., 1998). In *Delftia acidovorans*, the response to chlorophenoxy acid stress showed upregulation of one isoform of EF-Tu (TufA) and downregulation of another isoform (Benndorf et al., 2004). Since these effects were not observed in pure cultures of strain MT1, it is possible to argue that the presence of strain MT3 creates environmental signals sensed by strain MT1 that goes beyond the mere variations in upper degradative pathways but more into whole cell behavior.

At low dilution rate, from the identified oxidative stress proteins, SOD1 was the only one upregulated (DE 5.40 ± 0.08, Figure12, panel C), while SOD2 showed high expression levels at all dilution rates tested. SMP-30 was downregulated (DE 0.47 ± 0.31, Figure 12, panel D) and no variation in AhpC isoforms was observed, suggesting a possible higher concentration of ROS in mixed cultures compared to analog MT1 culture under low dilution rate of 0.1 d^{-1}.

Following the behavior of strain MT1 in low dilution rate cultures, strains MT1 and MT3 community culture showed upregulation of HemC (DE 2.10 ± 1.36, Figure 12, panel A). However, a difference was observed in the levels of protein FliS, that showed a different pattern being downregulated in the mixed culture (DE 0.40 ± 0.34, Figure 12, panel C). FliS is a chaperone protein that prevents the premature polymerization of flagellin, the main component of flagellar filaments (Muskotal et al., 2006). Chaperone FliS mutant strains of *Campylobacter jejuni*, presented a reduced capacity to form flocs, a known growth form that confers protection against environmental stress (Joshua et al., 2006).

Once more, outer membrane proteins as well as transporters showed a significant variation in their expression. OprF was highly overexpressed (DE 5.79 ± 1.68, Figure 12, panel A) and a series of transporters were upregulated (appendix Table ap-2b, spots 48, 52 and 109), being a different set compared to those overexpressed in pure MT1 culture. As it was observed in pure strain MT1 continuous cultures run at low dilution rate, a MFS permease was *de novo* synthesized (Figure 12, panel B, red circled).

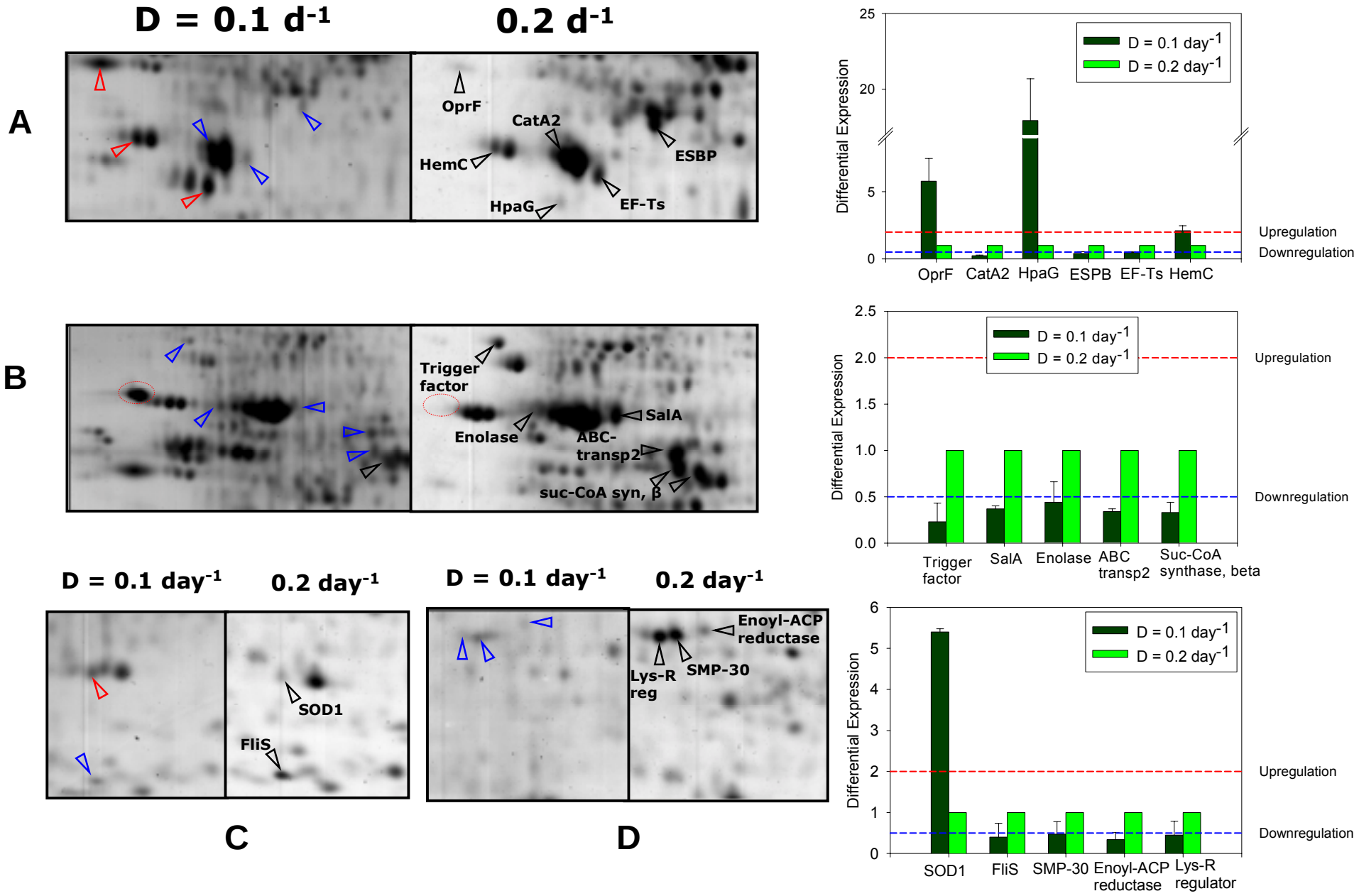

Figure12. Selected proteome comparative views of *Pseudomonas* sp. MT1 and *Achromobacter xylosoxidans* MT3 in mixed continuous cultures at two different dilution rates (*D*).

5.1.3 Comparison of steady state pure cultures of *Pseudomonas* sp. MT1 and community culture of *Pseudomonas* sp MT1 and *Achromobacter xylosoxidans* MT3 at the low dilution rate of 0.1 d^{-1}.

Due to the toxic intermediates produced in the 4CS degradation pathway in *Pseudomonas* sp. strain MT1, together with the low generation times of the strains used under present culture conditions, slow dilutions rates have been used in this study. At the lower 0.1 d^{-1} dilution rate, pure MT1 culture showed 2.36e08 ± 8.29e07 CFU/mL associated to an OD_{650} of 0.183 ± 0.051, while mixed culture of strains MT1 and MT3 presented an OD_{650} of 0.254 ± 0.050 with a corresponding 1.19e08 ± 4.13e07 CFU/mL value. This variation in culture turbidity, without the corresponding CFU increase, could be explained by the generation of metabolites in the mixed culture, such as polymers that could increase the optical density or also by an increase in the number of viable but not cultivable cells within the community. Metabolite concentration was similar in both cultures for *cis*-dienelactone (2.07 ± 1.32 µM for MT1 and 3.61 ± 0.30 µM for MT1 and MT3 cultures) but significantly lower levels of protoanemonin where detected in the community culture (24.36 ± 3.27 µM for MT1 and 11.36 ± 2.34 µM for mixed culture). It is possible to speculate that the carbon source could be more efficiently routed in the mixed culture, due that protoanemonin production is characteristic from degradation misleading of chloromuconates by enzymes of the 3-oxoadipate pathway (Blasco et al., 1995), since no direct proof of protoanemonin degradation has been obtained for strains MT1 and MT3.

An interesting proteomic scenario was registered using a lower dilution rate of 0.1 d^{-1}, showing the upregulation and *de novo* synthesis of outer membrane proteins and transporters as well as induction of parallel aromatic catabolic pathways.

A direct comparison between pure and community cultures under the lowest *D*, showed an important difference in the proteome pattern. Mixed culture presented downregulation of SalA (DE 0.23 ± 0.05, Figure 13, panel B) with respect to pure MT1 culture, with simultaneous upregulation of CatA2, indicating that both enzymes are apparently under different regulatory networks in *Pseudomonas* sp. MT1. Moreover, the community culture showed overexpression of parallel aromatic degradative pathways, with upregulation of Sal5 and HpaG (DE 2.33 ± 0.70 and 3.73 ± 0.66, respectively), proteins that are close related to the gentisate degradative pathway, unexpectedly induced at low dilution rates and enhanced by the presence of *A. xylosoxidans* MT3. Also XenB was upregulated in the mixed culture (DE 2.64 ± 0.90, Figure 13, panel A).

At the central metabolism a general dowregulation was observed in the community culture (ATP synthase DE 0.36 ± 0.01 and Succinyl-CoA synthase β subunit DE 0.21 ± 0.12, Figure 13, panel B) with the sole exception of glyceraldehydes 3-phosphate dehydrogenase that was overexpressed (DE 3.88 ± 0.82). However, it was not straight forward to infer a lower fitness of the mixed culture, since biomass content was comparable as shown above, and identified proteins related to cell division where upregulated, such as DNA polymerase III δ subunit (DE 2.27 ± 0.58, Figure 13, panel B) and cell division protein FtsA (DE 2.78 ± 0.78). In proteobacteria only DNA polymerase III holoenzyme plays a major role in chromosomal replication (Kelman & O'Donnell, 1995) and FtsA has been shown to be essential for bacterial cell division (Jensen et al., 2005).

A similar protein pattern was obtained in both cultures concerning general and oxidative stress proteins with only an observable differential expression of EF-Ts that was

downregulated in the community with respect to the single strain culture (DE 0.32 ± 0.02).

A major difference was observed at the outer membrane and transporters group where transporters of the extracellular solute-binding family 3 protein were downregulated (spots 52 and 65, Figure 13, panel B) as well as outer membrane proteins in the mixed culture. Porin D presented a DE of 0.30 ± 0.20 and OprF expression was significantly reduced (DE 0.18 ± 0.15, Figure 13, panel A).

5.1.4 Comparison of steady state pure cultures of *Pseudomonas* sp MT1 and mixed culture of *Pseudomonas* sp MT1 and *Achromobacter xylosoxidans* MT3 at reference dilution rate of 0.2 d^{-1}.

A reference dilution rate of 0.2 d^{-1} was set based on previous studies (Pelz et al., 1999). Under this dilution rate, there were significant variations when pure strain MT1 and mixed strains MT1 and MT3 cultures were compared. Biomass concentration determinations showed an inconsistency when plate counting was compared to optical density measurements. While pure MT1 continuous cultures gave an average of 7.24e08 ± 1.29e08 CFU/mL associated to an OD_{650} average value of 0.197 ± 0.066, mixed strains culture gave slightly lower results on plate counting (1.39e08 ± 9.11e07 CFU/mL) but significantly higher average optical density (OD_{650} 0.326 ± 0.073).

Incorporation of total, dead and alive cell counts per mL determinations by standardized Fluorescence Assisted Cell Sorting (FACS) as described in section 2.7.1, established that under current culture conditions, pure MT1 culture presented a stable total cells count per mL of 6.2e08 ± 1.4e07, including 5.7e08 ± 1.9e07 live (91.9%) and 2.3e07 ±

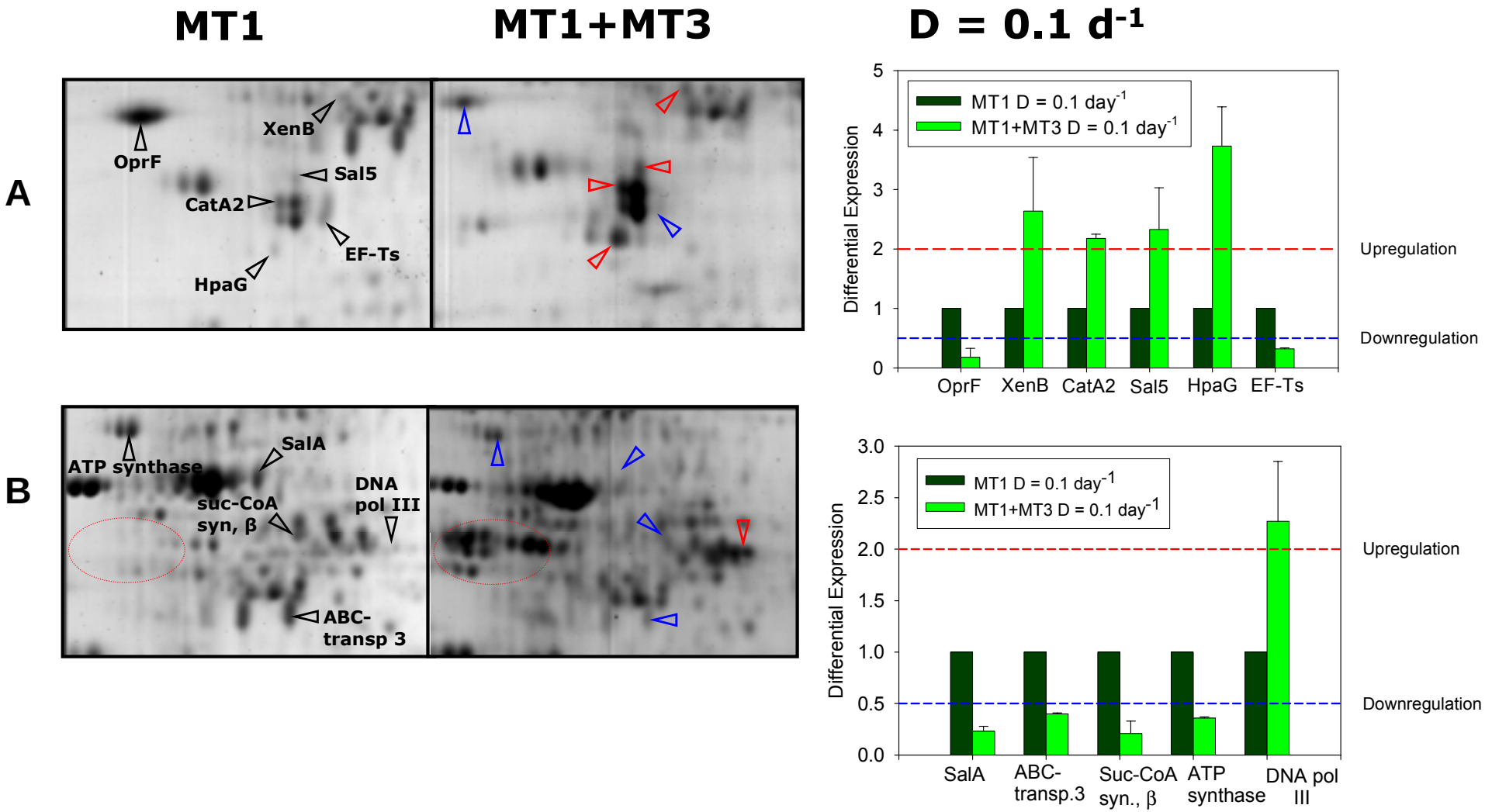

Figure 13. Selected proteome comparative views of pure *Pseudomonas* sp. MT1 and mixed *Pseudomonas* sp. MT1 with *Achromobacter xylosoxidans* MT3 steady state continuous cultures at a dilution rates of 0.1 d^{-1}.

3.6e06 dead (3.7%) cell counts/mL. Under the same conditions, strains MT1 and MT3 community culture presented a stable total amount of 7.2e08 ± 4.1e07 with 6.0e08 ± 3.2e07 (83.3%) live and 3.8e07 ± 1.1e07 (5.3%) dead cell counts/mL, showing no significant difference in biomass content between the cultures.

Comparing pure and community continuous cultures under these conditions, identified enzymes of the main degradative upper pathway were non-differentially expressed, as well as parallel catabolic pathways. Exceptions were proteins HpaG (DE 0.48 ± 0.09, Figure 15, panel B) and CatJ β subunit (DE 0.32 ± 0.15) that were downregulated (Figure 15, panel D). An interesting difference was observed for 3-oxoadipate enol-lactonase (CatD) that was *de novo* synthesized in the community

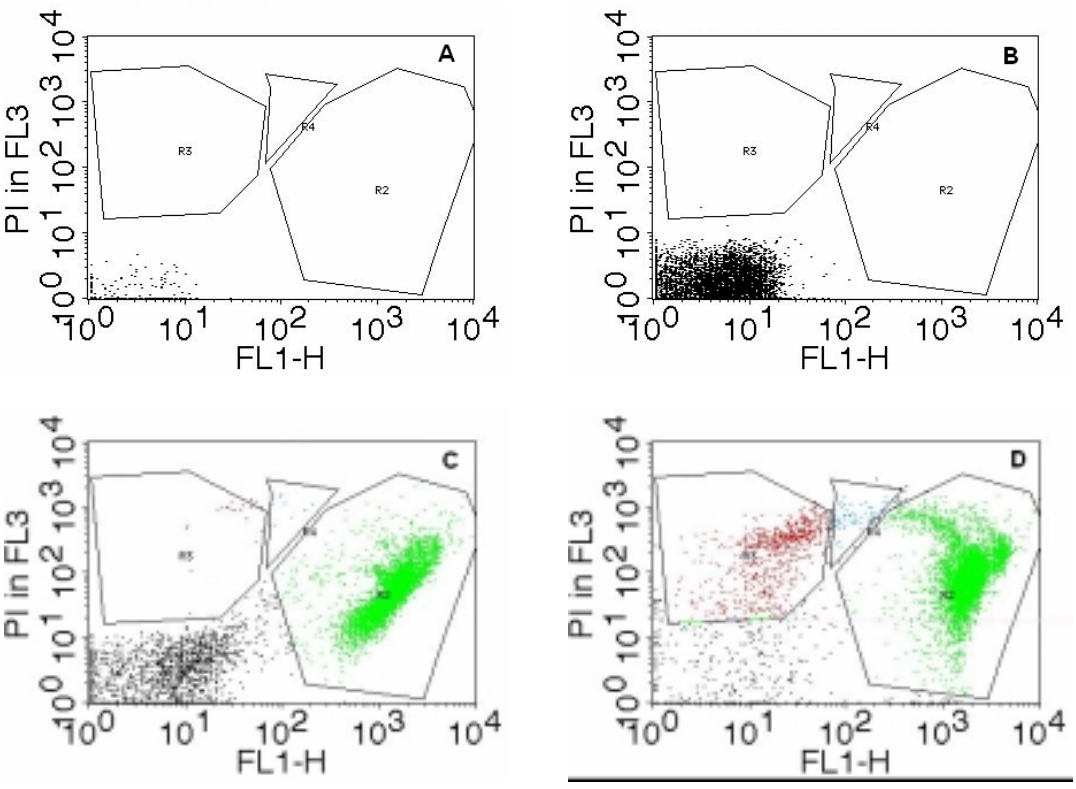

Figure 14**.** Total, live and dead cell determination. Panel A: filtered PBS solution + TWEEN (0.01%)). B: Cells without staining. C: Total cells (gate R2) stained with thiazole orange. D: Dead cells (gate R3) & Live cells (gate R2) stained with a mixture of thiazole orange and propidium iodide.

culture (Figure 15, panel D, red circled). CatD is an enzyme of the 3-oxoadipate pathway that catalyze the transformation of 3-oxoadipate enol-lactone to 3-oxoadipate. It has been associated to both catechol (Shanley et al., 1986) and protocatechuate pathways (Hughes et al., 1988).

Among the proteins that were upregulated, an uncharacterized conserved hypothetical protein (gi|23467370) showed the highest variation with a DE of 6.37 ± 1.99 (Figure 15, panel B). This protein shares conserved domains with the pseudouridine synthase, TruD family with 39% identity with Pseudouridylate synthase of *Pseudomonas fluorescens* PfO-1 (gi|62901246), involved in rRNA and tRNA biosynthesis (Sunita et al., 2006). In regards to stress proteins – both general and oxidative – no major variations were observed in the identified proteins of this group with the exception of chaperone Cpn10 that was upregulated in the mixed culture (DE 2.73 ± 0.79, Figure 15, panel C).

Analyzing the expression pattern of transporters and outer membrane proteins, the community culture showed downregulation of OprF (DE 0.47 ± 0.07, Figure 15, panel B) and ABC-type transporters spots 48 and 109 (DE 0.41 ± 0.03 and 0.35 ± 0.31, respectively). Conversely, porin D was upregulated (DE 2.43 ± 0.02, Figure 15, panel A) as well as transporter spot 103 (DE 3.86 ± 1.80). Furthermore, a TctC transporter was *de novo* synthesized (Figure 15, panel B, red circled). TctC belongs to the tripartite tricarboxylic transporters (TTT) family of multicomponent uptake and efflux systems. TctC in *Salmonella typhimurium* corresponds to a periplasmic tricarboxylate binding receptor and *P. putida* posses one homolog (gi|26988151) (Winnen et al., 2003). Interestingly, TctC contains a conserved domain of the *Bordetella* uptake gene (BUG) that includes a series of extra-cytoplasmic solute receptors from β-proteobacteria (Antoine et al., 2003) that can be related to proteins expressed in strain MT3.

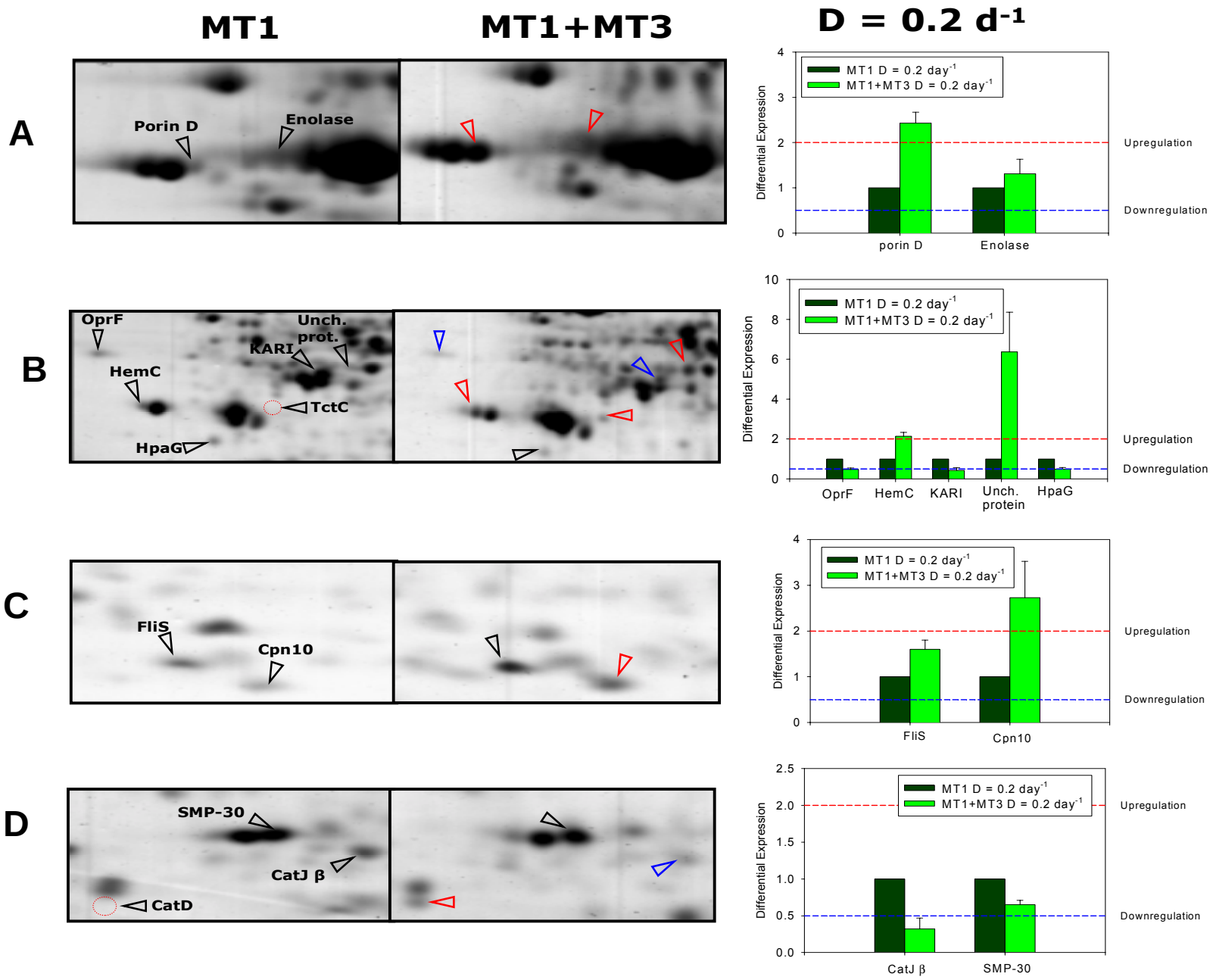

Figure 15. Selected proteome comparative views of pure *Pseudomonas* sp. MT1 and mixed *Pseudomonas* sp. MT1 with *Achromobacter xylosoxidans* MT3 steady state continuous cultures at a dilution rate of 0.2 d^{-1}.

5.1.5 Discussion overview of steady state cultures

A significant amount of proteins were identified with statistical significance during the study of *Pseudomonas* sp. MT1 steady state cultures. In several cases PMF was not specific enough, and *ab initio* sequencing coupled to peptide sequence homology search showed to be a powerful tool to identify proteins in non-sequenced organisms.

MT1 steady state cultures showed the characteristic inducible expression of aromatic catabolic enzymes. At low dilution rates, enzymes showed a general trend, being less expressed and in some cases even downregulated. Similar pattern was shown for parallel aromatic degradative pathways. However, in the presence of *A. xylosoxidans* MT3, the expression of a second pathway under a *D* of 0.1 d^{-1} was remarkably different. High levels of Sal5 and an 18-fold upregulation of HpaG, indicate that alternative carbon routing in the upper pathway possibly play an important role in the community under extreme carbon limiting conditions.

At the different *D* tested, the pure culture showed variations in transporters and outer membrane proteins. Perhaps the most interesting one was OprF. Its 11-fold increment in pure culture, at the lowest *D* used, while central metabolism activity seemed to be depressed, suggests that this major outer membrane protein plays a key role under these circumstances due to its inherent transport capacity, controlling the outer membrane permeability to a some extent. It is possible that OprF concentration increment, facilitates substrate diffusion into the cell, improving fitness under severe carbon limiting states. At a higher dilution rate, simple diffusion governs the transport of substrate and consequently OprF expression is reduced. Interestingly, a similar behavior was observed in the presence of *A. xylosoxidans* MT3, where OprF is also upregulated at lower *D*. Nevertheless, overexpression of OprF reached only a 6-fold

increment in the community culture, with a parallel increase in porin D. This corresponds to a significant change in the outer membrane composition, probably due to changes in the cell's environment and consequently to an alteration of the cell's requirements.

Taken together, HpaG upregulation and OprF downregulation, comparing pure and mixed cultures run at a low *D*, it is possible to speculate that at low 4CS loads, the community could benefit through the downregulation of the main degradative pathway and the simultaneous activation of parallel pathways, preventing the useless formation of protoanemonin, since its synthesis can be considered as a 'carbon waste'. If this is the case, the presence of strain MT3 may trigger parallel pathways in strain MT1, possibly through the generation of highly active inducers, improving the community fitness and reducing the accumulation of toxic intermediates. Consequently, only mild oxidative stress was observed in the mixed culture. The difference in the expression levels of OprF can be an outcome of starvation induction, which could be partially overcome in the mixed culture.

In summary, this study carried out in steady state cultures, shows that minor concentrations of a second community member (the proportion of *A. xylosoxidans* MT3 was only 10% as determined by specific CFUs) can have important effects on the protein expression levels of the most abundant community member, altering its metabolic performance as shown by the differences in the proteome and the metabolite profile.

5.2 Dynamic State Cultures

As previously stated, bacterial role in natural environments is fundamental to preserve the systems under equilibrium. Under most environmental conditions, bacteria face nutrient limiting stress disturbed by nutrient abundant events in the so-called feast and famine cycles (Kovarova-Kovar & Egli, 1998). Therefore, in order to understand the MT community response to drastic variations in substrate availability, carbon-limiting continues cultures under steady state were switched to batch mode and subject to 4CS shock loads, being monitored at constant time intervals for population dynamics and metabolite profile. Proteomic analysis was restricted to particularly interesting dynamic states.

5.2.1 Metabolic profile of *Pseudomonas* sp. MT1 dynamic state cultures

Steady state continuous cultures of *Pseudomonas* sp. MT1 run at a dilution rate of 0.2 d^{-1} were subject to independent 4CS shock load events in the range of 0.5 to 8 mM. Several replicates were performed at different concentrations and a representative set of experiences are shown on Figure 16. Interestingly, the average rate of degradation of 4CS showed a relatively constant value within the range from 0.5 to 3 mM. At concentrations higher than 3 mM, the degradation rate dramatically decreased and the biomass concentration, evaluated by plate counting and OD_{650} , was reduced. Within the range 0.5 – 3 mM, the degradation of 4CS was constantly monitored at several time intervals for substrate as well as metabolites, in all concentrations tested (Figure 16). Degradation rates, were determined from progress curve analysis and the kinetic

parameters were obtained by non-linear regression assuming simple Michaelis-Menten kinetics (Figure 17).

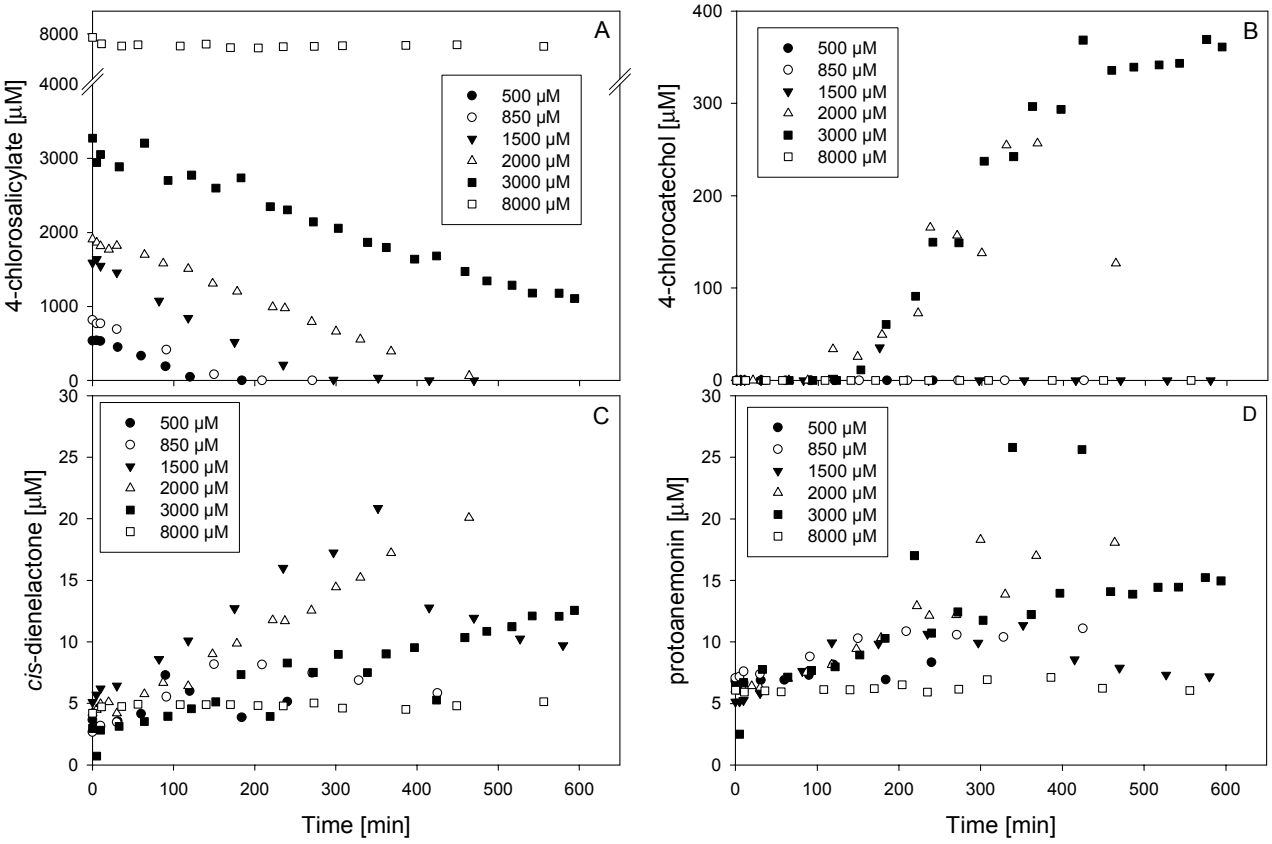

Figure 16. Depletion of 4CS (panel A) and formation of 4CC (panel B), *cis*-dienelactone (panel C) and protoanemonin (panel D) in steady state continuous cultures of *Pseudomonas* sp. MT1 subject to batch conditions at different shock loads of substrate.

Under the dynamic state created by substrate pulses, it was possible to observe not only products but more metabolites of the upper degradation pathway of 4CS. 3-chloromuconate (3CM) was detected up to a concentration of 50 µM, but no clear trend was observed (data not shown), showing intermittent levels probably due to its intrinsic instability (Kaulmann et al., 2001). Transient accumulation of 4CC, one of the most toxic intermediates of the main catabolic pathway, was consistently detected in shock loads

with a substrate concentration of 2 mM. Concentrations above 2 mM showed higher levels of 4CC, and the cultures turned dark impeding any further analysis. Moreover, a 4CS shock load performed at a concentration of 8 mM, showed no detectable substrate degradation and constant levels of dead-end products without detection of any other metabolite with the analytical techniques used, indicating that 4CS can be directly toxic, inhibiting growth at this concentration.

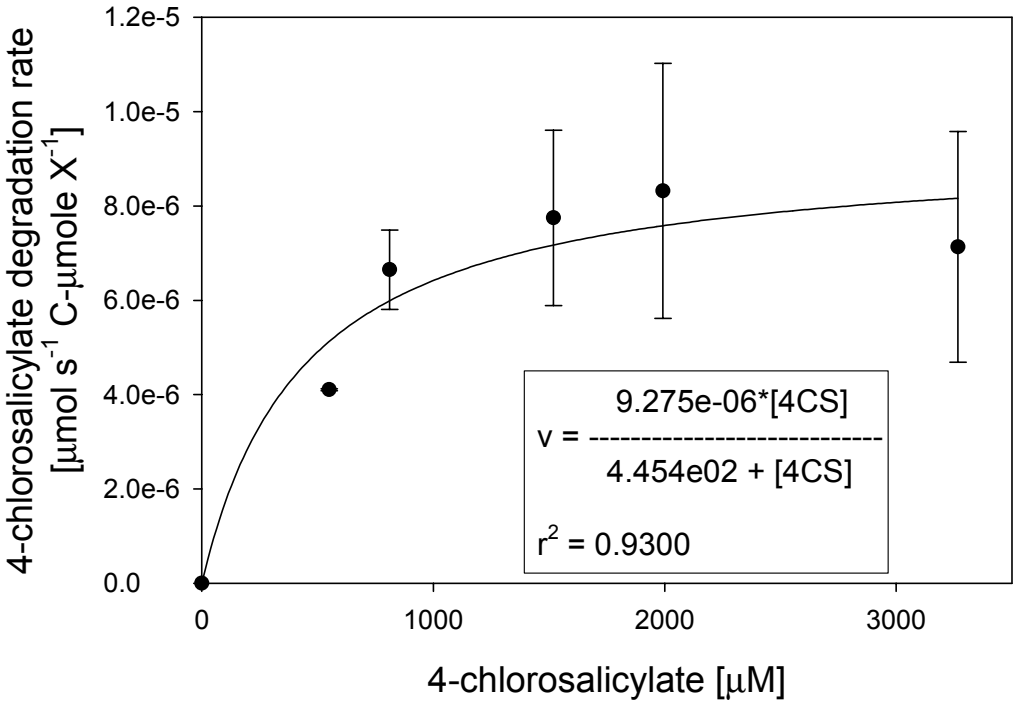

Figure 17. Rates of degradation of 4CS under different shock loads of substrate. Box shows the non-linear regression assuming Michaelis-Menten kinetics.

No clear trend was observed for the accumulation of dead-end metabolites, *cis*-dienelactone and protoanemonin. A constant increase was observed in all shock loads, but the final concentration was not proportional to the substrate load, indicating that the initial concentrations condition their accumulation.

The transient appearance of 4CC in pure cultures of strain MT1, up to a concentration of 250 µM, reported to be high enough to cause damage in the cellular membrane and uncoupling of the oxidative phosphorylation process by chlorinated catechols in *E. coli* (Schweigert et al., 2001a), was considered as a transient sub-lethal stress state, and a condition for further protein expression analysis in both pure and community cultures.

5.2.2 *Pseudomonas* sp. MT1 shock load stress dynamic state proteomics

Based on the observed metabolite profiles described previously, a sub-lethal shock load stress of 2 mM 4CS was performed on a steady state continuous culture of strain MT1 when switched to batch mode. Before and during the shock load, proteins were extracted at several time intervals (2, 5 and 7 h after shock load) according to the metabolite profile evolution. Triplicate cultures were monitored for proteomics, metabolite profile and population dynamics analyzed by dead & alive staining coupled to FACS quantification.

The metabolite analysis before the shock load, showed stable concentrations of *cis*-dienelactone and protoanemonin, as described before for current culture conditions. During the shock load, high levels of protoanemonin up to a concentration of 190 µM were detected, while *cis*-dienelactone showed no major variation with a maximum of 11.6 µM, both concentration peaks were observed 6 h after substrate addition. 4CC reached a maximal concentration of 240 µM at 4 h, being totally degraded two hours after. 4CS was completely removed from the cultures after 6 h, and monitoring was stopped at 7 h.

Population dynamics, showed and average initial total of 5.87e08 ± 1.74e07 with 5.48e08 ± 1.41e07 (93.4%) live and 3.76e07 ± 3.40e06 (6.4%) dead cell counts/mL.

These values were not significantly altered throughout the shock load as shown in Figure 18, panel A. Average final total cell counts per mL, after total 4CS and 4CC depletion were 6.18e08 ± 9.96e06 composed of 5.91e08 ± 7.08e06 (95.6%) live and 3.46e07 ± 1.11e07 (5.6%) dead cell counts/mL. The observed values clearly show that the cultures reached concentrations of toxic metabolites, protoanemonin and 4CC, previously reported to be enough to inhibit bacterial growth, were sub-lethal for *Pseudomonas* sp. MT1 under the culture conditions tested. It is important to stress that the antibiotic effect of protoanemonin has been tested with *Pseudomonas* strains with values reported for IC_{50} (50% inhibitory concentration) in the range from 60 to 800 μM, where *P. putida* KT2440 was the most resistant strain tested (Blasco et al., 1995).

As in prior proteomic analysis, differential expression of the identified enzymes of the main catabolic pathway of 4CS was first assessed. SalA showed no differential expression throughout the shock load. From the two catechol 1,2-dioxygenases, CatA1, was expressed at lower levels compared to initial conditions but only downregulated 7 h after the shock load (DE 0.32 ± 0.18). In the case of CatA2, downregulation was observed at both 2 h (DE 0.46 ± 0.09) and 7 h (DE 0.25 ± 0.15) after the shock load (Figure 19, panel A). Conversely, protein CatJ subunit α showed upregulation at all times after the shock load being highest at 2 h (DE 3.02 ± 0.21 at 2h, Figure 19,panel D). From the parallel aromatic degradative pathways, only XenB showed a consistent expression pattern, being upregulated throughout the shock load with a peak in DE of 4.67 ± 0.88 observed at 7 h (Figure 19, panel B).

Several of the central metabolism proteins identified presented lower expression levels, with downregulation of enolase (DE 0.38 ± 0.04), acetoacetyl-CoA reductase (0.37 ± 0.07) and citrate synthase (0.41 ± 0.21) at 2 h, being only F0F1-type ATP synthase α

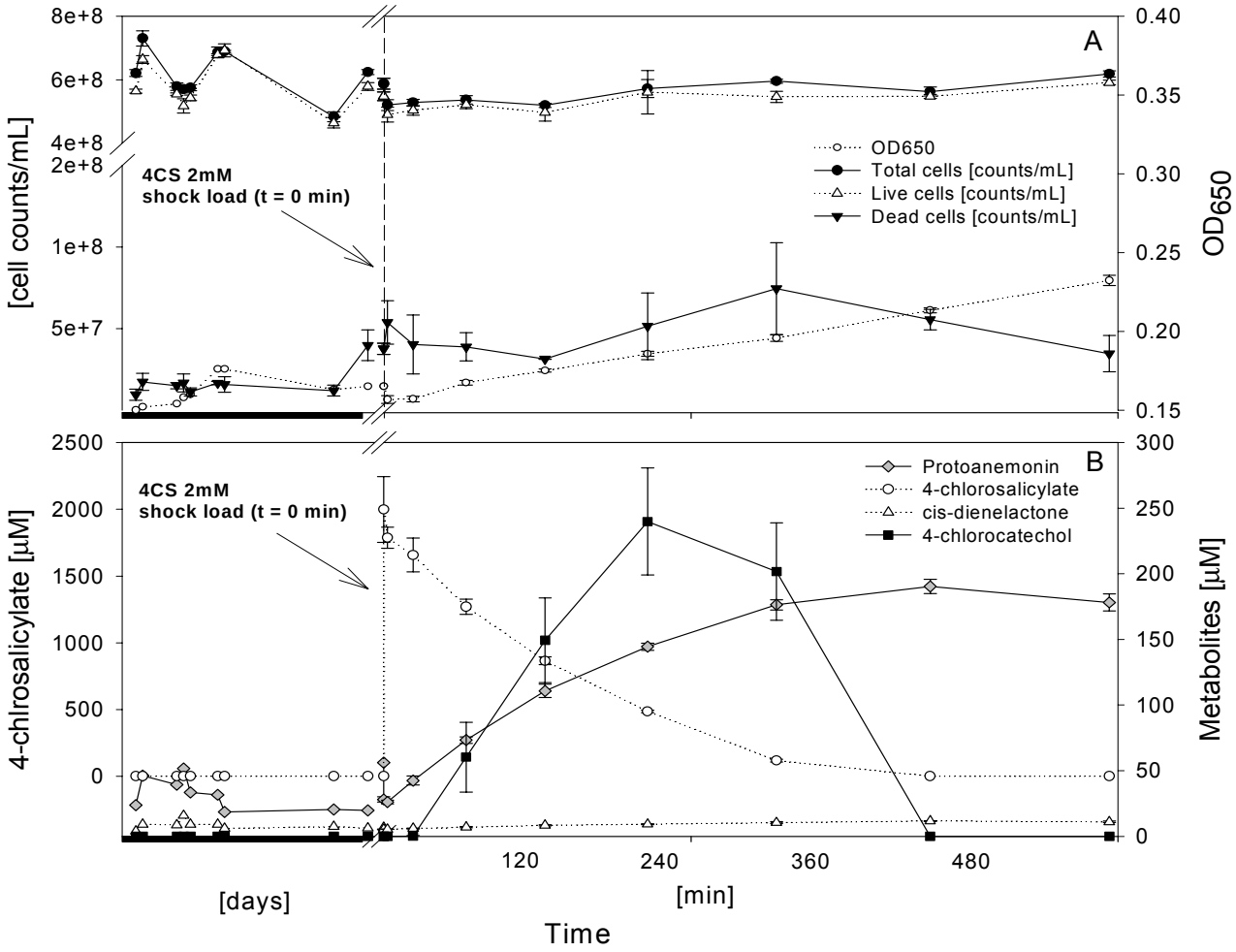

Figure 18. *Pseudomonas* sp. strain MT1 continuous culture monitoring before and during a 2mM 4CS shock load stress. A: population dynamics. B: metabolic profile.

subunit upregulated (DE 2.50 ± 0.23) at 2 h. However, the expression level of enolase varied during the shock load response, being upregulated with a highest DE of 7.91 ± 1.39 at 5 h. At the same time acetoacetyl-CoA reductase reached its lowest DE of 0.17 ± 0.15.

A significant variation in expression was observed in identified enzymes related to cell envelope biogenesis. Enoyl-[acyl-carrier-protein] reductase showed a constant

upregulation at all analyzed time intervals after the shock load, with a maximum DE of 4.81 ± 1.19 at 7 h (Figure 19, panel A). Moreover, an acyl-carrier protein phosphodiesterase (AcpH) was *de novo* synthesized (Figure 20). AcpH is a non-essential protein involved in fatty acid biosynthesis found only in Gram-negative organisms (Thomas & Cronan, 2005), suggesting a possible physiological role in lipid A biosynthesis, a major component of the Gram-negative's outer membrane (Vaara, 1996).

An important differential expression was also observed in proteins belonging to the general and oxidative stress response. UspA was less expressed during the shock load compared to initial conditions, being downregulated from 5h on (minimum DE 0.23 ± 0.06 at 7 h). In contrast, EF-Tu and chaperone protein Cpn10 were upregulated at all analyzed time intervals (highest DE of 5.60 ± 1.30 at 5 h and 4.31 ± 0.41 at 2h, respectively, Figure 19, panels B and C). Also chaperon FliS showed higher expression levels during the shock load, being maximally upregulated at 7 h (DE 4.72 ± 0.05, Figure 19, panel C).

Oxidative stress response protein AhpC isoforms 1 and 2 were highly upregulated, reaching a maximum DE of 10.43 ± 1.09 and 5.69 ± 1.20 at 5h, respectively, together with an hydrogen peroxide-inducible gene activator (OxyR) that showed upregulation with a maximum DE of 12.57 ± 1.68 at 7 h (Figure 19, panel D). SMP-30, apparently linked to oxidative stress response was downregulated throughout the shock load, showing a minimum DE of 0.18 ± 0.06 at 7 h (Figure 19, panel A). The observed expression pattern of general stress proteins, in concert with the high expression levels of oxidative stress response proteins, demonstrate that 2mM 4CS shock load generates a sub-lethal stress condition in *Pseudomonas* sp. MT1 with the intermediate 4CC as a

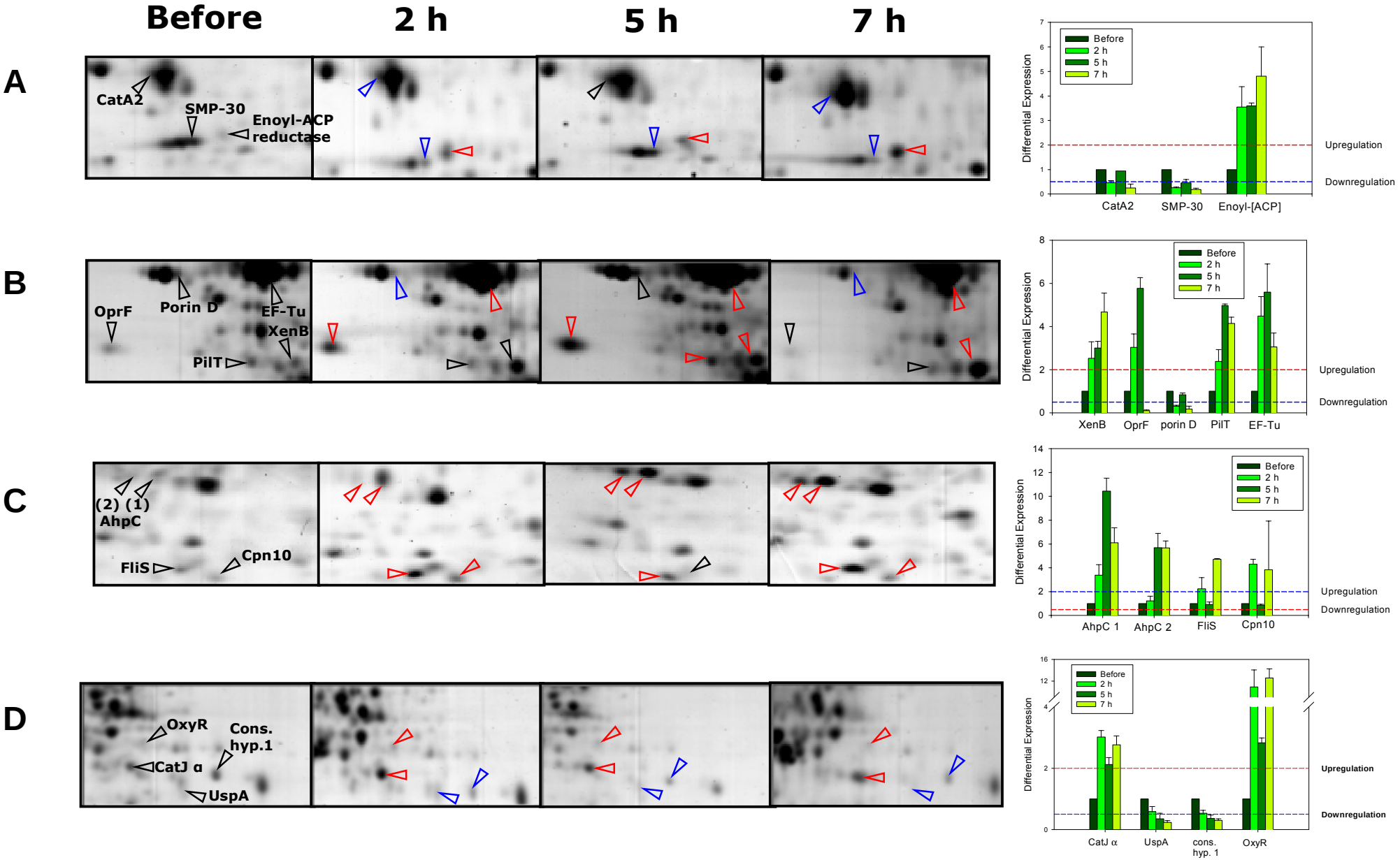

Figure 19. Selected proteome comparative views of continuous culture of *Pseudomonas* sp. strain MT1 exposed to 2mM 4CS shock load.

major stressor, since the highest expression levels of this protein group was associated to its maximum transient concentration around 5 h after the shock load.

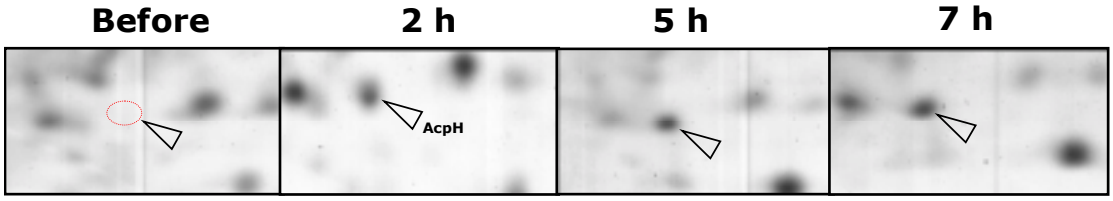

Figure 20. *De novo* synthesis of Acyl-carrier protein phosphodiesterase (AcpH) during 2 mM 4CS shock load stress in *Pseudomonas* sp. MT1.

Particularly interesting are the observations of the outer membrane and transporter groups of proteins identified. ABC-type amino acid transport/signal transduction systems showed a selective expression pattern being spots 103 and 126 upregulated (highest DE 5.31 ± 3.12 at 7 h and 12.15 ± 4.28 at 2 h, respectively), while spot 52 was downregulated at all time intervals analyzed (lowest DE 0.26 ± 0.07 at 7 h). Major outer membrane protein OprF was upregulated at 2 and 5 h after the shock load, with a maximal DE of 5.77 ± 0.50 at 5 h, and downregulated at 7 h (DE 0.10 ± 0.03, Figure 19, panel B). These observations puzzled the hypothesis of facilitated diffusion role of OprF as an important uptake mechanism of 4CS by *Pseudomonas* sp. MT1, since its upregulation was previously related to substrate-limiting conditions in continuous cultures. Therefore, OprF expression is probably related to complex regulatory events, triggered by substrate availability under the different conditions tested. On the other hand, porin D was intermittently downregulated with a minimum DE of 0.17 ± 0.14 at 7 h (Figure 19, panel B). Another outer membrane related protein, a YceI precursor, was consistently upregulated during the shock load with a highest DE of 4.84 ± 0.63 at 5 h. YceI corresponds to a non-characterized periplasmic protein that has been reported to be overexpressed in *E. coli* under pH stress (Stancik et al., 2002) and in *Delftia acidovorans* MC1 proteomic response to chlorophenoxy herbicides stress (Benndorf et al., 2004).

Another protein that showed an interesting expression pattern was PilT, an ATPase responsible for the retraction of type IV pili related to 'twitching motility', a motion mechanism of bacteria in low water environments (Chiang et al., 2005). During the shock load, PilT was upregulated at all sampled time intervals with a highest DE of 4.97 ± 0.08 observed at 5 h (Figure 19, panel B).

5.2.3 *Pseudomonas* sp. MT1 and *Achromobacter xylosoxidans* MT3 community shock load stress dynamic state proteomics

Based on the shock load analysis performed over *Pseudomonas* sp. MT1 cultures, and in order to compare the proteome expression pattern under dynamic state of pure strain MT1 and mixed culture of strains MT1 and MT3, a sub-lethal shock load stress of 4-clhorosalicylate was analyzed in the community culture. As before, a steady state continuous culture of strain MT1 run at the reference dilution rate of 0.2 d^{-1} was inoculated with strain MT3, and after new steady state achievement the culture was turned to batch mode in triplicate, and spiked with 4CS to a final concentration of 2 mM. Proteomics, metabolite profile and population dynamics were followed at several time intervals before and during the shock load.

The metabolite profile before inoculation of *A. xylosoxidans* MT3 showed stable concentrations of *cis*-dienelactone and protoanemonin as described before for current culture conditions. After addition of strain MT3, the concentration of *cis*-dienelactone and protoanemonin remained at constant levels, as shown before on mixed strains steady state cultures (Section 5.1.2).

After the shock load, the metabolic profile showed a rather different situation compared to the one observed in pure strain MT1 culture (Figure 21, panel B). Substrate depletion was slower, being completely degraded after 16 h. Accumulation of the toxic metabolite

protoanemonin was reduced 4-fold compared to single strain culture, with a maximum of 53.61 ± 2.08 µM at 12 h, and 4CC was practically absent and only detected in one replicate, 9 h after the shock load at a low concentration level (9.60 µM).

Population dynamics determined by dead & alive staining coupled to FACS quantification, showed initial stable concentrations of cell counts per mL with a total of 9.58e08 ± 4.33e07, live 8.05e08 ± 3.24e07 (84.0%) and dead 9.29e07 ± 7.93e06 (9.7%) cell counts/mL in the mixed culture, with a considerable higher proportion of dead cells compared to strain MT1 pure culture. During the shock load stress no major variation was observed, and after 16 h the total counts per mL remained in the same order of magnitude (8.71e08 ± 3.94e07) with similar proportions of live (7.33e08 ± 7.57e07, equivalent to 84.2%) and dead (7.43e07 ± 9.08e06, equivalent to 8.5%) cell counts/mL as those for initial conditions (Figure 21, panel A).

In order to establish the composition of the mixed culture, Fluorescent *in situ* hybridization (FISH) with specific oligonucleotide probes fluorescently labeled with Alexa Fluor 488 (Kaminski et al., 2006), was carried out before and after the shock load in the mixed culture. Due to the high loss of bacterial counts during the fixation and hybridization steps, only a qualitative approach was possible. Initial composition of the culture showed 68% of the active population to be specifically stained with strain MT1 probe and 10% to MT3 probe. Taken together, a 78% approximate closely to the 84% live cell counts determined by dead & alive staining, considering that rRNA targeted FISH gives a strong signal mainly in active cells (Zwirglmaier, 2005). At the end of the shock load, the proportion of strain MT1 remained constant giving 70% while the proportion of strain MT3 significatively increased up to 16%, being the sum (86%) comparable again with the live population observed in dead & alive determinations at this stage (84.2%). These measurements confirm the proportions observed in the community cultures quantified by specific CFU determinations.

Analysis of the proteomic profile of *Pseudomonas* sp. MT1 and *A. xylosoxidans* MT3 community culture under 4CS shock load stress, restricted to the comparison of initial conditions to 5 h after the shock load, showed no variations in the expression levels of the identified enzymes that belong to the main degradative pathway. SalA, as well as CatA 1 and 2 were non-differentially expressed (DE 1.50 ± 0.06, 1.20 ± 0.41 and 1.18 ± 0.05, respectively).

Minor variations in the expression levels of parallel catabolic pathways were observed, and only downregulation of catechol 2,3-dioxygenase, 4-HPPD and Sal5 was observed (DE 0.21 ± 0.02, 0.18 ± 0.11 and 0.43 ± 0.05, respectively). Central metabolism was practically not affected and differences were observed in aminoacid metabolism with upregulation of Arginine deaminase (ADE) presenting a DE of 3.95 ± 0.38 and downregulation of Argininosuccinate synthase (Assyn) that showed a DE of 0.34 ± 0.12 (Figure 22, panel C).

Cell division protein FtsA and a TraN-like protein were upregulated (DE 2.83 ± 0.48 and 2.77 ± 0.11, respectively). FtsA is a highly conserved protein, that constitutes an essential bacterial component due to its protein–protein interaction with proteins involved into the Z-ring formation that allows the physical separation of daughter cells (Paradis et al., 2005). In the case of the TraN-like protein identified (gi|29611516), it corresponds to an unknown function protein found in conjugative transposons present in bacteria from the genus *Bacteroides* an *Flavobacterium* with no homology nor conserved domains detected.

Identified proteins related to cell envelope biogenesis, were divergently expressed with downregulation of a NmrA-like protein (DE 0.20 ± 0.01) and upregulation of AcpH (DE 2.62 ± 0.92) a protein that was *de novo* synthesized during shock load stress in pure MT1 cultures. Identified stress response proteins were non-differentially expressed with

the exception of AhpC1 that showed a mild upregulation (DE 2.14 ± 0.11, Figure 22, panel B).

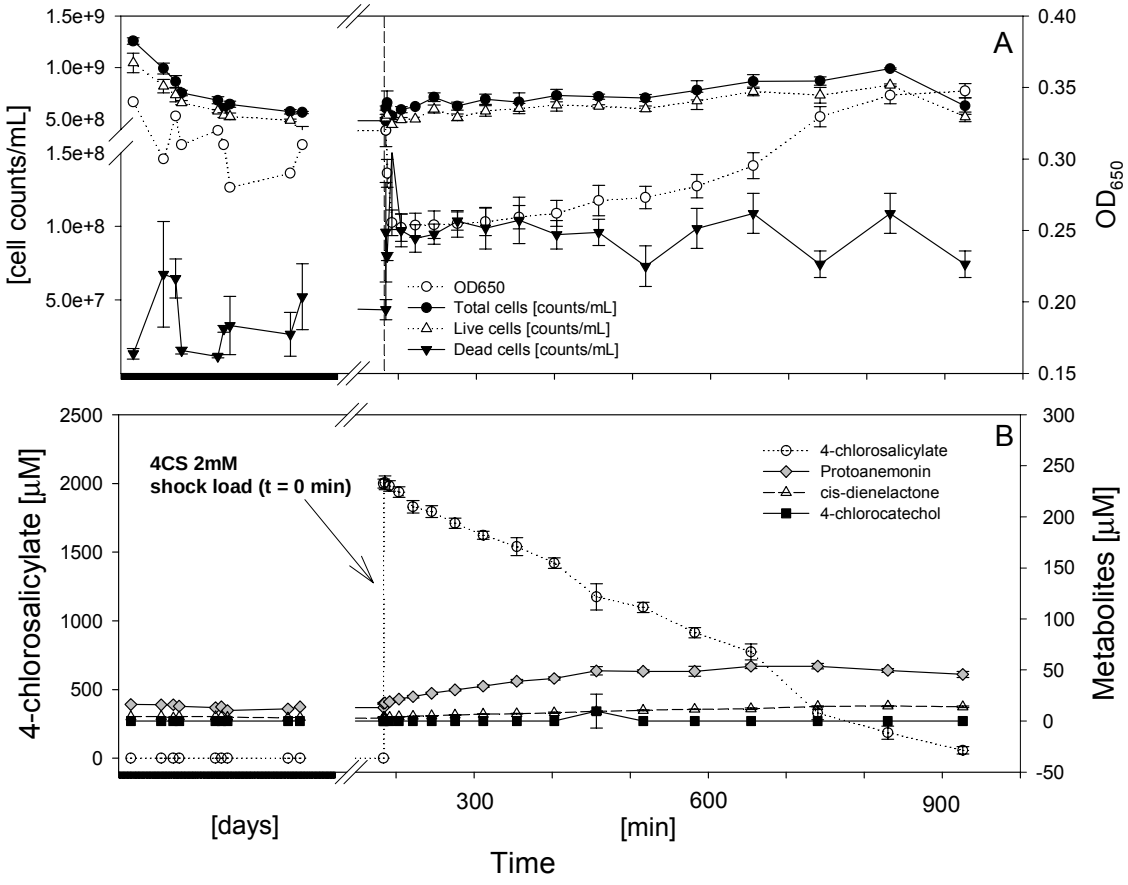

Figure 21. *Pseudomonas* sp. strain MT1 and *Achromobacter xylosoxidans* strain MT3 community continuous culture monitoring before and during a 2mM 4CS shock load stress. A: population dynamics. B: metabolic profile.

Once more, transporters presented an important variation, with two ABC-type transporters upregulated (spots 48 and 52 with DE of 2.21 ± 0.97 and 2.93 ± 0.63, respectively), showing again a selective expression that differs from the pure culture condition. OprF was non-differentially expressed and porin D showed upregulation with a DE of 4.80 ± 2.33 (Figure 22, panel A).

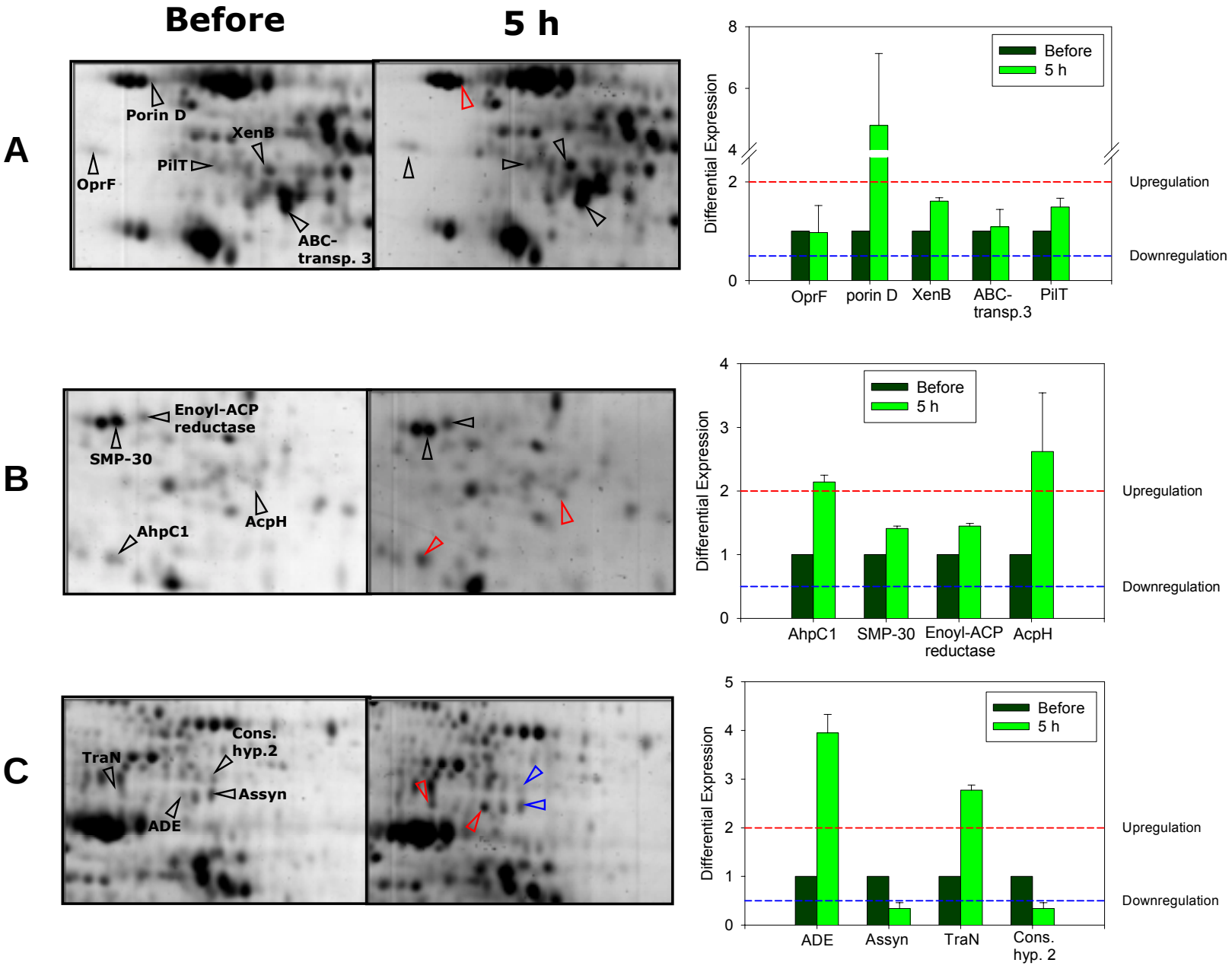

Figure 22. Selected proteome comparative views of mixed continuous culture of *Pseudomonas* sp. strain MT1 and *Achromobacter xylosoxidans* strain MT3 exposed to 2mM 4CS shock load.

5.2.4 Discussion overview of dynamic state cultures

Growing conditions found by bacteria in the environment are extremely variable. Hence, the capacity to adapt to those changes is the key for survival and persistence. That is, nutrient limitation is probably the most common stress condition faced by environmental bacterial communities, a situation that is perturbed by intermittent nutrient abundance events. Examples of such events, both natural and man-made, can be found in aquatic environments, for example, when algae blooms generate high organic matter loads or in the case of contamination events, such as oil spills and industrial effluent discharges, creating a sudden increase in organic matter concentrations. Particularly interesting for bioremediation is the response of microorganisms to high xenobiotic loads, represented in this study by 4CS shock loads.

A remarkably different response to 4CS shock load was observed comparing pure strain MT1 and community cultures. *Pseudomonas* sp. MT1 accumulate high levels of toxic intermediates in a fast degradative process, generating a sub-lethal stress condition, tackled by high upregulation of the oxidative stress response protein system. Despite rapid degradation, cellular fitness is probably impaired since central metabolism enzymes were downregulated and a high loss of carbon, due to high levels of protoanemonin, was generated.

In the presence of *A. xylosoxidans* MT3, the community response to 4CS shock load showed a slower degradation capacity with respect to the pure culture, but at the same time, there was no significant accumulation of toxic metabolites and consequently, no major stress response. This may be traduced into a better fitness, since the mixed culture showed no variation in most of the central metabolism expression of identified proteins and moreover, upregulation of the aminoacid metabolism was observed. To this

respect, induction of the arginine deiminase pathway has been reported in *Pseudomonas aeruginosa* under low oxygen concentrations, using arginine as an alternative source of ATP (Mercenier et al., 1980).

Thus, it is possible to conclude that a 2 mM 4CS shock load generates a stress response in pure culture and a 'metabolic response' in the mixed culture. The accumulation of 4CC in pure strain MT1 cultures, a known stressor (Schweigert et al., 2001a), is probably the major cause of this difference.

A. xylosoxidans MT3 helps to prevent 4CC accumulation and therefore provides a more robust biodegradative capacity to the community. Former studies have shown that once stable isotopic labeled 4CC is added to the MT community, the label incorporates faster into MT3 specific fatty acids (Pelz et al., 1999). The present study demonstrates that strain MT3 is directly involved in the degradation of 4CC, but not simply due to its catabolic potential, but rather by altering the 4CS degradation rates by strain MT1. At first glance, this can be simply caused by an alteration of inducer concentrations, but the variations observed suggest a more sophisticated interaction, apparently not involving the induction of the upper degradation pathways in the main strain MT1, but rather altering the cellular envelope composition and the selective transport mechanisms probably involved in the degradative process.

One interesting fact was the differential expression of the outer membrane proteins, OprF and porin D. In this study, OprF was initially related to substrate transport, possibly increasing the 4CS uptake by facilitated diffusion in continuous cultures at low *D*. However, a more complex scenario was observed, since OprF was also upregulated under shock load stress. This observation draws the attention to refined sensing mechanism that may regulate the outer membrane permeability, and that unspecific

porins such as OprF may play different roles under different culture conditions. A possible explanation for such behavior may relate OprF overexpression on one hand, to higher substrate uptake under carbon limiting conditions (from the environment towards the cell), and on the other hand, to allow toxic intermediate diffusion (from the cell towards the environment), in both cases increasing the outer membrane permeability. The later can come from the tight correlation of 4CC transient accumulation with OprF expression in the pure culture during the shock load (Figure 22a) and moreover, from the fact that OprF was not upregulated in the mixed culture where there was no 4CC accumulation. OprF has been classified as a 'slow porin' (Nikaido, 2003), residing at the outer membrane in both open and closed states (Sugawara et al., 2006). Possibly, different environmental signals can alter the proportion of OprF states according to the metabolic requirements of the cell. Moreover, *P. putida* KT2440 stress response to chlorophenoxy herbicides includes the upregulation of OmpA (OprF homolog) and a TolC homolog, possibly involved in efflux detoxification systems (Benndorf et al., 2006).

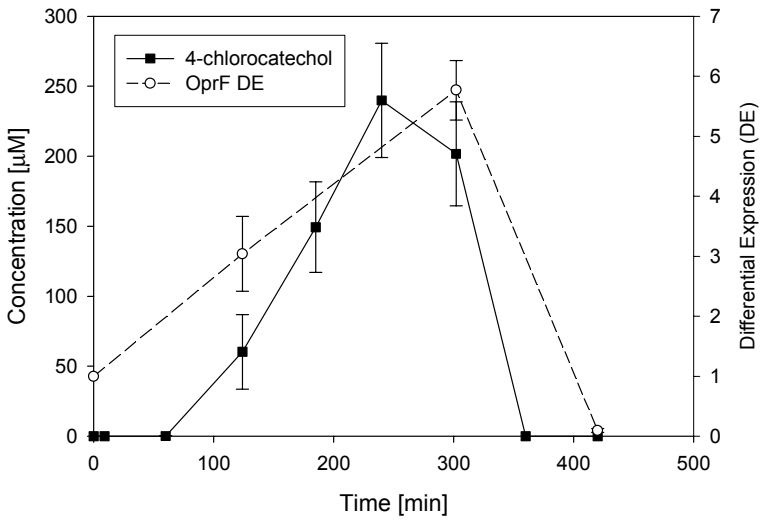

Figure 22a. Correlation of OprF expression and 4-chlorocatechol transient accumulation in 2mM 4CS shock load on *Pseudomonas* sp. MT1 culture (linear $r^2 = 0.9442$).

In the case of porin D (gi|70732098), an outer membrane protein from the OprD family, sharing 25 and 30% aminoacid sequence identity with VanP and BenF, respectively, being both aromatic transport proteins (Metzgar et al., 2004; Nelson et al. 2002), its expression followed a different pattern compared to OprF. During the shock load, porin D was downregulated in pure strain MT1 culture and upregulated in the presence of strain MT3, indicating that *Pseudomonas* sp. MT1 has a rather different outer membrane composition that it is strongly influenced by the presence of *A. xylosoxidans* MT3.

Finally, many studies have been done on stress response, centered on the variations in the cellular response to a stressor. Protein and gene expression, among other parameters have been studied, focusing on the differences at the pure culture level. However, no study has been carried out so far concerning the stress response in a mixed culture and few studies are available on metaproteomics. Hence, this study constitutes to my knowledge, the first analysis of the variation of the response from stress in a pure culture to non-stress in a bacterial community, being one step closer to real environmental conditions, where the stress response is coordinated at the community level.

5.2.5 Kinetic metabolic modeling of dynamic states

To understand the essential qualitative and quantitative features of complex systems, it is necessary to gather an important amount of information about different aspects but particularly, requires a systematic integration of the collected data. Metabolic modeling can be considered as a method to organize what sometimes seems to be untidy and diffuse knowledge. A straight forward application of modeling goes through the exploration of potential system's behavior, helping to reject false hypotheses and aiming to focus on the most feasible explanations for the observed performance of the system. Finally, modeling and simulation can be of tremendous help for experimental design when a validated and robust model with predictive capacity is available.

During the metabolic and proteomic analysis performed, it was particularly interesting to develop a kinetic model of the upper degradation pathway of 4CS in *Pseudomonas* sp. MT1, as well as mixed cultures in the presence of *A. xylosoxidans* MT3, with the aim to develop a mechanistic explanation of the essential parts of the upper degradation pathway able to describe the global dynamic behavior and, after validation, to become a tool to predict the behavior of the system under different conditions, e.g., community cultures under high substrate loads.

5.2.5.1 Kinetic Modeling of *Pseudomonas* sp. MT1 dynamic states

As it was initially described, under the culture conditions used in this study, the MT community relies on the metabolic capacity of *Pseudomonas* sp. strain MT1 to degrade 4CS, in order to establish a carbon sharing network among the community members. Additionally, strain MT1 constitutes the majority of the population in the community

(>80%) being a particularly interesting model community to study bacterial interactions in terms of the influence of low abundant strains on the major community member.

Detailed information of the upper degradation pathway, including a proposed mechanism of reaction for some of the involved enzymes was generated by Nikodem and co-workers, showing that the degradation of 4CS goes via 4CC and 3-chloromuconate, and suggesting 4-chloromuconolactone as the intermediate and *trans*-dinelactone hydrolase as the enzyme involved in further formation of maleylacetate and prevention of protoanemonin dead-end formation (Nikodem et al., 2003). Moreover, the mechanism of reaction of salicylate hydroxylase, the first enzyme in the pathway, has been thoroughly studied (Katagiri et al., 1966; White-Stevens et al., 1972) as well as the reaction kinetics (Takemori et al., 1972) and new isofunctional enzymes have been recently characterized in Pseudomonad (Zhao et al., 2005; Balshova et al., 2001). Salicylate hydroxylase corresponds to a flavin-dependent monooxygenase that uses NAD(P)H as reductant, catalyzing the insertion of one oxygen atom from O_2 into (chloro)salicylate forming (chloro)catechol, being the second oxygen atom reduced to water (Katagiri et al., 1966). Stable ternary complex of salicylate hydroxylase, NADH and salicylate have been detected and characterized as enzimatically active, since the introduction of air gave stoichiometric formation of catechol (Katagiri et al., 1966; Wang & Tu, 1984).

The second degradative step, catalyzed by catechol 1,2-dioxygenase, presents less complexity, since only two substrates are involved (4CC and O_2). A proposed mechanism of reaction is available (Walsh et al., 1983), assuming ternary complex formation with initial binding of catechol and later incorporation of molecular oxygen. Also *in vitro* kinetic parameters have been determined (Nakai et al., 1988; Riddler et al., 1998).

As described in Nikodem's work, a combination of two muconate cycloisomerases and a *trans*-dinelactone hydrolase is required for efficient transformation of 3-chloromuconate to maleylacetate, preventing protoanemonin formation, with *cis*-dienelactone as a potential product of 3CM spontaneous decarboxylation, and/or as a misleading catalyzed reaction in the muconate cycloisomerization process (Nikodem et al., 2003). Later, the transformation of maleylacetate by means of a maleylacetate reductase to 3-oxoadipate, could be considered as one of the last steps before conversion to central metabolism intermediates. This last study provided a good base for the development of a kinetic metabolic model of the upper degradation pathway of 4CS by *Pseudomonas* sp. MT1.

5.2.5.1.1 *Pseudomonas* sp. MT1 kinetic metabolic mathematical statements and model structure

A model structure was created based on the information obtained from the present, as well as previous studies, assuming an homogeneous system (perfect mixing), with constant volume, temperature and pH. Only suspended cells (planktonic culture), growing with 4-chlrosalicylate as the single limiting nutrient in a saturated dissolved oxygen environment, presenting a constant yield, was assumed. The set of assumptions create the boundaries of the system, constrained to mass conservation. Boundaries simplified the kinetic expressions for the initial two degradation steps, since oxygen was assumed to be not limiting in the reactions, being reduced to second and first order respectively. This assumption can be supported by the high dissolved oxygen levels maintained in the cultures (>200 μM), since previous studies have shown that concentrations higher than 150 μM correspond to zero order kinetics for O_2 in catechol

1,2-dioxygenase catalyzed reactions (Riddler et al., 1998). Moreover, NADH intracellular pool was considered constant, reducing the 4CS degradation kinetic expressions to first order.

However, all reactions were considered first order with respect to biomass concentration, assumed to be variable during the dynamic state and therefore, increasing them to second order. Finally, experimental determination reduced the number of significant metabolites since only consistent concentrations were obtained for 4CS, 4CC, protoanemonin and *cis*-dienelactone. A diagram of the kinetic model developed for *Pseudomonas* sp. MT1 is shown in Figure 23. As described in Nikodem's work, 3CM was considered as a key intermediate from which all pathway products, including biomass, were produced. Finally, due to the reported toxic effects of 4CC on biomass (Schweigert et al., 2001a), and since there was no clear toxic effect of 4CS at concentrations lower than 3 mM, a biomass decay rate was included for the toxic intermediate 4CC.

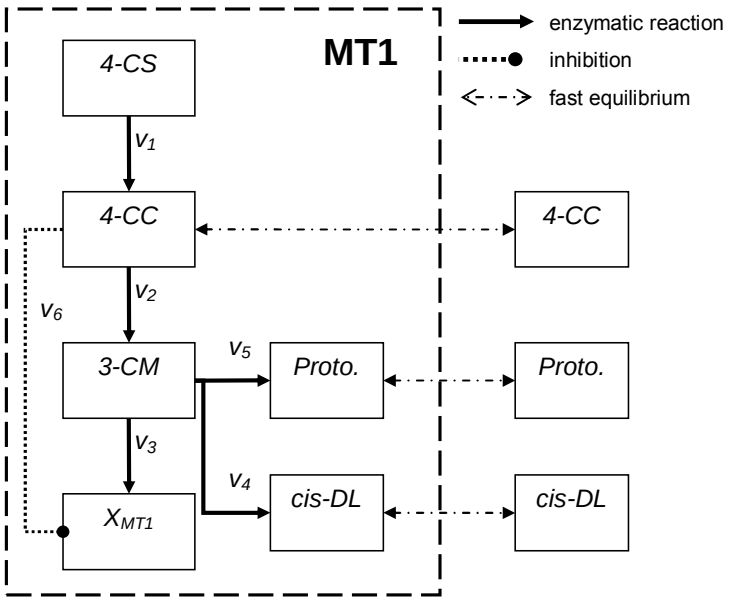

Figure 23. Kinetic metabolic model structure of the upper degradation pathway of 4CS by *Pseudomonas* sp. MT1. 4-CS: 4-chlorosalicylate, 4-CC: 4-chlorocatechol, 3-CM: 3-chloromuconate, cis-DL: *cis*-dienelactone, Proto: protoanemonin.

Kirchhoff's node laws or mass balance equations for the state variables included in the model are given by:

$$\frac{d[4CS]}{dt} = -v_1[X_{MT1}]$$
$$\frac{d[4CC]}{dt} = (v_1 - v_2)[X_{MT1}]$$
$$\frac{d[3CM]}{dt} = (v_2 - (v_3 / Y_{MT1}) - v_4 - v_5)[X_{MT1}]$$
$$\frac{d[X_{MT1}]}{dt} = v_3[X_{MT1}] - v_6$$
$$\frac{d[cis-dienelactone]}{dt} = v_4[X_{MT1}]$$
$$\frac{d[\mathrm{Pr}\,otoanemonin]}{dt} = v_5[X_{MT1}]$$

Based on the previous assumptions, the kinetic expressions followed simple Michaelis-Menten for individual enzymatic reactions and Monod kinetics for biomass growth:

$$v_1 = \frac{V_{\max 1}[4CS]}{K_{M1} + [4CS]}$$
$$v_2 = \frac{V_{\max 2}[4CC]}{K_{M2} + [4CC]}$$
$$v_3 = \frac{\mu_{\max}[3CM]}{K_S + [3CM]}$$
$$v_4 = \frac{V_{\max 3}[3CM]}{K_{M3} + [3CM]}$$
$$v_5 = \frac{V_{\max 4}[3CM]}{K_{M4} + [3CM]}$$
$$v_6 = k_{tox}[4CC]$$

MATLAB® version 7.2.0.232 R2006a and SIMULINK® version 6.4.1 R2006a+ software was used to build the kinetic model expression and to visualize simulations. SIMULINK-based Parameter Estimator version 1.1.3 software was used to perform multi-parameter fitting, solving the set of ordinary differential equations using a multi-step method solver of variable-order based on numerical differentiation formulas (ode15s build-in MATLAB®).

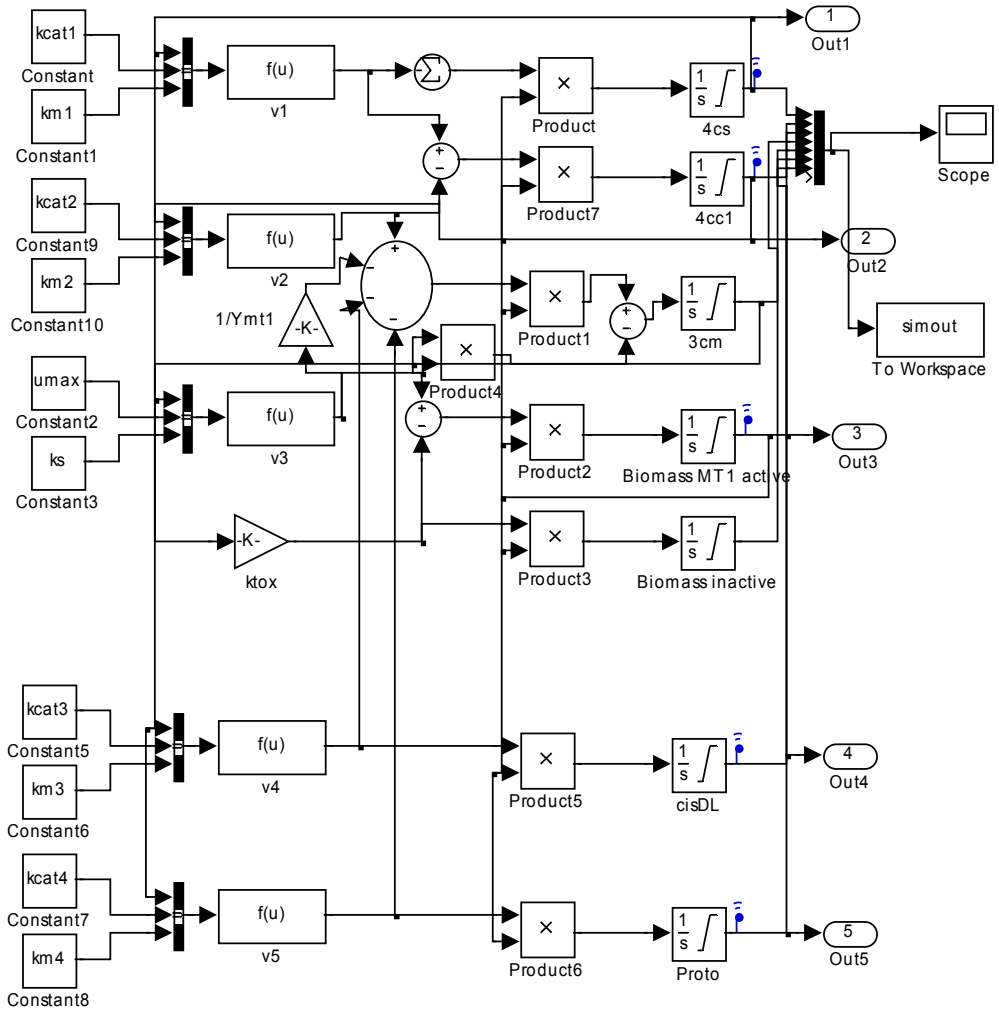

Figure 24. Example of a model build-up in SIMULINK®.

5.2.5.1.2 Experimental determination of initial parameter values for *Pseudomonas* sp. MT1 kinetic model

Initial parameter values (also referred to as initial guess) for the parameter estimation optimization step were obtained from direct analysis of progress curves from dynamic

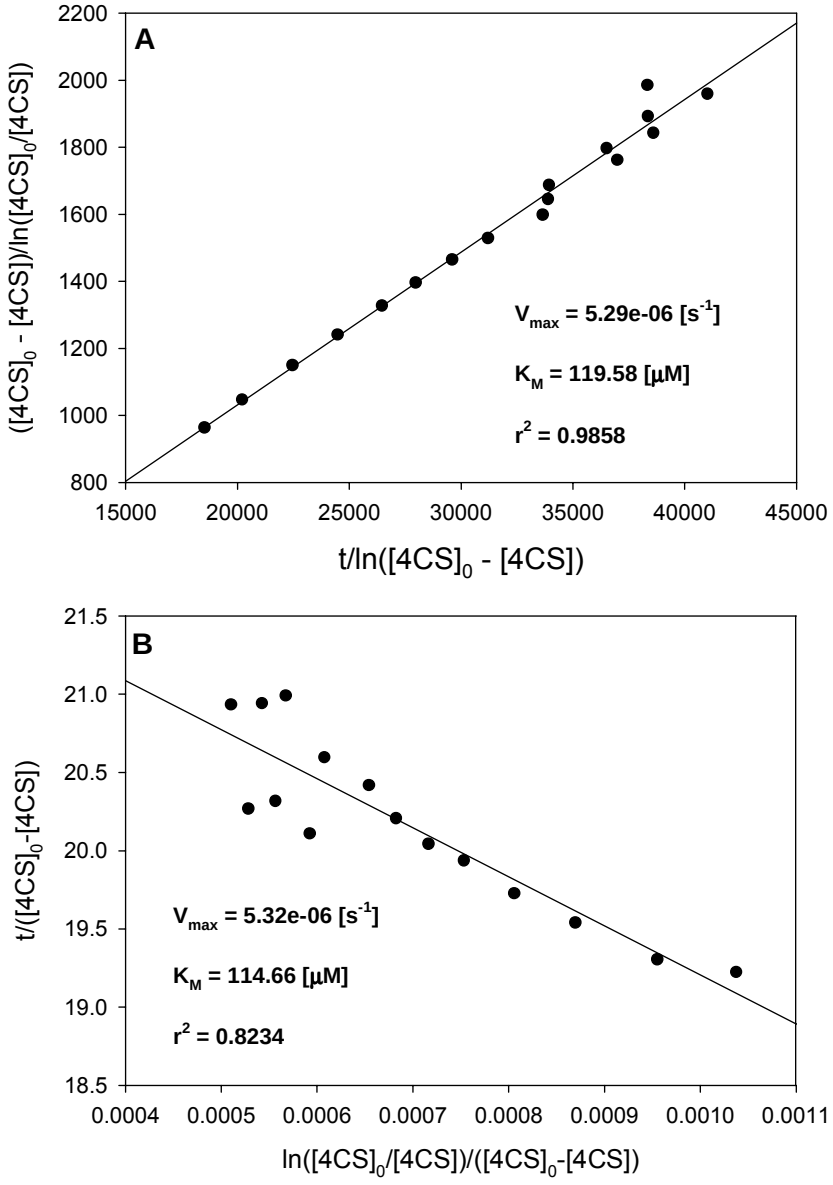

Figure 25. Examples of two linearized forms (A, equation (8) and B, equation (10)) of the integrated Michaelis-Menten equation (7) to obtain initial parameter values for 4CS degradation.

state experiences using both non-linear regression (as shown on Figure 17 and 26) and linearized forms of the integrated Michaelis-Menten equation (equations (8) and (10)), as shown in Figure 25. Values are listed in Table 3.

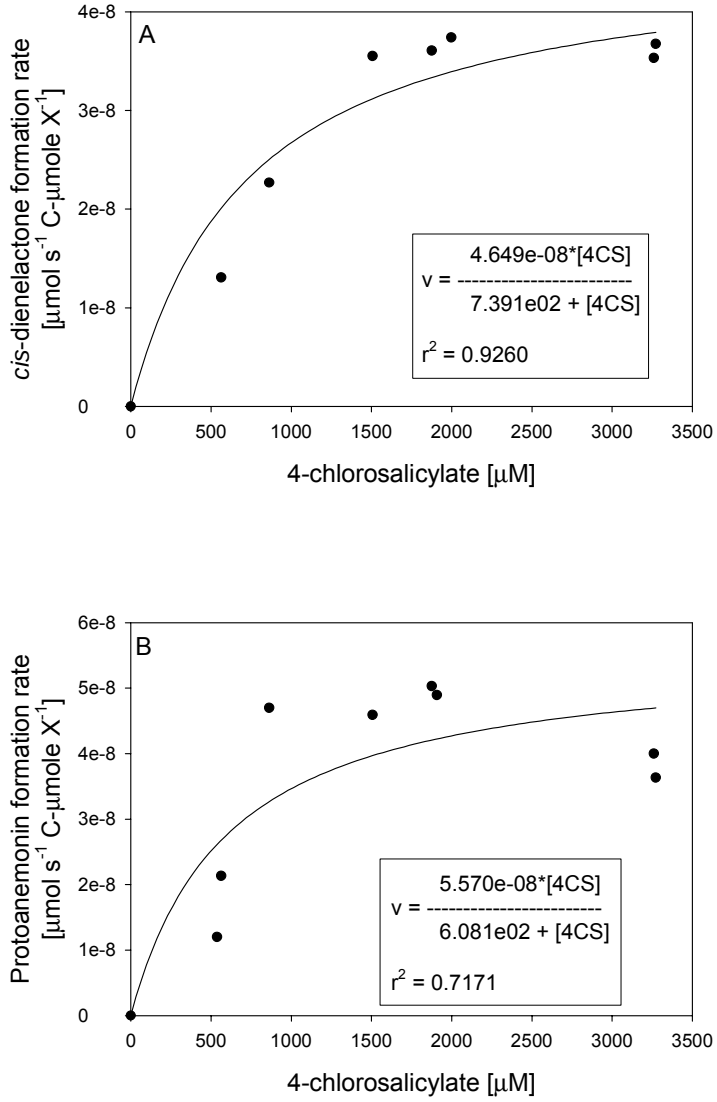

Figure 26. Rates of formation of A, *cis*-dienelactone and B, protoanemonin under different shock loads of substrate. Box shows the non-linear regression assuming Michaelis-Menten kinetics.

Biomass quantification was done by simple determinations of optical density (OD_{650}) and correlated to biomass concentration values obtained from previous experiences as shown in Figure 27, panel A (Hecht, unpublished data).

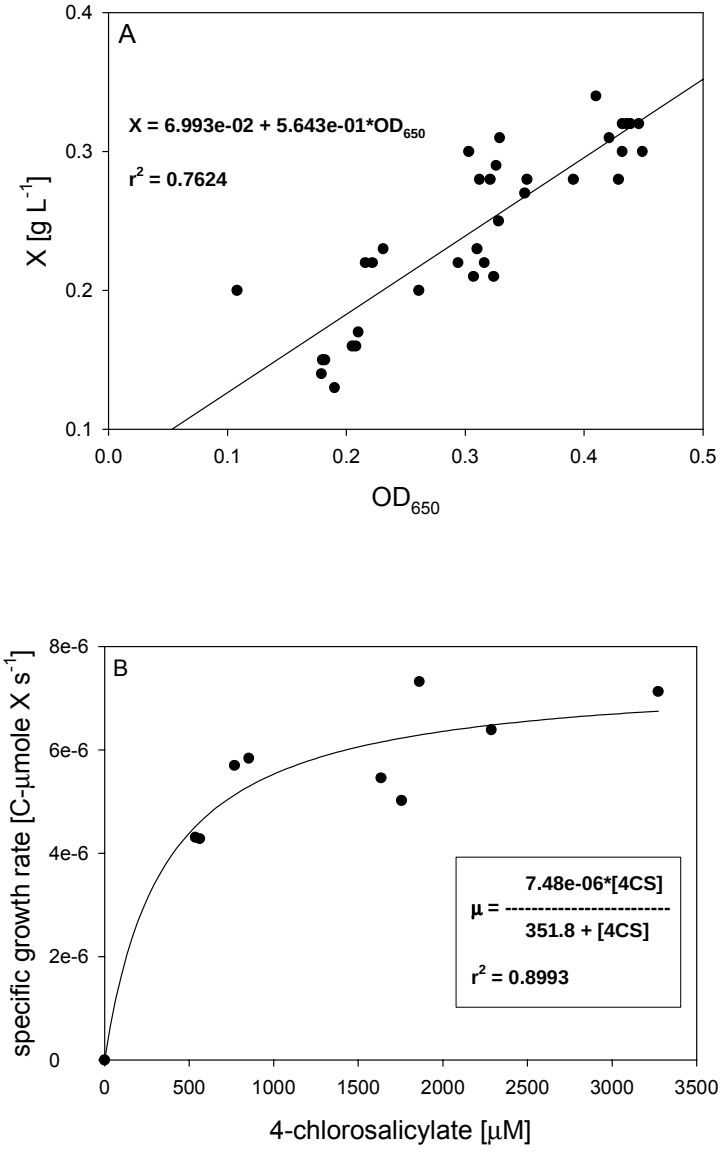

Figure 27. A: Correlation of optical density at 650 nm (OD_{650}) to biomass concentration *X*. B: non-linear regression assuming Monod kinetics for biomass growth.

It is important to highlight that biomass concentrations are referred to as a carbon mole basis (C-mole), assuming a standard biomass chemical formula:

$$CH_{1.8}O_{0.5}N_{0.2}$$

which corresponds to a molecular weight of 24.6 g (C-mole biomass)$^{-1}$ (Nielsen et al., 2003).

The maximal specific growth rate (μ_{max}) was calculated directly from dynamic state experiences by non-linear regression. Determinations were restricted to the linear increase in biomass. Figure 27, panel B shows the obtained regression in the range of concentration of 4CS from 500 to 3000 µM.

Finally, the yield coefficient ($Y_{S,X}$) was obtained from the observed biomass increase as a function of the substrate degradation rate. In this case, substrate must be expressed in C-mole units, to be directly proportional to the biomass concentration. It is important to point out that the yield coefficient obtained corresponds to the observed yield coefficient ($Y_{obs\ S,X}$) that includes biomass maintenance (Nielsen et al., 2003). A constant yield was obtained in the range of concentrations tested as shown in Figure 28.

Initial values for V_{max2}, K_{M2} and k_{tox} where obtained by guess work in order to fit the experimental results, constrained to literature reported and/or available values (BRENDA database).

Initial parameter values were introduced into the kinetic expression of *Pseudomonas* sp. MT1 model and multiparameter fitting was carried out in order to optimize the parameter values.

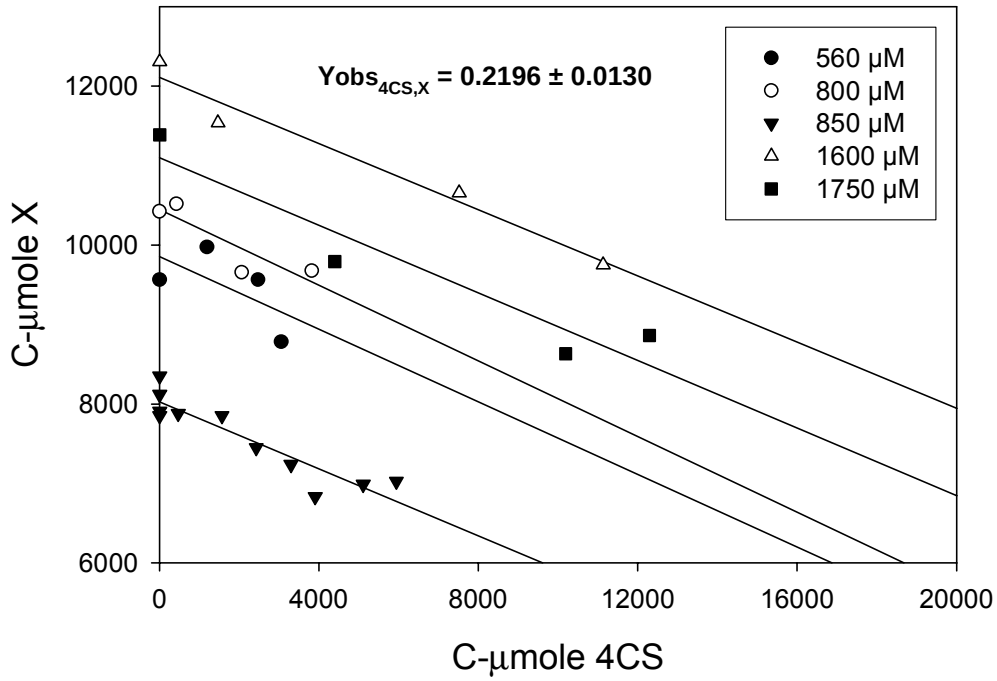

Figure 28. Determination of the yield coefficient for different dynamic states.

Table 3. Initial kinetic parameter values for parameter optimization

Parameter	Value	Units	Source
V_{max1}	7.79e-06 ± 3.16e-06	[s^{-1}]	Non-linear regression
V_{max3}	4.65e-08 ± 6.29e-09	[s^{-1}]	Non-linear regression
V_{max4}	5.57e-08 ± 1.28e-08	[s^{-1}]	Non-linear regression
μ_{max}	7.48e-06 ± 7.10e-07	[s^{-1}]	Non-linear regression
K_{M1}	2.90e02 ± 1.41e02	µM	Non-linear regression
K_{M3}	7.39e02 ± 3.34e02	µM	Non-linear regression
K_{M4}	6.08e02 ± 4.88e02	µM	Non-linear regression
K_S	3.52e02 ± 1.46e02	µM	Non-linear regression
$Y_{obs\ 4CS,X}$	0.2196 ± 0.0130	unit less	Linear regression

5.2.5.1.3 Parameter sensitivity analysis of *Pseudomonas* sp. MT1 kinetic model

Multi-parameter sensitivity analysis was performed directly evaluating the variation in model prediction with respect to observed values. Three-dimensional visualization of the error space, expressed as the natural logarithm of the sum of the squared errors for each state variable in the model (logSSE), as a function of the simultaneous variation of the parameter pair of each individual kinetic expression, leaving the other parameters at a constant value, allowed the observation of local minima and to evaluate the determination of the true global minimum, during the parameter estimation iterative process. Parameter values were considered sensitive and valid only when the values were in the area of global minimum error.

Parameter sensitivity was not restricted to overall sensitivity, since it can mask the effects of parameter variation on low magnitude quantities. Therefore, parameter sensitivity was evaluated independently for the error on each predicted state variable of the model that could be compared to consistent experimental data. An example is shown in Figure 29 for the simultaneous variation of V_{max1} and K_{M1} showed high parameter sensitivity (top panel),when the error space was evaluated for the discrepancy between observed and predicted values for substrate depletion (logSSE[4CS]). For the same error space, Figure 29 (bottom panel) shows low parameter sensitivity for simultaneous variation of V_{max2} and K_{M2}. However, the evaluation for the discrepancy between observed and predicted values for 4CC transient accumulation (logSSE[4CC]) for simultaneous variation of V_{max2} and K_{M2} showed high parameter sensitivity.

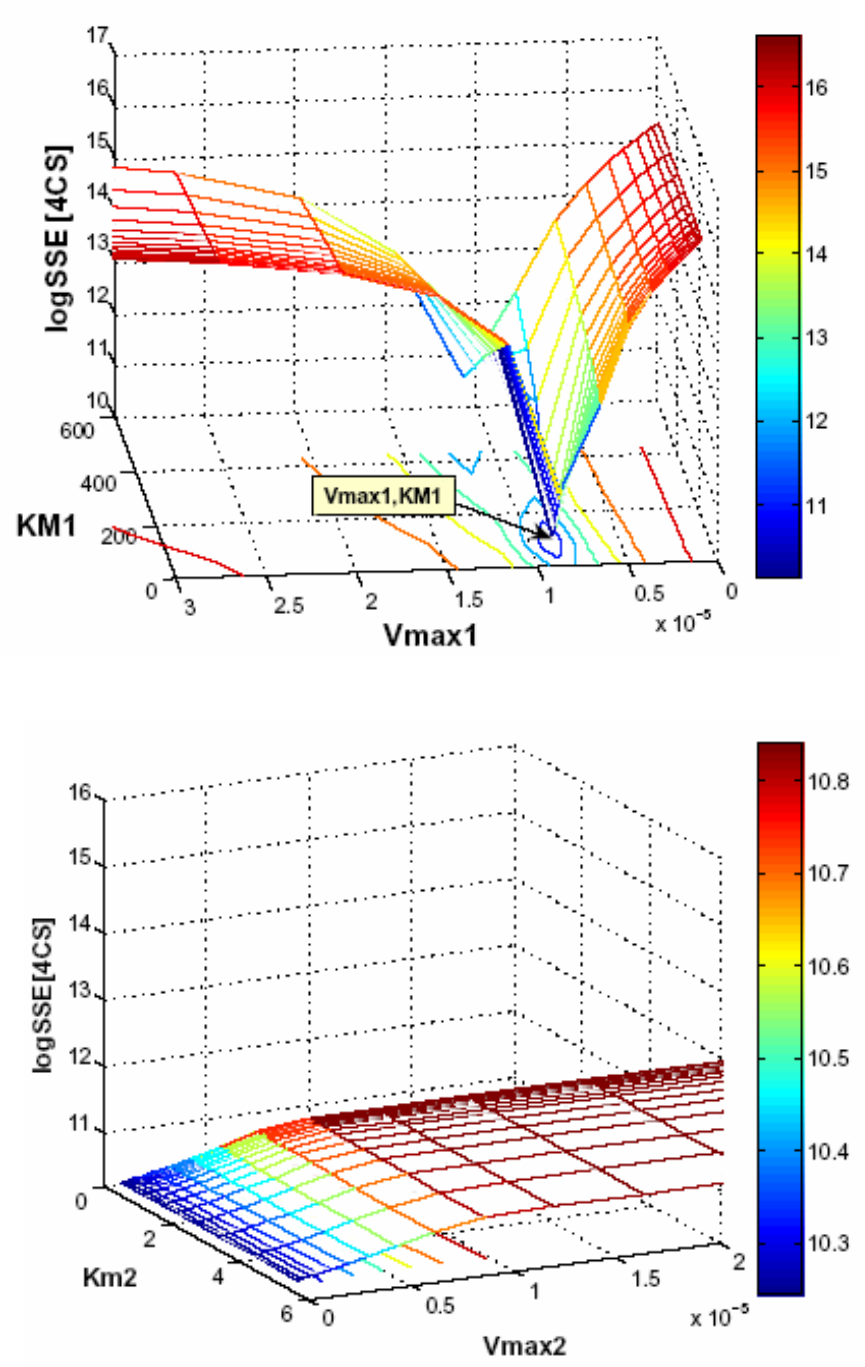

Figure 29. Examples of the three-dimensional visualization of the error space. Top, simultaneous variation of the high sensitivity parameters V_{max1} and K_{M1}. Bottom, simultaneous variation of low sensitivity parameters V_{max2} and K_{M2}, both evaluated for logSSE[4CS]. Color bar shows the logarithm of the error variation range.

It is important to highlight that parameter sensitivity was determined for all state variables in order to establish the overall sensitivity and to determine the optimal parameter values within the global minimum (Figure 31). As shown in Figures 29 and 30, it is equivalent to visualize the error surface in a two dimensional contour plot for the simultaneous variation of the parameters. The range of variation of the error values (logSSE) is represented by the color bar and the contour lines, and can be used as an indication of the sensitivity (Goudar et al., 2004). Finally, no linear dependency among parameters of the same kinetic expression was detected since no linear compensation in the error was observed.

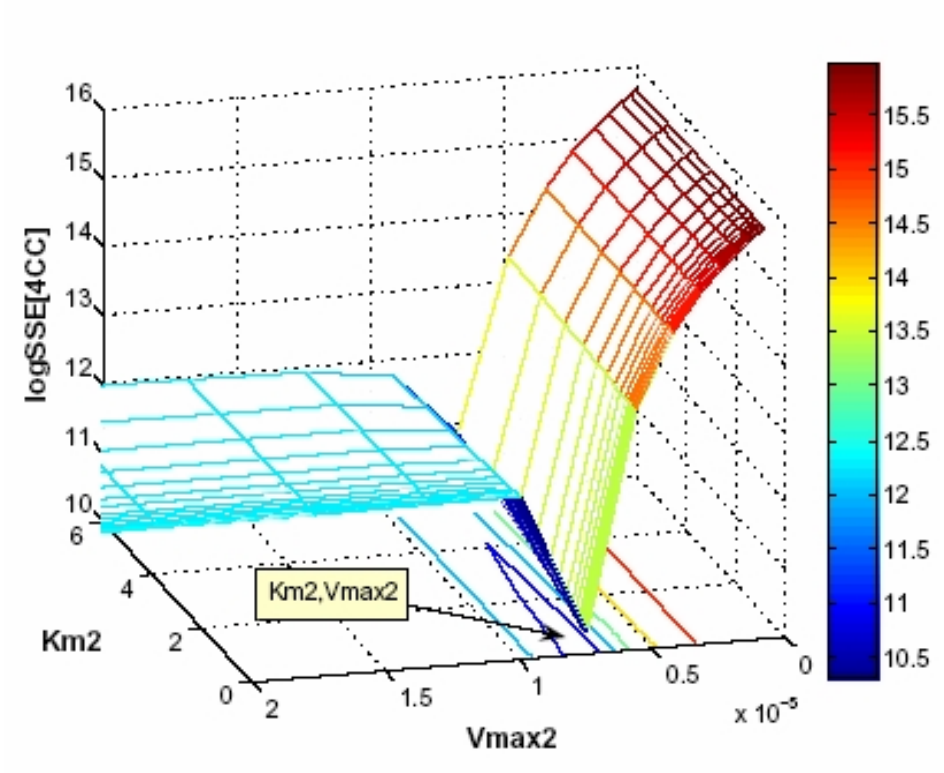

Figure 30. Example of the three-dimensional visualization of the error space for simultaneous variation of the high sensitivity parameters V_{max2} and K_{M2} evaluated for logSSE[4CC]. Color bar shows the logarithm of the error variation range.

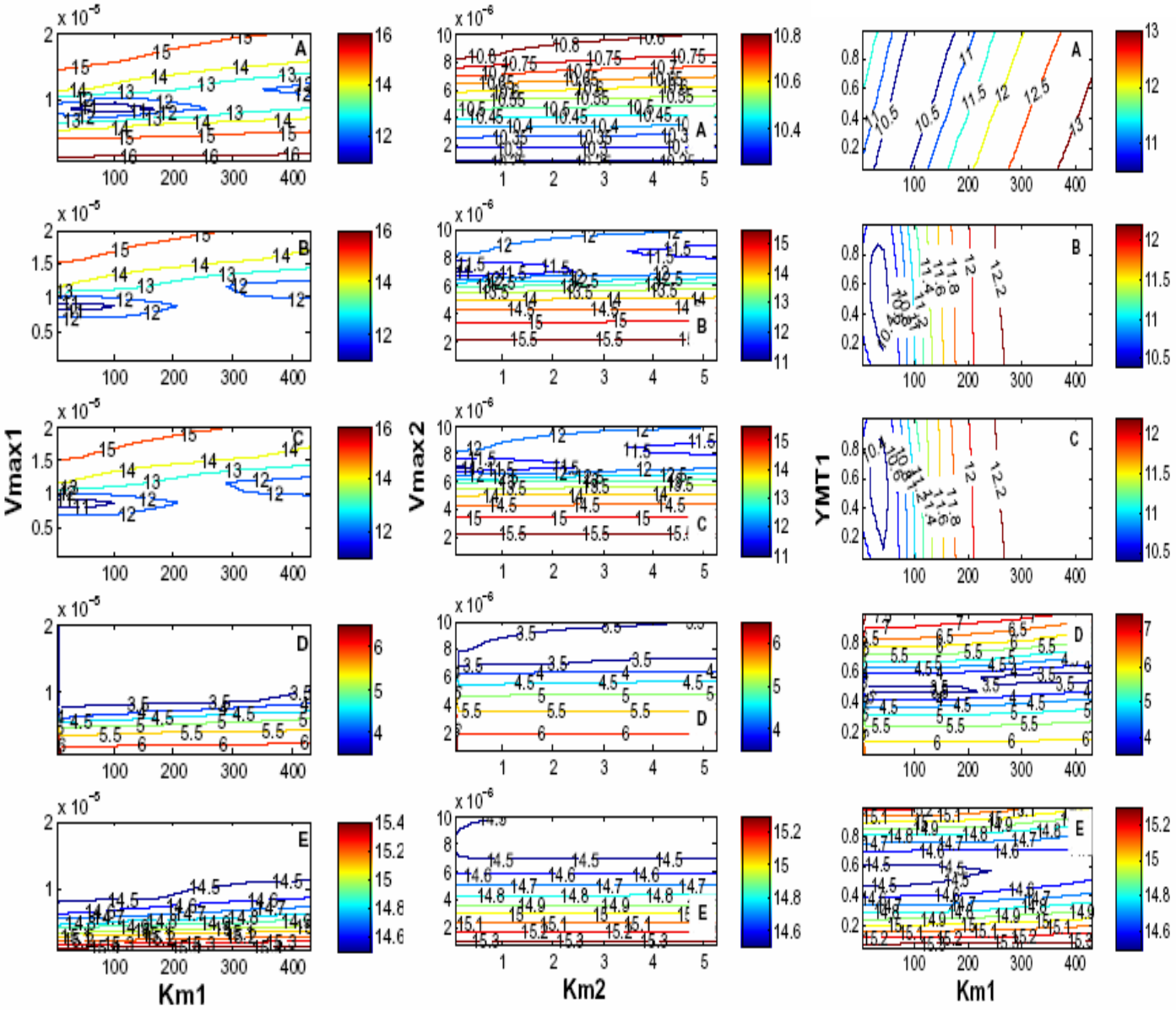

Figure 31. Examples of the visualization of the error surface (logSSE values) as a bi-dimensional contour plot for the simultaneous variation of: Left, K_{M1} and V_{max1}; Center, K_{M2} and V_{max2}; and Right, K_{M1} and Y_{MT1}, for the evaluated error in A: 4-chlorosalicylate, B: 4-chlorocatechol, C: *cis*-dienelactone, D: protoanemonin and E: C-µmole X_{MT1} predictions. Color bar shows the logarithm of the error variation range.

Table 4. Optimal set of parameters for *Pseudomonas* sp. MT1 kinetic model*

Parameter	Value	Units
V_{max1}	8.73e-006	$[s^{-1}]$
V_{max2}	7.40e-006	$[s^{-1}]$
V_{max3}	2.42e-01	$[s^{-1}]$
V_{max4}	1.58e-01	$[s^{-1}]$
μ_{max}	1.54e-005	$[s^{-1}]$
K_{M1}	4.30e01	μM
K_{M2}	5.24e-01	μM
K_{M3}	7.39e02	μM
K_{M4}	6.08e02	μM
K_S	6.48e-004	μM
k_{tox}	4.78e-010	$[s^{-1}]$
Y_{MT1}	0.4975	unit less

*All parameter values were obtained from the iterative process of parameter estimation coupled to parameter sensitivity analysis.

From the parameter estimation step combined with the multiparameter sensitivity analysis in an iterative process, an optimal set of parameters was obtained (Table 4) and further used for simulations. In the case of V_{max3}, V_{max4}, K_{M3} and K_{M4}, there was a considerable variation of the optimized values with respect to the initial guess. Also a higher yield coefficient was obtained. This could be caused by the fact that the regressions were obtained as a function of 4CS (Figures 26 and 28) since no accurate determinations of 3CM could be obtained.

5.2.5.1.4 *Pseudomonas* sp. MT1 kinetic model validation

In order to validate and to assess its predictive value, the model was set to initial conditions determined for the state variable, biomass and metabolites, for different dynamic states evaluated experimentally. Model output showed a good correlation to observed values as shown in Figure 32 for a considerable range of concentrations.

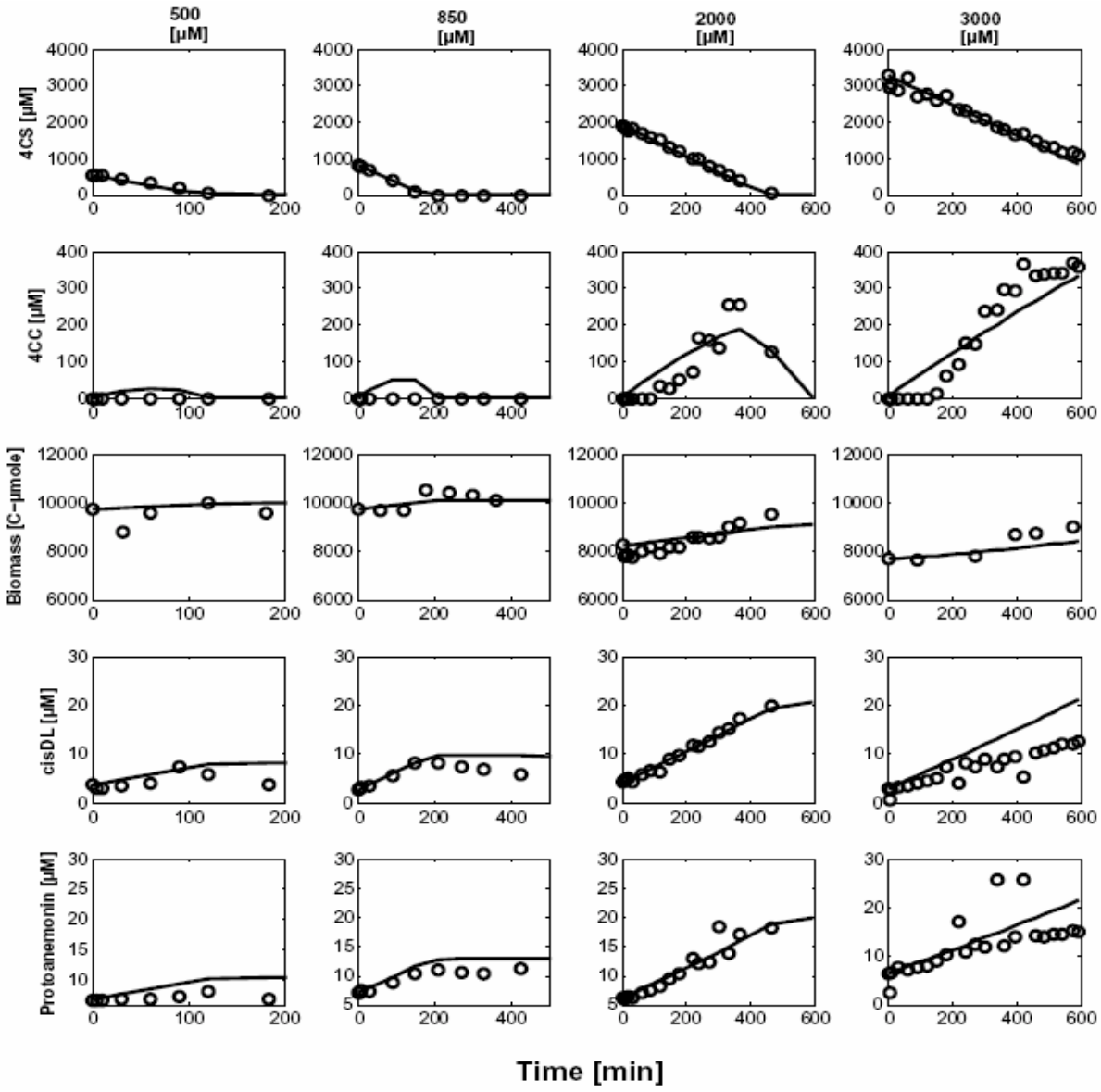

Figure 32. Model validation for a dynamic state series from 500 to 3000 µM 4-chlorosalicylate shock loads in *Pseudomonas* sp. MT1 cultures. Circles and lines represent experimental values and model predictions, respectively.

An interesting aspect arose at this stage with respect to the predicted values generated by model simulations for 4CC at initial concentrations lower than 2000 μM. Experimental determinations showed no traceable amounts, indicating that 4CC concentrations were below the detection limit. However, the model predicts a transient accumulation at all concentrations, proportional to the initial concentration of substrate. In the analysis of shock loads at initial concentrations of 4CS equal to or higher than 2000 μM, the model predict accurate forecasts with a good correlation between predicted and observed values. Nevertheless, there is an observed delay in the experimental appearance of 4CC that the model is not able to predict. This particular issue can be explained considering the experimental procedure, in which the measured concentrations were obtained from the culture supernatants after biomass removal. Therefore, only those metabolites that are able to diffuse out of the cell could be determined. Following this rationale, and taking into account that halogenated catechols can accumulate in membranes due to their high octanol-water partition coefficients (Schweigert et al., 2001), it is possible to argue that 4CC can be initially accumulated in the membrane when its formation exceeds its degradation rate and, after reaching a certain concentration, starts diffusing out of the cell. Using a model for membrane partitioning (Hüsken et al., 2003) and standard volumetric mass transfer and octanol-water partition coefficients for aromatic compounds, concentrations of 4CC up to 215 μM can be predicted in the membrane for a 3000 μM shock load. In addition, it has been reported that the outer membrane imposes a diffusion rate-limiting barrier for hydrophobic compounds, that diffuse through by entirely different mechanisms from those used by hydrophilic molecules (Nikaido, 1976). In the case of protoanemonin, model predictions were relatively close to experimental observations, and an apparent negative correlation with biomass content was observed.

5.2.5.2 Kinetic Modeling of *Pseudomonas* sp. MT1 and *A. xylosoxidans* MT3 community dynamic states

The metabolic behavior of mixed cultures of *Pseudomonas* sp. MT1 and *A. xylosoxidans* MT3 resemble the pure culture in terms of dead-end products under the steady states analyzed. However in the dynamic states, a major difference was observed in the substrate degradation rate as well as in the accumulation of the toxic intermediates, 4CC and protoanemonin. Several hypotheses rose after the combined analysis carried out at the metabolite, population dynamics as well as proteomic stages.

5.2.5.2.1 *Pseudomonas* sp. MT1 and *A. xylosoxidans* MT3 community kinetic metabolic mathematical statements and model structure

The analysis of complex systems requires a systematic approach in order to gather all the information pieces to be able – at least in part – to describe the dynamic behavior of the system from a global perspective. In this particular case, the behavior of a simple two-membered bacterial community can be considered as a starting point to unravel and understand the elemental bacterial interactions that thrive in more complex biological systems.

The comparison of single *Pseudomonas* sp. strain MT1 cultures to community cultures in the presence of *A. xylosoxidans* strain MT3, showed a different behavior in both steady as well as dynamic states. Particularly interesting was the difference in the metabolite profile under 2 mM 4CS shock load described before, where lower 4CS degradation rates and no accumulation of 4CC was observed for the community culture. Looking for a mechanistic explanation to these differences, and having a validated kinetic model with predictive value developed for strain MT1, the next step was to incorporate minor

additions in order to obtain a kinetic model for the community culture under dynamic conditions. To this respect, the observed metabolite profile showed an enhanced 4CC degradative capacity in the community. This could be produced by a combination of a slower 4CS degradation rate by strain MT1 and increased 4CC degradation rate by strain MT3. It is highly probable that complex mechanisms of transport are involved as well, since the composition of the outer membrane of *Pseudomonas* sp. MT1 was significantly changed in the presence of *A. xylosoxidans* MT3, as shown in the proteomic analysis. However, for the seek of simplicity, all compounds are assumed to freely diffuse within the system.

Also a remarkable reduction in protoanemonin accumulation was observed in the community compared to the single strain MT1 culture during the 2 mM shock loads and moreover, the accumulation of protoanemonin and *cis*-dienelactone showed a transient trend, indicating a possible degradative potential for these compounds within the community.

Protoanemonin detoxification by dienelactone hydrolase has been described in *Pseudomonas* sp. B13 as a poor catalytic process with *cis*-acetylacrylate as the main product (Brückmann et al., 1998). In this present study, no detectable levels of acetylacrylate were observed under the conditions tested. Former studies have shown that protoanemonin binds unspecifically to protein thiol groups, giving an alternative explanation for protoanemonin removal (Schlömann, 1988).

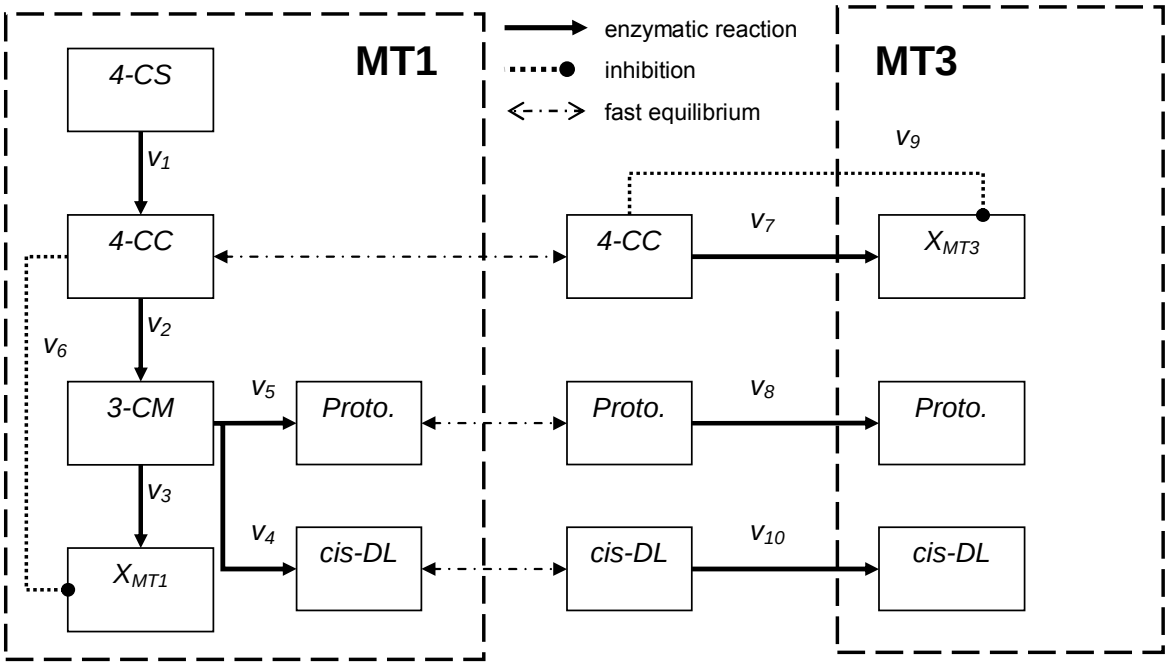

Figure 33. Kinetic metabolic model structure for the upper degradation pathway of 4-chlrosalicylate by *Pseudomonas* sp. MT1 and *Achromobacter xylosoxidans* MT3 community. 4-CS: 4-chlorosalicylate, 4-CC: 4-chlorocatechol, 3-CM: 3-chloromuconate, cis-DL: *cis*-dienelactone, Proto: protoanemonin.7

All the assumptions considered for strain MT1 model were kept and extended for the additional kinetic expressions. From the analyzed substrate shock loads, an inhibitory effect of 4CC on biomass was considered for both strains. The difference in 4CC concentration was attributed to MT3 4CC degrading capacity assuming simple Michaelis-Menten kinetics. Since no direct proof of protoanemoin nor *cis*-dienelactone biodegradation are available, an adsorption and/or unspecific binding to proteins was included to account for the reduced levels as previously described, simplifying the kinetic expressions to one kinetic parameter, assuming saturation conditions. Finally, a fast equilibrium for 4CC, protoanemonin and *cis*-dienelactone was assumed, and no transport mechanism was considered. A schematic representation of the community model structure is shown in Figure 33.

The mass balance equations for the state variables included in the model was given by :

$$\frac{d[4CS]}{dt} = -v_1[X_{MT1}]$$

$$\frac{d[4CC]}{dt} = (v_1 - v_2)[X_{MT1}] - (v_7 / Y_{MT3})[X_{MT3}]$$

$$\frac{d[3CM]}{dt} = (v_2 - (v_3 / Y_{MT1}) - v_4 - v_5)[X_{MT1}]$$

$$\frac{d[X_{MT1}]}{dt} = v_3[X_{MT1}] - v_6$$

$$\frac{d[cis - dienelactone]}{dt} = v_4[X_{MT1}] - v_{10}$$

$$\frac{d[\mathrm{Pr}\,otoanemonin]}{dt} = v_5[X_{MT1}] - v_8$$

$$\frac{d[X_{MT3}]}{dt} = v_7[X_{MT3}] - v_9$$

Based on the previously described assumptions, the kinetic expressions followed simple Michaelis-Menten for individual enzymatic reactions, Monod kinetics in the case of growth and first order irreversible mass action kinetics for protoanemonin and *cis*-dienelactone removal:

$$v_1 = \frac{V_{\max 1}[4CS]}{K_{M1} + [4CS]}$$

$$v_2 = \frac{V_{\max 2}[4CC]}{K_{M2} + [4CC]}$$

$$v_3 = \frac{\mu_{\max MT1}[3CM]}{K_{SMT1} + [3CM]}$$

$$v_4 = \frac{V_{\max 3}[3CM]}{K_{M3} + [3CM]}$$

$$v_5 = \frac{V_{\max 4}[3CM]}{K_{M4} + [3CM]}$$

$$v_6 = k_{tox}[4CC]$$

$$v_7 = \frac{\mu_{\max MT3}[4CC]}{K_{SMT3} + [4CC]}$$

$$v_8 = k_{bind}[X_{MT3}]$$

$$v_9 = k_{tox1}[4CC]$$

$$v_{10} = k_{bind1}[X_{MT3}]$$

5.2.5.2.2 Parameter estimation and sensitivity analysis of *Pseudomonas* sp. MT1 and *A. xylosoxidans* MT3 community kinetic model

Multi-parameter fitting coupled to sensitivity analysis was performed directly evaluating the variation in the model predictions with respect to observed values as described before. Parameter estimation was strongly constrained by the fixed values of the former kinetic parameters reducing the number of possible solutions. Estimation of the yield as well as the specific growth rate was restricted to a range of known values for bacteria (Nielsen et al., 2003).

Table 5. Optimal set of parameters for *Pseudomonas* sp. MT1 and *A. xylosoxidans* MT3 community kinetic model

Parameter	Value	Units
V_{max1}	8.73e-006	[s^{-1}]
V_{max2}	7.40e-006	[s^{-1}]
V_{max3}	2.42e-01	[s^{-1}]
V_{max4}	1.58e-01	[s^{-1}]
μ_{maxMT1}	1.54e-005	[s^{-1}]
μ_{maxMT3}	4.60e-006	[s^{-1}]
K_{M1}	4.30e01	µM
K_{M2}	5.24e-01	µM
K_{M3}	7.39e02	µM
K_{M4}	6.08e02	µM
K_{SMT1}	6.48e-004	µM
K_{SMT3}	3.04e-005	µM
k_{tox}	4.78e-010	[s^{-1}]
K_{tox1}	3.89e-014	[s^{-1}]
K_{bind}	8.61e-011	[s^{-1}]
K_{bind1}	4.82e-011	[s^{-1}]
Y_{MT1}	0.4975	unit less
Y_{MT3}	0.1230	unit less

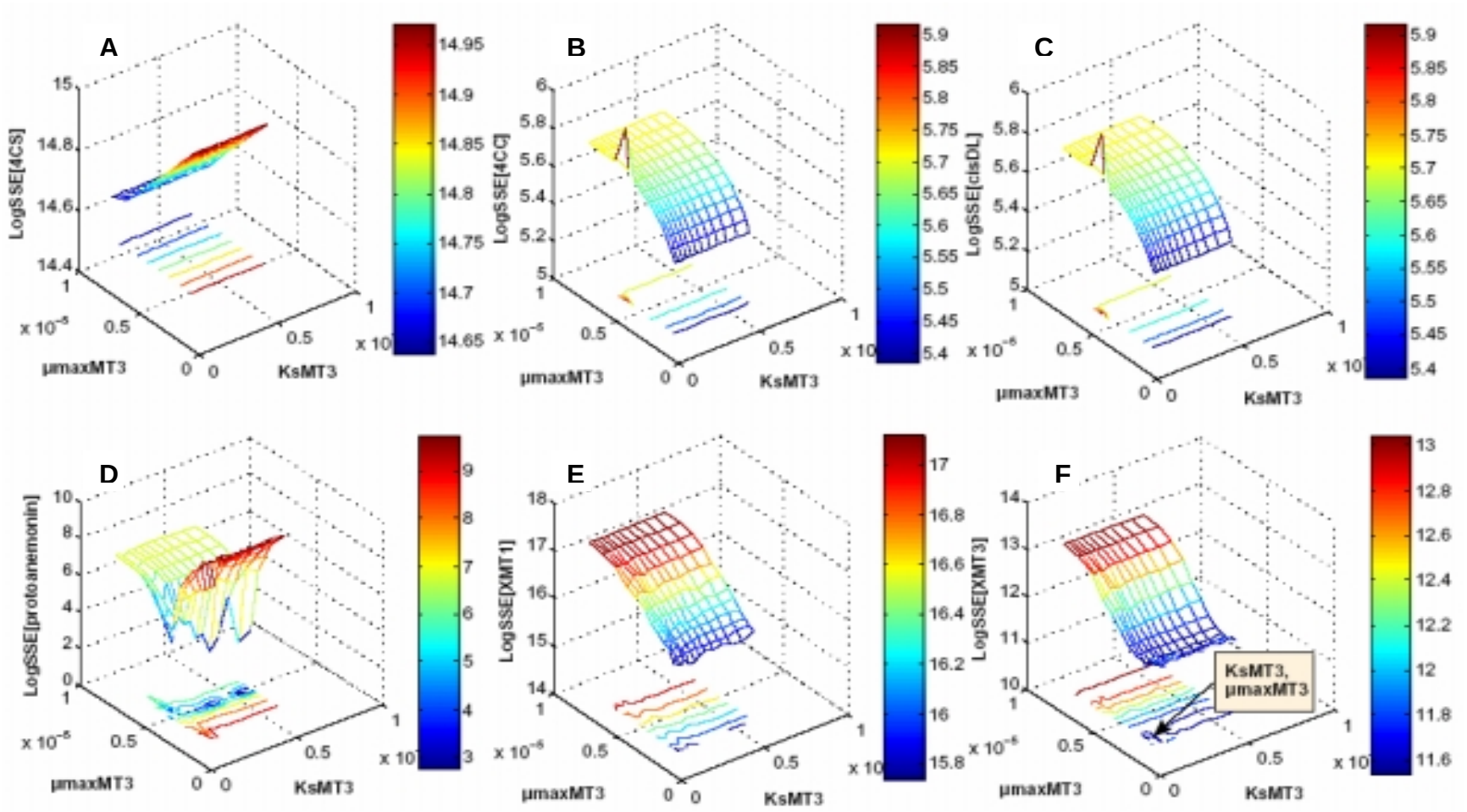

Figure 33. Three-dimensional error space in the kinetic model for *Pseudomonas* sp. MT1 and *A. xylosoxidans* MT3 community model for simultaneous variation of k_{sMT3} and μ_{maxMT3} evaluated for: A, LogSSE[4CS]; B, LogSSE[4CC]; C, LogSSE[*cis*-dienelactone]; D, LogSSE[protoanemonin]; E, LogSSE[X_{MT1}] and F, LogSSE[X_{MT3}]. Color bar shows the logarithm of the error variation range.

5.2.5.2.3 Community model validation

Experimental determinations of dynamic states were used to validate the kinetic model developed for the community. In this case, substrate (4CS) as well as 4CC shock loads were analyzed in order to determine the predictive capacity of the model under different scenarios. Initial conditions for the state variables were used as an input for the model.

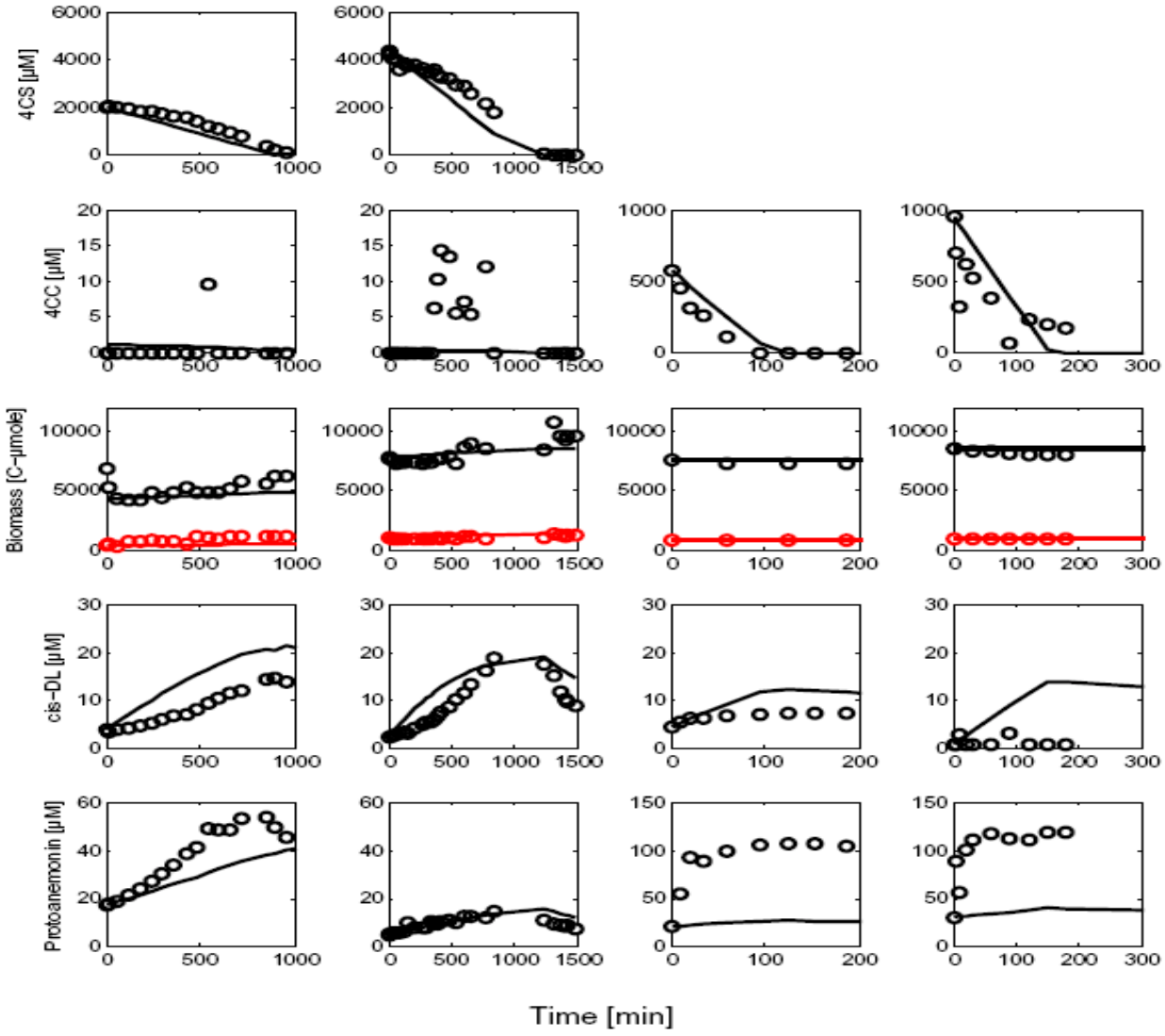

Figure 34. Model validation for a series of dynamic states created by 4-chlorosalicylate and 4-chlorocatechol shock loads in *Pseudomonas* sp. MT1 and *A. xylosoxidans* MT3 community cultures. Biomass panel shows in black X_{MT1} and in red X_{MT3}. Circles and lines represent experimental and predicted values, respectively.

5.2.6 Discussion overview of kinetic modeling in dynamic states

The simplification of complex systems through a series of assumptions, based on accurate determinations of crucial variables, can provide important advances to approach such systems in a systematic way. Simple mathematical models together with standard computational capacity, are powerful tools than can be integrated into the analysis of biological systems. A major drawback for this integration is probably the skepticism of the biological scientific community, based on the poor performance or low predictive power of available models.

During this present study, the analysis of dynamic states in pure strain MT1 culture and in a community culture composed by strains MT1 and MT3 showed a different response. In order to establish a possible mechanistic explanation to such differences, a kinetic metabolic model was initially developed for strain MT1 and, after minor additions, for the community. After optimization, both models showed predictive capacity, provided accurate data for initial conditions were available, attributing the robustness of the community to enhanced biodegradative potential of toxic intermediates. However, the model was unable to predict rapid changes in active biomass content, a critical variable for the system under investigation. These changes, mainly observed by optical density determinations, could be considered as artifacts, since cell aggregation, a known mechanism of bacterial protection, could be the cause of such changes. However, only accounting for this effect, accurate predictions for substrate depletion could be obtained.

After the model optimization stage, a set of sensitive kinetic parameters were obtained. The comparison of these parameters with values published for purified enzymes, show a major discrepancy at the turnover values, being several orders of magnitude different. In the case of salicylate hydroxylase (SalA), reported values are in the order of 2.7 s^{-1}

(BRENDA database) while the value found in the present study was 8.73e-06 s^{-1}. This discrepancy is not compensated in the variation of the second parameter of the corresponding kinetic expression, since the values previously reported for K_M (from 143 to 2.7 μM (BRENDA database)) and the one obtain in this study, 43 μM, where comparable. Similar situations were observed for catechol 1,2-dioxygenase (CatA) and muconate cycloisomerase (MCI). CatA values reported in literature are in the order of 3.1 s^{-1} for the turnover number (Riddler et al., 1998) and in the present study the value obtained was 7.40e-06 s^{-1}. In the case of MCI, the values obtained after optimization were more closed to reported values in both the turnover number (reported 1.07 s^{-1}, this study 0.24 s^{-1}) and the Michaelis constant (reported 1700 μM, this study 739 μM) (Nikodem et al., 2003). This discrepancy has been reported before, where a major difference in the turnover number is attributed to the complex interactions that take place *in vivo*, such as protein-protein interactions or transport mechanisms that are completely absent *in vitro* (Shiraishi & Savageau, 1992; Kuile & Cook, 1994). Therefore, it may be considered that the set of kinetic parameters obtained is taking into account such interactions and consequently, the Michaelis-Menten kinetics are no longer applicable, being the kinetic expression more close to an empirical approach such it is the Monod kinetics for growth. Nevertheless, the simple kinetic expressions are clearly valid showing to be a robust approximation to predict the dynamic behavior of the system under study.

Despite the good correlation between predicted and experimental values for 4CC shock load depletion, a major difference was observed in the prediction of protoanemonin formation. High levels of protoanemonin were registered experimentally while the model predicted fives time lower concentrations. Interestingly, this observation can be related to the importance in substrate uptake and transformation within the community, in view of

the fact that the community response to high substrate loads is not only reduced to higher 4CC degradation capacity, but also to modifications in substrate uptake, preventing higher formation rates of toxic 4CC.

It is clear that the kinetic models developed within this study are limited to a restricted concentration range, and only to those metabolites included as state variables. However, the range of concentrations where the models have shown predictive power vary in one order of magnitude (from 0.5 to 4 mM), and the metabolites include the key intermediates with reported toxicity, becoming a useful tool for *in silico* experimental design and a good base for further modeling development, incorporating more complex kinetic expressions, transport and regulation. Finally, the complementation of simple kinetic models with more complete stoichiometric models, with a detailed description of the central metabolism pathways, assuming a *pseudo*-steady state for the carbon fluxes at this level, can give considerable predictive power to such integrated models in a whole cell scale.

VI. CONCLUSIONS

Bacterial communities perform essential functions for the environmental balance. Their complexity constitutes a major challenge for modern science and step-wise advances in the study of such systems are extremely important.

In this work, a sub-group from a real bacterial community isolated by enrichment from a polluted sediment, was used as a model system to study the metabolic interactions that take place in a rigorous environment, under nutrient limiting conditions and under exposure to toxic compounds, trying to represent conditions more close to real environmental situations. The consortium composed by *Pseudomonas* sp. MT1 and *A. xylosoxidans* MT3, showed to be stable and a particularly interesting model system due to the abundance of strain MT1, being on average 90% of the culture, allowing the specific analysis on the effects of a minor abundant strain in the performance of the first one.

In general terms, the community culture showed a better fitness with higher biomass yields and lower formation of dead-end metabolites. These observations were associated to a higher metabolic versatility within the community, since significant protein expression variations in parallel catabolic pathways were only observed in the mixed culture. To this respect, *Pseudomonas* sp. MT1 posses an enormous metabolic potential reflected in the high redundancy in several key enzymes such as, catechol 1,2-dioxygenases and muconate cycloisomerases with particular combinations of gene clusters producing novel catabolic capacities (Nikodem et al., 2003), and also in oxidative stress response proteins, with two superoxide dismutase and two alkyl hydroperoxide reductase isoenzymes, possibly allowing bacterial persistence under oxidative stress.

A remarkable effect of the presence of strain MT3 was observed in the different expression profile of the outer membrane proteins and transport systems, indicating that changes in the environmental conditions are rapidly sensed, forcing a fast cell response in *Pseudomonas* sp. MT1 to the new conditions. The nature of the signals remained unknown, but certainly a mixture of inducers play a central role, possibly altering the DNA/protein (promoter/regulator) interactions (interaction 3 in Figure 35).

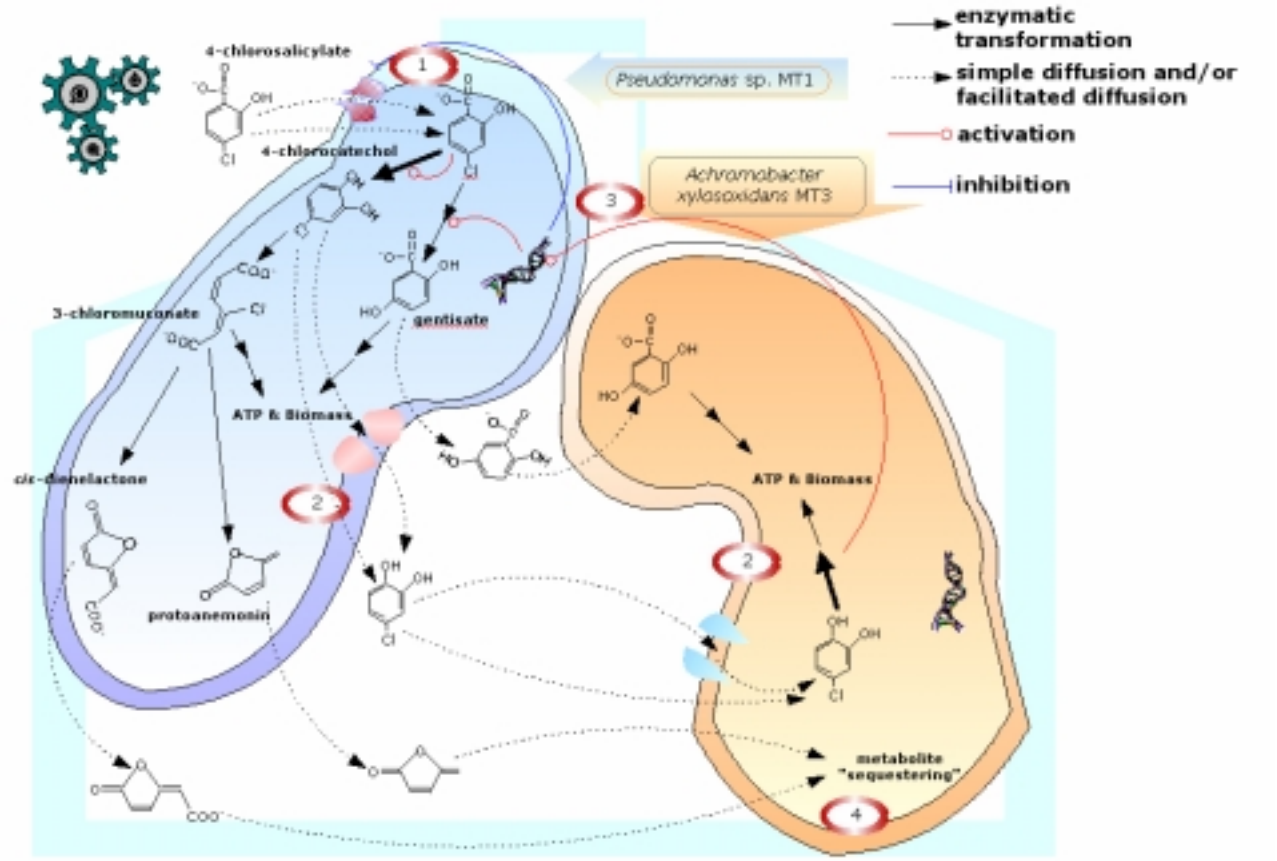

Figure 35. Scheme of proposed bacterial interactions at the upper degradation pathway of 4CS in the 'sub-MT community' composed by *Pseudomonas* sp. MT1 and *Achromobacter xylosoxidans* MT3. 1: altered substrate uptake. 2: alteration of outer membrane permeability. 3: activation of parallel pathways. 4: possible mechanism for dead-end product quenching.

The outer membrane seems to act as an important barrier for the selective transport of substrate and pathway intermediates under the conditions tested (interactions 1 and 2 in Figure 35), as well as a protective layer showing important changes in protein content (porin concentration and composition), and possibly in lipid and/or carbohydrate constitution, depending on the cell requirements.

Perhaps the most striking outcome of the present study was the observation of a remarkably different response to 4CS shock loads. The response of the pure culture involved a strong oxidative stress response, while the community showed an enhanced central metabolism response, clearly related to the transient accumulation of toxic intermediates possibly due to a less efficient combination of upper degradative enzymes leading to formation of higher concentrations of the dead-end metabolite protoanemonin.

As previously discussed, kinetic models can be valuable tools for experimental design provided enough accurate information is available. Simple algebraic expressions can produce interesting outputs with predictive value, that might be able to guide the experimental process, and work as a summary instrument for the obtained knowledge of the system under study.

In summary, the comparison between cultures of *Pseudomonas* sp. strain MT1 and the consortium composed by strain MT1 plus *Achromobacter xylosoxidans* strain MT3, appeared as an attractive model system to study bacterial interactions under restricted environments, including carbon limiting and culture exposure to toxic compounds, providing the following conclusions:

(1) The presence of minor proportions (~10%) of *A. xylosoxidans* strain MT3 significantly affect the metabolic performance of the most abundant community member, *Pseudomonas* sp. MT1 (i) activating the expression of parallel catabolic pathways under carbon-limiting conditions, and (ii) changing its cellular envelope with a new arrangement of outer membrane proteins and transport systems both under carbon-limiting conditions as well as at high concentrations of toxic intermediates 4CC and protoanemonin.

(2) The observed bacterial interactions between strains MT1 and MT3 included an efficient biodegradative capacity, with a strong reduction in toxic intermediate accumulation rates due to (i) a higher metabolic versatility and (ii) a combination of selective transport mechanisms and modifications of the outer membrane permeability.

(3) Overall, the bacterial community studied showed higher stability and robustness compared to the single strain culture, showing a better fitness under severe carbon-limiting conditions and high xenobiotic loads.

VII. OUTLOOK

Bacterial communities represent one of the most important biological components of ecosystems, involving complex spatial and temporal organization and their study and analysis constitutes a major challenge for modern science.

The MT community represents a unique model system where bacterial interactions in a community formed by environmental isolates can be evaluated. The present study analyze some aspects of the interactions among the most abundant members of the MT community, *Pseudomonas* sp. MT1 and *A. xylosoxidans* MT3. The metabolite and proteomic profiles showed important effects under stress conditions, where the response of the most abundant community member changed in the presence of the second strain.

Several aspects can be considered for further studies in this model system. First, the interactions that affect the community performance by alteration of the substrate uptake and the role of the outer membrane as a selective permeation barrier. Particularly, the analysis of genetically modified strains of *Pseudomonas* sp. MT1, mainly K*opf* mutants, could elucidate the role of this major outer membrane protein under the culture conditions tested. Most studies carried out in aromatic transport are related to detoxification mechanism for the active efflux of solvents and antibiotics outside the cell. Several gene clusters containing sets of catabolic enzymes include transporters that are assumed to be involved in aromatic substrate uptake, however, specific deletions of single transporter genes have shown non-essential functions. Therefore, the role of aromatic substrate transport, though probably shared among several transport systems, could be restricted by the outer membrane permeability, where unspecific porins may constitute the major gate.

Second, considering the complexity of natural bacterial communities and the environmental conditions in which this biological systems develop, the incorporation of a third strain and the alternation of different carbon sources can give some insight into more complex interactions. In the first case, a straight forward approach is the incorporation of *Pseudomonas veronii* strain MT4, previously related to protoanemonin detoxification within the MT community (Pelz et al., 1999). Since the abundance of strain MT4 is considerably low (>10%) under similar culture conditions as the ones used in this study (Pelz et al., 1999; Tillmann, 2004), an analogous approach can be achieved, analyzing the metabolite profile and particularly the variations in the proteome of strain MT1 in a three strains community. However, incorporation of a third strain at extreme low composition (>1%) may not significantly alter the behavior. An interesting approach was carried out adding alternative carbon sources in order to promote significant variations in MT community composition (Rabenau, 2004). The non-chlorinated analog salicylate appears as an attractive substrate, due that both strains MT1 and MT3 are able to mineralize it. Moreover, strain MT1 degrades salicylate via catechol and strain MT3 does it via gentisate (data not shown), showing an interesting scenario where both strains will compete for the substrate. In the best case, single substrate or mixtures can be used to achieve a steady state with an equilibrated proportion of both strains (ideally 50:50), where the metaproteome can be assessed, provided there is previous information on the single strain proteome, such as a reference map for pure strains MT1 and MT3 grown in salicylate. The use of DIGE could also reduce gel-to-gel variations improving the reproducibility and allowing the comparison of different samples in the same gel slab.

An ambitious but certainly interesting approximation, could be the creation of a protein database derived after sequencing and annotation of all MT community members (or at

least the most abundant), in a similar way as the community proteomic approach used by Ram and co-workers (Ram et al., 2005). This would facilitate the proteome analysis since the PMF searches can be carried out directly on a database specifically created containing all annotated proteins, with an improvement in protein identification. Besides, sequencing has the advantage to provide full information about the community genetic

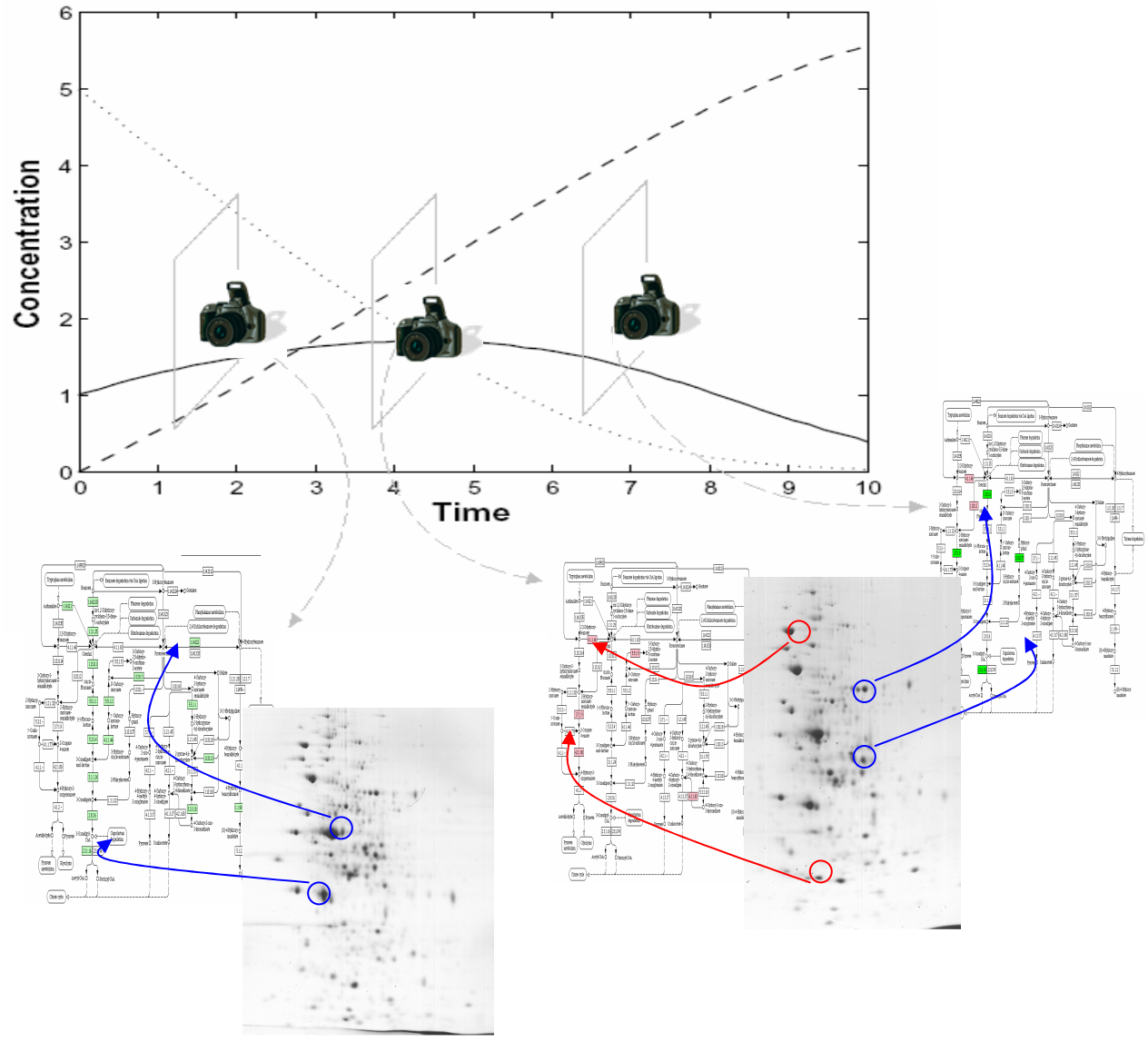

Figure 36. Integration of kinetic and stoichiometric models via metabolic snapshot views as a tool for complex proteomic pattern interpretation.

potential, allowing the reconstruction of independent as well as mixed metabolic networks that could give rise to the first metabolic model at a community scale.

The integration of metabolic models and proteomic analysis is certainly one of the most interesting aspects that should be considered for future studies. Bearing in mind the predictive capacity of the kinetic metabolic model developed in this study, the integration with models of central metabolism can give a qualitative analysis of the fluxes under specific substrate and upper degradation metabolite concentrations given by the kinetic model and used as the input for the stoichiometric model, in particularly interesting dynamic states, assuming a *pseudo*-steady state in a metabolic 'snapshot view' as described in Figure 36, constituting an analysis tool for the interpretation of complex proteomic profiles. Noticeably, intrincate regulatory events are involved and only an integrated analysis including this aspect will lead not only to a more complete description of the system but also to understand complex regulatory networks. To this respect, simple approaches incorporating regulators and gene expression can be initially used, for example, assuming possible activation/inhibition effects on the expression of the upper degradation enzymes in order to determine possible inducer/inhibitor affecting the system's performance. An illustrative example is shown on Figure 37, assuming an inhibition effect of 4CC on CatA expression giving rise to a possible explanation for lower expression levels of this enzyme in single culture with respect to the community culture.

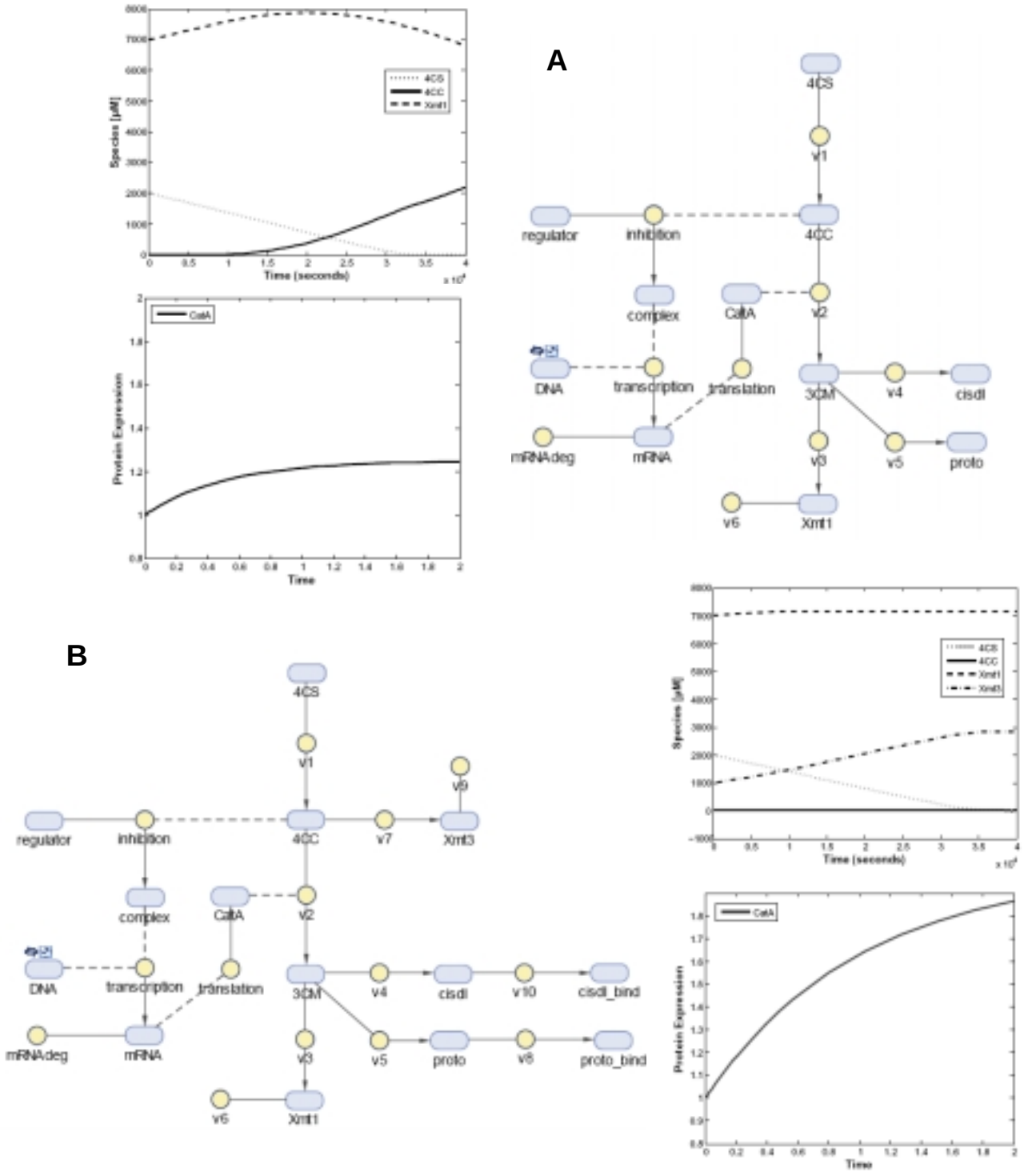

Figure 37. Kinetic model with the incorporation of regulatory events build in MATLAB R2006a and SimBiology version 2.0 (R2006a+) (The Mathworks, Inc., Natick, MA, USA). In the example, 4CC is assumed to inhibit the expression of CatA (catechol 1,2-dioxygenase) in the degradative pathway of strain MT1, showing an enhanced inhibitory effect on the pure culture (A), compared to the community culture (B). CatA protein expression in arbitrary units, without considering protein turnover.

VIII. REFERENCES

Adamczyk J, Hesselsoe M, Iversen N, Horn M, Lehner A, Nielsen PH, Schloter M, Roslev P & Wagner M. 2003. "The isotope array, a new tool that employs substrate-mediated labeling of rRNA for determination of microbial community structure and function". Appl. Environ. Microbiol. 69(11): 6875–6887

Antoine R, Jacob-Dubuisson F, Drobecq H, Willery E, Lesjean S & Locht C, 2003. "Overrepresentation of a gene family encoding extracytoplasmic solute receptors in Bordetella". J. Bacteriol. 185(4):1470-4

Balashova, N. V., Stolz, A., Knackmuss, H. J., Kosheleva, I. A., Naumov, A. V. & Boronin, A. M. 2001. Purification and characterization of a salicylate hydroxylase involved in 1-hydroxy-2-naphthoic acid hydroxylation from the naphthalene and phenanthrene-degrading bacterial strain *Pseudomonas putida* BS202-P1. Biodegradation 12(3): 179-88

Barbour M & Bayly R, 1981. “Control of *meta*-cleavage degradation of 4-hydroxyphenylacetate in *Pseudomonas putida*”. J. Bacteriol. 147(3): 844-50

Benndorf D, Davidson I, & Babel W, 2004. "Regulation of catabolic enzymes during long-term exposure of *Delftia acidovorans* MC1 to chlorophenoxy herbicides". Microbiology 150(Pt 4): 1005-14

Benndorf D, Thiersch M, Loffhagen N, Kunath C, Harms H., 2006. "*Pseudomonas putida* KT2440 responds specifically to chlorophenoxy herbicides and their initial metabolites". Proteomics 6: 1-11

Blasco R, Wittich RM, Mallavarapu M, Timmis KN, Pieper DH., 1995. "From xenobiotic to antibiotic, formation of protoanemonin from 4-chlorocatechol by enzymes of the 3-oxoadipate pathway". JBC 270(49): 29229-35

Blehert D, Fox B & Chambliss G, 1999. "Cloning and sequence analysis of two *Pseudomonas* flavoprotein xenobiotic reductases". J. Bacteriol. 181(20):6254-63

Boening D, 1998. "Toxicity of 2,3,7,8-tetrachlorodibenzo-p-dioxin to several ecological receptor groups: a short review". Ecotoxicol. Environ Saf. 39(3):155-63

Branda SS, Vik S, Friedman L, Kolter R."Biofilms: the matrix revisited". 2005. Trends Microbiol. 13(1): 20-26

Briggs G & Haldane J., 1925."A Note on the Kinetics of Enzyme Action". Biochem. J. 19(2): 338-9

Brückmann M, Blasco R, Timmis K N & Pieper D H, 1998. “Detoxification of protoanemonin by dienelactone hydrolase”. J. Bacteriol. 180(2): 400-2

Bunai K & Yamane K., 2005."Effectiveness and limitation of two-dimensional gel electrophoresis in bacterial membrane protein proteomics and perspectives" J. Chromatogr B. 815(1-2): 227-36

Burk D & Lineweaver H.1930. "The influence of fixed nitrogen on *Azotobacter*". J Bacteriol. 19(6):389-414

Caldas T, El Yaagoubi A & Richarme G., 1998."Chaperone properties of bacterial elongation factor EF-Tu". J. Biol. Chem. 273: 11478–11482

Chen G, 2004. "Reductive dehalogenation of tetrachloroethylene by microorganisms: current knowledge and application strategies". Appl. Microbiol. Biotechnol. 63: 373-77

Chevalier S, Burini J, Freulet-Marriere M, Regeard C, Schoofs G, Guespin-Michel J, De Mot R & Orange N., 2000."Characterization of an OprF-deficient mutant suggests that OprF is an essential protein for *Pseudomonas fluorescens* strain MF0". Res. Microbiol. 151: 619-27

Chiang P, Habash M & Burrows L, 2005. "Disparate subcellular localization patterns of *Pseudomonas aeruginosa* Type IV pilus ATPases involved in twitching motility". J. Bacteriol. 187(3):829-39

Christensen B, Haagensen J, Heydorn A & Molin S. 2002. "Metabolic commensalism and competition in a two-species microbial consortium". Appl. Environ. Microbiol. 68(5): 2495-502

Cornish-Bowden A, 1975. "The use of the direct linear plot for determining initial velocities". Biochem. J. 149(2): 305-12

Crey C, Dumy P, Lhomme J & Kotera M, 2003. “A convenient synthesis of protoanemonin”. Synth. Comm. 33(21): 3727-32

DeLong E, Wickham G & Pace N. 1989. "Phylogenetic stains: ribosomal RNA-based probes for the identification of single cells". Science 243:1360-3

Ditty J & Harwood C, 1999, "Conserved cytoplasmic loops are important for both the transport and chemotaxis functions of PcaK, a protein from *Pseudomonas putida* with 12 membrane-spanning regions". J. Bacteriol. 181(16):5068-74

Edman K, 1950. "The action of ouabain on heart actomyosin". Acta Chem. Scand. 4: 283
Edwards J & Palsson B, 1999."Systems properties of the Haemophilus influenzae Rd metabolic genotype". J. Biol. Chem. 274: 17410-6

Egland P, Palmer R & Kolenbrander P, 2004. "Interspecies communication in *Streptococcus gordonii-Veillonella atypica* biofilms: signaling in flow conditions requires juxtaposition". Proc. Natl. Acad. Sci. 101(48): 16917-22

Famili I, Forster J, Nielsen J & Palsson BO, 2003. "*Saccharomyces cerevisiae* phenotypes can be predicted by using constraint-based analysis of a genome-scale reconstructed metabolic network". Proc. Natl. Acad. Sci. 100: 13134-9

Fayet O, Ziegelhoffer T & Georgopoulos C, 1989. "The groES and groEL heat shock gene products of *Escherichia coli* are essential for bacterial growth at all temperatures". J. Bacteriol. 171(3):1379-85

Fenn J, Mann M, Meng C, Wong S & Whitehouse C, 1989."Electrospray ionization for mass spectrometry of large biomolecules". Science 246: 64-71

Fischer S & Lerman L, 1983. "DNA fragments differing by single base-pair substitutions are separated in denaturing gradient gels: correspondence with melting theory". Proc. Natl. Acad. Sci. 80(6): 1579-83

Fligge T, Bruns K & Przybylski M, 1998. "Analytical development of electrospray and nanoelectrospray mass spectrometry in combination with liquid chromatography for the characterization of proteins". J. Chromatogr. B 706(1): 91-100

Gerlt J, Babbitt P, 2003. "Divergent evolution of enzymatic function: mechanistically diverse superfamilies and functionally distinct suprafamilies". Annu. Rev. Biochem. 70:209-46

Gilligan P, 1991. "Microbiology of airway disease in patients with cystic fibrosis". Clin. Microbiol. Rev. 4:35–51

Gombert A & Nielsen J, 2000. "Mathematical modelling of metabolism". Curr. Opin. Biotechnol. 11: 180-6

Goudar C, Harris S, McInerney M & Suflita J, 2004."Progress curve analysis for enzyme and microbial kinetic reactions using explicit solutions based on the Lambert W function". J. Microbiol. Meth. 59: 317-26

Handelsman J, 2004. "Metagenomics: application of genomics to uncultured microorganisms". Microbiol. Mol. Biol. Rev. 68(4): 669-85

Harder W & Dijkhuizen L, 1983. "Physiological responses to nutrient limitation". Ann. Rev. Microbiol. 37:1-23

Harwood C & Parales R, 1996. "The β-ketoadipate pathway and the biology of self-identity". Annu. Rev. Microbiol. 50:553–90

Heim S, Ferrer M, Heuer H, Regenhardt D, Nimtz M & Timmis K N, 2003. "Proteome reference map of *Pseudomonas putida* strain KT2440 for genome expression profiling: distinct responses of KT2440 and *Pseudomonas aeruginosa* strain PAO1 to iron deprivation and a new form of superoxide dismutase". Environ. Microbiol. 5(12): 1257-69

Hofmann B, Hecht H, Flohé L, 2002. "Peroxiredoxins". Biol. Chem. 383: 347-64

Holben W & Harris D, 1995. "DNA-based monitoring of total bacterial community structure in environmental samples". Mol. Ecol. 4:627-31

Hoskisson P & Hobbs G, 2005. “Continuous culture – making a comeback?”. Microbiology. 151: 3153-9

Hughes E, Shapiro M, Houghton J & Ornston L. 1988."Cloning and expression of pca genes from *Pseudomonas putida* in *Escherichia coli*". J. Gen. Microbiol. 134(11): 2877-87

Hüsken L, Hoogakker J, de Bont J, Tramper J & Beeftink H, 2003. "Model description of bacterial 3-methylcatechol production in one- and two-phase systems". Bioprocess Biosyst. Eng. 26:11 –17

Inoue A & Horikoshi K, 1989. "A *Pseudomonas* thrives in high concentrations of toluene". Nature 338: 264-6

Jensen S, Thompson L & Harry E, 2005. "Cell division in *bacillus subtilis*: ftsz and ftsa association is z-ring independent, and FtsA is required for efficient midcell Z-ring assembly". J. Bacteriol. 187(18): 6536-44

Joshua G, Guthrie-Irons C, Karlyshev A & Wren B, 2006. "Biofilm formation in *Campylobacter jejuni*". Microbiology 152(Pt 2):387-96

Kaminsky F, Bobadilla R & Martins dos Santos V A P, 2006. “Quantitative population dynamics of a 4-chlorosalicylate degrading community by multi-fluorescence *in situ* hybridization coupled to fluorescent-activated cell sorting”. Manuscript in preparation.

Kan J, Hanson T, Ginter J, Wang K & Chen F, 2005."Metaproteomic analysis of Chesapeake Bay microbial communities". Saline Systems 19: 1-7

Kapp E, Schutz F, Connolly L, Chakel J, Meza J, Miller C, Fenyo D, Eng J, Adkins J, Omenn G & Simpson R, 2005. "An evaluation, comparison, and accurate benchmarking of several publicly available MS/MS search algorithms: sensitivity and specificity analysis". Proteomics 5: 3475-90

Karas M & Hillenkamp F, 1988."Laser desorption ionization of proteins with molecular masses exceeding 10,000 daltons". Anal Chem. 60: 2299-301

Katagiri M, Takemori S, Suzuki K & Yasuda H. 1966. "Mechanism of the salicylate hydroxylase reaction". J. Biol. Chem. 241(23):5675-7

Kaulmann U, Kaschabek S & Schlömann M, 2001. "Mechanism of chloride elimination from 3-chloro- and 2,4-dichloro-*cis,cis*-muconate: new insight obtained from analysis of muconate cycloisomerase variant CatB-K169A". J. Bacteriol. 183(15): 4551–61

Keller L & Surette M, 2006."Communication in bacteria: an ecological and evolutionary perspective". Nature 4(4): 249-58

Kelman Z & O'Donnell M, 1995. "DNA polymerase III holoenzyme: structure and function of a chromosomal replicating machine". Annu. Rev. Biochem. 64:171-200

Kent A & Triplett E. 2002. "Microbial communities and their interactions in soil and rhizosphere ecosystems". Annu. Rev. Microbiol. 56:211–36

Kerr R. 1997. "Life goes to extremes in the deep earth--and elsewhere?". Science 276(5313): 703-704

Kim Y, Cho K, Yun S, Kim J, Kwon K, Yoo J & Kim S, 2006. "Analysis of aromatic catabolic pathways in *Pseudomonas putida* KT2440 using a combined proteomic approach: 2-DE/MS and cleavable isotope-coded affinity tag analysis". Proteomics 6(4): 1301-18

Kolker E, Purvine S, Galperin M, Stolyar S, Goodlett D, Nesvizhskii A, Keller A, Xie T, Eng J, Yi E, Hood L, Picone A, Cherny T, Tjaden B, Siegel A, Reilly T, Makarova K, Palsson B & Smith A, 2003."Initial proteome analysis of model microorganism *Haemophilus influenzae* strain Rd KW20". J. Bacteriol. 185(15): 4593-602

Kovarova-Kovar K & Egli T, 1998. "Growth kinetics of suspended microbial cells: from single-substrate-controlled growth to mixed-substrate kinetics". Microbiol. Mol. Boil. Rev. 62(3): 646-66

Kubota K, Kosaka T & Ichikawa K, 2005. "Combination of two-dimensional electrophoresis and shotgun peptide sequencing in comparative proteomics". J. Chromatogr. B 815: 3-9

Kuile, B & Cook M, 1994. “The kinetics of facilitated diffusion followed by enzymatic conversion of the substrate”. Biochim. Biophys. Acta 1193: 235-9

Laidler K, 1955. "Theory of the transient phase in kinetics, with special reference to enzyme systems". Can. J. Chem. 33: 1614-24

Lasa I, 2006. "Towards the identification of the common features of bacterial biofilm development". Int. Microbiol. 9: 21-8

Lazazzera B, 2000. "Quorum sensing and starvation: signals for entry into stationary phase". Curr. Opin. Microbiol. 3(2):177-82

Manefield M, Whiteley A, Griffiths R & Bailey M. 2002. "RNA stable isotope probing, a novel means of linking microbial community function to phylogeny". Appl. Environ. Microbiol. 68(11): 5367-73

Master E, Lai V, Kuipers B, Cullen W & Mohn W. 2002. "Sequential anaerobic-aerobic treatment of soil contaminated with weathered Aroclor 1260". Environ. Sci. Technol. 36: 100-3

Mendes P, 1997. "Biochemistry by numbers: simulation of biochemical pathways with Gepasi 3". Trends Biochem Sci. 22(9):361-3

Mercenier A, Simon J, Vander Wauven C, Haas D, Stalon V, 1980. "Regulation of enzyme synthesis in the arginine deiminase pathway of *Pseudomonas aeruginosa*". J. Bacteriol. 144(1):159-63

Metzgar D, Bacher J, Pezo V, Reader J, Doring V, Schimmel P, Marliere P, de Crecy-Lagard V, 2004. "*Acinetobacter* sp. ADP1: an ideal model organism for genetic analysis and genome engineering". Nucleic Acids Res. 32: 5780-90

Michaelis & Menten, 1913. “Die Kinetik der Invertinwirkung“. Biochem. Z. 49: 333-69

Mohr C, Sonsteby S & Deretic V, 1994. "The *Pseudomonas aeruginosa* homologs of *hemC* and *hemD* are linked to the gene encoding the regulator of mucoidy AlgR". Mol. Gen. Genet. 1994 Jan;242(2):177-84

Monod J, 1949. "The growth of bacterial cultures". Annu. Rev. Microbiol. 3: 371-94

Muskotal A, Kiraly R, Sebestyen A, Gugolya Z, Vegh B & Vonderviszt F, 2006."Interaction of FliS flagellar chaperone with flagellin". FEBS Lett. 580(16):3916-20

Nelson K, Weinel C, Paulsen I, Dodson R, Hilbert H, Martins dos Santos V A, Fouts D, Gill S, Pop M, Holmes M, Brinkac L, Beanan M, DeBoy R, Daugherty S, Kolonay J, Madupu R, Nelson W, White O, Peterson J, Khouri H, Hance I, Chris Lee P, Holtzapple E, Scanlan D, Tran K, Moazzez A, Utterback T, Rizzo M, Lee K, Kosack D, Moestl D, Wedler H, Lauber J, Stjepandic D, Hoheisel J, Straetz M, Heim S, Kiewitz C, Eisen JA, Timmis K N, Dusterhoft A, Tummler B & Fraser C M, 2002. "Complete genome sequence and comparative analysis of the metabolically versatile *Pseudomonas putida* KT2440". Environ. Microbiol. 2002 Dec;4(12):799-808

Nakae T, 1976. "Outer membrane of *Salmonella*. Isolation of protein complex that produces transmembrane channels". J. Biol. Chem. 251(7):2176-8

Nakai C, Nakazawa T, Nozaki M, 1988. "Purification and properties of catechol 1,2-dioxygenase (pyrocatechase) from *Pseudomonas putida* mt-2 in comparison with that from *Pseudomonas arvilla* C-1". Arch. Biochem. Biophys. 267(2):701-13

Nemergut D, Costello E, Meyer A, Pescador M, Weintraub M & Schmidt S. 2005. "Structure and function of alpine and arctic soil microbial communities". Res. Microbiol. 156: 775-84

Nicas T & Hancock R, 1983. "*Pseudomonas aeruginosa* outer membrane permeability: isolation of a porin protein F-deficient mutant". J. Bacteriol. 153(1): 281-5

Nielsen J, Villadsen J & Lidén G. 2003. “Bioreaction Engineering Principles”. 2nd Ed. Kluwer Academic, New York, USA

Nikaido H, 1976. “Outer membrane of *Salmonella typhimurium* transmembrane diffusion of some hydrophobic substances”. Biochim Biophys. Acta 433: 118-32

Nikaido H, 2003. "Molecular basis of bacterial outer membrane permeability revisited". Microbiol. Mol. Biol. Rev. 67(4):593-656

Nikodem P, Hecht V, Schlomann M, Pieper D H. 2003. "New bacterial pathway for 4- and 5-chlorosalicylate degradation via 4-chlorocatechol and maleylacetate in *Pseudomonas* sp. strain MT1". J. Bacteriol. 185(23):6790-800

Nikodem P, 2003. “New bacterial pathways of 4- and 5-chlorosalicylate degradation via 4-chlorocatechol and maleylacetate in a *Pseudomonas* strain". Ph. D. thesis, Fakultät für Lebenswissenschaften, Universität Carolo-Wilhelmina, Braunschweig, Germany

O'Farrell P, 1975. "High resolution two-dimensional electrophoresis of proteins". J. Biol. Chem. 250(10): 4007-21

Oda Y, Huang K, Cross F, Cowburn D & Chait B, 1999. "Accurate quantitation of protein expression and site-specific phosphorylation". Proc. Natl. Acad. Sci. 96(12): 6591-6

Orita M, Suzuki Y, Sekiya T & Hayashi K., 1989. "Rapid and sensitive detection of point mutations and DNA polymorphisms using the polymerase chain reaction". Genomics 5(4): 874-9

Pace N, 1997. "A molecular view of microbial diversity and the biosphere". Science 276(5313):734-40

Pak J, Knoke K, Noguera D, Fox B & Chambliss G, 2000. "Transformation of 2,4,6-trinitrotoluene by purified xenobiotic reductase B from *Pseudomonas fluorescens* I-C". Appl. Environ. Microbiol. 66(11):4742-50

Papin J, Price N, Wiback S, Fell D & Palsson B, 2003. "Metabolic pathways in the post-genome era". TRENDS Biochem. Sci. 28(5): 250-8

Paradis-Bleau C, Sanschagrin F & Levesque R, 2005. "Peptide inhibitors of the essential cell division protein FtsA". Protein Eng. Des. Sel. 18(2):85-91

Pelz O, Tesar M, Wittich R, Moore E, Timmis K N, Abraham W R, 1999. "Towards elucidation of microbial community metabolic pathways: unravelling the network of carbon sharing in a pollutant-degrading bacterial consortium by immunocapture and isotopic ratio mass spectrometry". Environ. Microbiol. 1(2): 167-74

Peng X, Xu C, Ren H, Lin X, Wu L & Wang S, 2005. "Proteomic analysis of the sarcosine-insoluble outer membrane fraction of *Pseudomonas aeruginosa* responding to ampicilin, kanamycin, and tetracycline resistance". J. Proteome Res. 4(6):2257-65

Perkins D, Pappin D, Creasy D & Cottrell J, 1999. "Probability-based protein identification by searching sequence databases using mass spectrometry data". Electrophoresis 20: 3551-67

Price N, Reed J & Palsson B, 2004. "Genome-scale models of microbial cells: evaluating the consequences of constraints". Nature Rev. 2: 886-97

Priscu J, Fritsen C, Adams E, Giovannoni S, Paerl H, McKay C, Doran P, Gordon D, Lanoil B & Pinckney J. 1998. "Perennial Antarctic lake ice: an oasis for life in a polar desert". Science. 280(5372):2095-8

Rabenau A, 2004. "Influence of biotic and abiotic factors on the composition and function of a 4-chlorosalicylate degrading consortium". Ph. D. thesis, Fakultät für Lebenswissenschaften, Universität Carolo-Wilhelmina, Braunschweig, Germany

Radajewski S, Ineson P, Parekh N, Murrell J, 2000. "Stable-isotope probing as a tool in microbial ecology". Nature 10;403(6770):646-9

Raghunathan A, Price N, Galperin M, Makarova K, Purvine S, Picone A, Cherny T, Xie T, Reilly T, Munson R, Tyler R, Akerley B, Smith A, Palsson B & Kolker E., 2004. "n Silico Metabolic Model and Protein Expression of *Haemophilus influenzae* Strain Rd KW20 in Rich Medium". OMICS 8(1): 25-41

Ram R, Verberkmoes N, Thelen M, Tyson G, Baker B, Blake R, Shah M, Hettich R & Banfield J, 2005. "Community proteomics of a natural microbial biofilm". Science 308: 1915-20

Ramos J L, Duque E, Gallegos M, Godoy P, Ramos-González M, Rojas A, Terán W & Segura A, 2002. "Mechanisms of solvent tolerance in Gram-negative bacteria". Annu. Rev. Microbiol. 56: 743-68

Reineke W & Knackmuss H J, 1988. "Microbial degradation of haloaromatics. Annu. Rev. Microbiol. 42:263-87

Righetti P, Castagna A, Antonucci F, Piubelli C, Cecconi D, Campostrini N, Antonioli P, Astner H & Hamdan M, 2004. "Critical survey of quantitative proteomics in two-dimensional electrophoretic approaches". J. Chromatogr . A. 1051(1-2): 3-17

Robinson J & Characklis W, 1984. "Simultaneous estimation of Vmax, Km, and the rate of endogenous substrate production (R) from substrate depletion data". Microb. Ecol. 10: 164-78

Rodriguez-Varela F, 2004. “Environmental genomics, the big picture?”. FEMS Microbiol. Lett. 231: 153-8

Santos P, Benndorf D & Sa-Correia I, 2004. "Insights into *Pseudomonas putida* KT2440 response to phenol-induced stress by quantitative proteomics". Proteomics 4: 2640-52

Sato T, Seyama K, Sato Y, Mori H, Souma S, Akiyoshi T, Kodama Y, Mori T, Goto S, Takahashi K, Fukuchi Y, Maruyama N & Ishigami A. 2006. "Senescence marker protein-30 protects mice lungs from oxidative stress, aging, and smoking". Am. J. Respir. Crit. Care Med. 174(5):530-7

Schilling C, Covert M, Famili I, Church G, Edwards J & Palsson B, 2002. "Genome-scale metabolic model of *Helicobacter pylori* 26695". J. Bacteriol. 184: 4582-93

Schilling C, Edwards J, Letscher D & Palsson B, 2001. "Combining pathway analysis with flux balance analysis for the comprehensive study of metabolic systems". Biotechnol. Bioeng. 71(4): 286-306

Schlömann M, 1988. "Die Verschiedenen typen der dienlacton-hydrolase und Ihre rolle beim bakterielien Abbau von 4-Fluobenzoat". Ph. D. thesis, Fakultät Geo- und Biowissenschaften, Universität Stuttgart, Stuttgart, Germany

Schnell S & Mendoza C, 1997. "Closed form solution for time-dependent enzyme kinetics". J. Theor. Biol. 187: 207-12

Schuster S, Fell D & Dandekar T, 2000. "A general definition of metabolic pathways useful for systematic organization and analysis of complex metabolic networks". Nat Biotechnol. 18(3):326-32

Schweigert N, Hunziker R, Escher B & Eggen R, 2001. "Acute toxicity of (chloro-)catechols and (chloro-)catechol-copper combinations in *Escherichia coli* corresponds to their membrane toxicity in vitro". Environ. Toxicol. Chem. 20: 239-47

Schweigert N, Zehnder A & Eggen R,2001. "Chemical properties of catechols and their molecular modes of toxic action in cells, from microorganisms to mammals". Environ. Microbiol. 3(2): 81-91

Segura A, Godoy P, van Dillewijn P, Hurtado A, Arroyo N, Santacruz S & Ramos J L, 2005. "Proteomic analysis reveals the participation of energy- and stress-related proteins in the response of *Pseudomonas putida* DOT-T1E to toluene". J. Bacteriol. 187(17): 5937-45

Shanley M, Neidle E, Parales R, Ornston L, 1986."Cloning and expression of Acinetobacter calcoaceticus catBCDE genes in *Pseudomonas putida* and *Escherichia coli*". J. Bacteriol. 165(2): 557-63

Shelton D & Tiedje J, 1984. "Isolation and Partial Characterization of Bacteria in an Anaerobic Consortium That Mineralizes 3-Chlorobenzoic Acid". Appl. Environ. Microbiol. 48(4): 840-48

Shim H, Hwang B,Lee S & Kong S, 2005. "Kinetics of BTEX biodegradation by a coculture of Pseudomonas putida and *Pseudomonas fluorescens* under hypoxic conditions". Biodegradation 16:319 –327

Shiraishi F & Savageau M, 1992. "The tricarboxylic acid cycle in *Dictyostelium discoideum*. I. Formulation of alternative kinetic representations". J. Biol. Chem. 267(32): 22912-8

Skiba A, Hecht V & Pieper D H, 2002. “Formation of protoanemonin from 2-chloro-*cis,cis*-muconate by the combined action of muconate cycloisomerase and muconolactone isomerase”. J. Bacteriol. 184(19): 5402-09.

Sparling G, Ord B & Vaughan D. 1981. "Changes in microbial biomass and activity in soils amended with phenolic acids". Soil Biol. Biochem., 13(6): 455-60

Stancik L, Stancik D, Schmidt B, Barnhart M, Yoncheva Y & Slonczewski J, 2002. "pH-Dependent Expression of Periplasmic Proteins and Amino Acid Catabolism in *Escherichia coli*". J. Bacteriol. 184(15): 4246-58

Straathof A, 2001. "Development of a computer program for analysis of enzyme kinetics by progress curve fitting". J. Molec. Catal. B. 11: 991-8

Sugawara E, Steiert M, Rouhani S & Nikaido H, 1996. "Secondary structure of the outer membrane proteins OmpA of *Escherichia coli* and OprF of *Pseudomonas aeruginosa*". J. Bacteriol. 178(20): 6067-9

Sugawara E, Nestorovich E, Bezrukov S, Nikaido H, 2006. "*Pseudomonas aeruginosa* porin OprF exists in two different conformations". J. Biol. Chem. 281(24):16220-9

Sunita S, Zhenxing H, Swaathi J, Cygler M, Matte A & Sivaraman J., 2006."Domain organization and crystal structure of the catalytic domain of *E. coli* RluF, a pseudouridine synthase that acts on 23S rRNA". J. Mol. Biol. 359(4): 998-1009

Taga M & Bassler B, 2003. “Chemimcal communication among bacteria”. Proc. Nat. Acad. Sci. 100(2): 14546-54

Takemori S, Nakamura M, Suzuki K, Katagiri M & Nakamura T, 1972. "Mechanism of the salicylate hydroxylase reaction. V. Kinetic analyses". Biochim Biophys Acta. 284(2):382-93

Tamber S, Ochs M & Hancock R., 2006. "Role of the Novel OprD Family of Porins in Nutrient Uptake in *Pseudomonas aeruginosa*". J. Bacteriol. 188(1): 45-54

Thomas J & Cronan J, 2005. "The enigmatic acyl carrier protein phosphodiesterase of *Escherichia coli*: genetic and enzymological characterization. J. Biol. Chem. 280(41):34675-83

Tillmann S, 2004. “Abschätzung des Abbaupotentials mikrobieller Biozönosen und Identifizierung der am organischen Abbau beteiligten Bakteriengruppen mittels Isotopenmassenspektrometrie (IRMS)”. Ph. D. thesis, Fakultät für Lebenswissenschaften, Universität Carolo-Wilhelmina, Braunschweig, Germany

Tyagi R, Lee Y, Guddat L & Duggleby R, 2005. "Probing the mechanism of the bifunctional enzyme ketol-acid reductoisomerase by site-directed mutagenesis of the active site". FEBS J. 272(2): 593-602

Tyson G, Chapman J, Hugenholtz P, Allen E, Ram R, Richardson P, Solovyev V, Rubin E, Rokhsar D & Banfield J, 2004."Community structure and metabolism through reconstruction of microbial genomes from the environment". Nature 428: 37-43

Unlu M, Morgan M, Minden J, 1997. "Difference gel electrophoresis: a single gel method for detecting changes in protein extracts". Electrophoresis 18(11):2071-7

Vaara M, 1996. "Lipid A: target for antibacterial drugs". Science 274: 939-40

Varma & Palsson, 1993. “Metabolic Capabilities of *Escherichia coli* II. Optimal Growth Patterns”. J. Theor. Biol. 165(4): 503-22

Varma A & Palsson B, 1994. "Stoichiometric flux balance models quantitatively predict growth and metabolic by-product secretion in wild-type Escherichia coli W3110". Appl. Environ. Microbiol. 60(10):3724-31

Varma A, Morbidelli M & Wu H, 1999. Parametric sensitivity in chemical systems. Cambridge university press, 1st Ed., New York, USA

Venter J, Remington K, Heidelberg J, Halpern A, Rusch D, Eisen J, Wu D, Paulsen I, Nelson KE, Nelson W, Fouts D, Levy S, Knap AH, Lomas MW, Nealson K, White O,

Peterson J, Hoffman J, Parsons R, Baden-Tillson H, Pfannkoch C, Rogers Y & Smith H, 2004. "Environmental genome shotgun sequencing of the Sargasso Sea". Science 304(5667): 66-74

Voit E & Savageau M, 1987. "Accuracy of alternative representations for integrated biochemical systems". Biochemistry 26:6869-80

Waage & Guldberg, 1864. Forhandlinger: Videnskabs-Selskabet i Christiana 1864, 35
Wackett L, 2003. "*Pseudomonas putida* a versatile biocatalyst". Nat. Biotechnol. 21(2): 136-8

Wagner M, Nielsen P, Loy A, Nielsen J & Daims H, 2006. "Linking microbial community structure with function: fluorescence *in situ* hybridization-microautoradiography and isotope arrays". Curr. Opin. Biotechnol. 17(1):83-91

Walsh T, Ballou D, Mayer R & Que L, 1983. "Rapid reaction studies of the oxygenation reactions of catechol dioxygenase". J. Biol. Chem. 258(23): 14422-7

Wang L & Tu S, 1984. "The kinetic mechanism of salicylate hydroxylase as studied by intial rate measurement, rapid reaction kinetics, and isotope effects". J. Biol. Chem. 259(17): 10682-8

Washburn M, Wolters D & Yates J, 2001. "Large-scale analysis of the yeast proteome by multidimensional protein identification technology". Nat. Biotechnol. 19(3):242-7

Widmer F, Seidler R, Gillevet P, Watrud L & Di Giovanni G, 1998. "A highly selective PCR protocol for detecting 16S rRNA genes of the genus *Pseudomonas* (*sensu stricto*) in environmental samples". Appl. Environ. Microbiol. 64(7):2545-53

Wittich R, Strompl C, Moore E, Blasco R, Timmis K N, 1999. "Interaction of Sphingomonas and *Pseudomonas* strains in the degradation of chlorinated dibenzofurans". J. Ind. Microbiol. Biotechnol. 23(4-5):353-358

White-Stevens RH, Kamin H, Gibson QH. 1972. "Studies of a flavoprotein, salicylate hydroxylase. I. Enzyme mechanism". J. Biol. Chem. 247(8):2371-81

Wieland G, Neumann R & Backhaus H, 2001. "Variation of microbial communities in soil, rhizosphere, and rhizoplane in response to crop species, soil type, and crop development". Appl. Environ. Microbiol. 67(12): 5849-54

Wilkinson T, Topiwala H & Hamer G, 1974. "Interactions in a mixed bacterial population growing on methane in continuous culture". Biotechnol. Bioeng. 16(1):41-59

Wilmes P & Bond P, 2004. "The application of two-dimensional polyacrylamide gel electrophoresis and downstream analyses to a mixed community of prokaryotic microorganisms". Environ. Microbiol. 6(9): 911-20

Wilmes P & Bond P, 2006. "Metaproteomics: studying functional gene expression in microbial ecosystems". TRENDS Microbiol. 14(2): 92-7

Winnen B, Hvorup R & Saier M, 2003. "The tripartite tricarboxylate transporter (TTT) family". Res. Microbiol. 154(7):457-65

Wright B, 1960. "On enzyme-substrate relationships during biochemical differentiation". Proc. Natl. Acad. Sci. 46(6):798-803

Yu L, Johnson M, Conrads T, Smith R, Morrison R & Veenstra T, 2002. "Proteome analysis of camptothecin-treated cortical neurons using isotope-coded affinity tags". Electrophoresis 23(11): 1591-8

Zhao H, Chen D, Li Y & Cai B, 2005. "Overexpression, purification and characterization of a new salicylate hydroxylase from naphthalene-degrading *Pseudomonas* sp. strain ND6". Microbiol Res. 160(3):307-13

Zhu H, Bilgin M & Snyder M, 2003. "Proteomics". Annu. Rev. Biochem. 72:783-812

Zwirglmaier K, 2005. "Flurorescence *in situ* hybridization (FISH) – the next generation". FEMS Microbiol. Lett. 246: 151-8

IX. APPENDIX

Table ap-1a. Proteome Reference Map List of Proteins Identified in *Pseudomonas* sp. strain MT1 by MALDI-ToF. Scores greater than 1.645 are significant (p<0.05).

Spot No.	Protein Description	Theoretical MW [kDa]	Theoretical pI	Score	Sequence coverage %	Peptides matched	Peptides not-matched	NCBInr accession No.
	Aromatic degradation enzymes							
9	3-carboxy-cis,cis-muconate cycloisomerase	48.869	6.08	1.75	26	5	6	gi|26988113
23	2,3-dihydroxybiphenyl 1,2-dioxygenase	34.969	4.99	2.43	32	8	5	gi|3059192
24	3-oxoadipate:succinyl-CoA transferase, A subunit	31.24	5.9	2.33	22	8	7	gi|48732882
37	3-oxoadipate:succinyl-CoA transferase, B subunit	27.39	5.17	1.75	26	11	56	gi|77381498
57	Protocatechuate 3,4-dioxygenase alpha subunit	20.72	4.8	1.98	21	4	11	gi|48732886
72	hydroxyphenylpyruvate dioxygenase	40.632	5.1	2.43	33	15	12	gi|15596062
81	biphenyl dioxygenase	44.3	5.0	1.98				gi|510288
82	2-keto-4-pentenoate hydratase/2-oxohepta-3-ene-1,7-dioic acid hydratase (catechol pathway)	27.41	5.6	1.84	20	5	3	gi|23015330
84	reductase component of salicylate 5-hydroxylase	36.0	6.2	1.76	40	8	22	gi|27372222
87	catechol 2,3-dioxygenase	35.12	5.4	1.91	32	9	21	gi|14715448
90	Acyl CoA:acetate/3-ketoacid CoA transferase, beta subunit	27.39	5.2	1.68	27	7	6	gi|48732883
114	3-oxoadipate:succinyl-CoA transferase, alpha subunit	25.76	5.5	2.40	34	9	14	gi|48732993
130	xenobiotic reductase B	37.90	5.3	2.43	30	11	12	gi|24982339
	Periplasmic, outer membrane proteins and transporters							

Spot No.	Protein Description	Theoretical MW [kDa]	Theoretical pI	Score	Sequence coverage %	Peptides matched	Peptides not-matched	NCBInr accession No.
27	Uncharacterized protein conserved in bacteria (hypothetical membrane associated protein)	38.87	9.3	1.91	25	7	3	gi|48859490
30	Outer membrane porin F precursor	37.422	4.73	2.43	41	8	7	gi|4530365
31	OprF (Outer membrane protein and related peptidoglycan-associated (lipo)proteins)	37.67	4.80	2.43	30	12	8	gi|48731955|
36	glr2336 (high homology with probable RND efflux membrane fusion protein precursor [Pseudomonas aeruginosa PAO1] gi|9949671)	29.38	8.1	1.69	23	6	3	gi|35212904
42	ABC-type amino acid transport/signal transduction systems, periplasmic component/domain (extracellular solute-binding protein, family 3)	34.194	6.45	2.38	48	21	14	gi|77384759
47	Membrane protease subunits, stomatin/prohibitin homologs (HflC-like protein)	34.26	7.8	1.68	41	9	38	gi|46311920
48	ABC-type amino acid transport/signal transduction systems, periplasmic component/domain	27.56	5.5	2.43	36	11	27	gi|48732828
52	ABC-type amino acid transport/signal transduction systems, periplasmic component/domain (extracellular solute-binding protein, family 3)	27.68	5.5	1.85	48	15	7	gi|48732828
63	yojA (periplasmic ferredoxin-type protein, subunit of nitrate reductase)	15.4	10.9	1.80	63	8	9	gi|405930

Spot No.	Protein Description	Theoretical MW [kDa]	Theoretical pI	Score	Sequence coverage %	Peptides matched	Peptides not-matched	NCBInr accession No.
88	Starvation-inducible outer membrane lipoprotein	21.60	5.9	1.67	55	8	12	gi|42629847
93	ABC-type amino acid transport/signal transduction systems, periplasmic component/domain	36.9	6.5	1.78	24	9	12	gi|48732598
103	ABC-type amino acid transport/signal transduction systems, periplasmic component/domain (extracellular solute-binding protein, family 3)	37.80	6.5	2.08	27	11	5	gi|48732598
109	ABC-type Fe3+-hydroxamate transport system, periplasmic component	37.88	5.6	1.74	34	9	19	gi|66046323
111	outer membrane porin (OprD homolog)	46.46	5.7	2.08	37	14	8	gi|48729184
126	ABC-type amino acid transport/signal transduction systems, periplasmic component/domain (extracellular solute-binding protein, family 3)	37.80	6.5	1.81	26	9	8	gi|48732598
133	porin D	48.46	5.48					gi|70732098
	Cell envelope biogenesis							
5,6,7	Dihydrolipoamide dehydrogenase (E3 component of 2-oxoglutarate dehydrogenase complex) (LPD-GLC) (Dihydrolipoamide dehydrogenase) (Glycine oxidation system L-factor)	51.31	5.9	2.43	40	17	5	gi|1706442
45	Enoyl-[acyl-carrier-protein] reductase (NADH)	28.81	5.27	2.35	36	9	14	gi|48731665
95	Glycosyltransferases involved in cell wall biogenesis	34.4	9.3	2.43	42	10	21	gi|71899363

Spot No.	Protein Description	Theoretical MW [kDa]	Theoretical pI	Score	Sequence coverage %	Peptides matched	Peptides not-matched	NCBInr accession No.
105	UDP-N-acetylglucosamine enolpyruvyl transferase	23.22	10.50	1.70	55	11	8	gi|23006264
122	(3R)-hydroxymyristoyl-[acyl carrier protein] dehydratase ((3R)-hydroxymyristoyl ACP dehydrase)	17.0	6.1	2.43	28	7	9	gi|47605657
	Stress Response							
1	penicillin acylase	98.14	7.33	1.78	18	15	6	gi|46310114
2	Transcription termination factor NusA	55.29	4.5	2.43	12	8	7	gi|23470955
11	D-alanyl-D-alanine carboxypeptidase, fraction A; penicillin-binding protein 5	45.66	8.5	2.43	15	6	11	gi|24050895
16	Translation elongation factor TU	44.32	5.20	2.09	35	13	9	gi|48728524
34	Translation elongation factor Ts	29.90	5.20	1.72	26	7	9	gi|48732722
54	Alkyl hydroperoxide reductase, subunit C	20.428	4.94					
55	Alkyl hydroperoxide reductase, subunit C	20.39	5.0	2.43	34	7	15	gi|48733206
77	CagA (cytotoxin associated protein A)	38.11	9.1	2.40	39	12	13	gi|22335887
92	Universal stress protein UspA	31.388	5.92	2.28	43	11	18	gi|46164823
94	NTP pyrophosphohydrolases including oxidative damage repair enzymes	23.01	4.9	1.76	13	4	21	gi|48834691
99	Chaperonin GroEL	58.499	4.99	1.77	14	9	12	gi|77384725
101	beta-lactamase	33.102	9.5	2.43	43	15	6	gi|76583829
106	Chaperonin Cpn10	10.551	5.68	2.43	46	7	8	gi|77384726
121	Hydrogen peroxide-inducible genes activator	36.13	6.90	2.09	13	4	7	gi|17989239
	Central Metabolism							
4	glutamine synthetase, type I	53.03	5.2	1.95	24	10	18	gi|24986826
10	FKBP-type peptidyl-prolyl cis-trans isomerase (trigger factor)	48.11	4.80	2.00	46	21	8	gi|77383923

Spot No.	Protein Description	Theoretical MW [kDa]	Theoretical pI	Score	Sequence coverage %	Peptides matched	Peptides not-matched	NCBInr accession No.
12	F0F1-type ATP synthase, beta subunit	50.32	4.90	1.83	47	15	16	gi|23469339
13	F0F1-type ATP synthase, beta subunit	50.32	4.90	2.43	45	21	7	gi|23469339
14	ATP synthase F1, alpha subunit	56.44	5.50	2.28	29	24	16	gi|28855956
128	ATP synthase F1, alpha subunit	55.48	5.5	2.28	27	12	3	gi|28855956
129	F0F1-type ATP synthase, alpha subunit	55.5	5.4	2.22	34	16	11	gi|48731319
17	Enolase	46.75	4.90	2.25	27	11	10	gi|48732741
20	succinyl-CoA synthase, beta subunit	41.5	5.8	2.25	37	19	8	gi|48729501
32	Fructose-1,6-bisphosphate aldolase	39.29	5.3	2.43	33	8	4	gi|22995491
39	Succinyl-CoA synthetase, alpha subunit	30.849	6.08	2.24	41	14	11	gi|68343411
56	Acetoacetyl-CoA reductase protein	26.0	6.2	1.78	33	6	31	gi|15967014
73	glyceraldehyde 3-phosphate dehydrogenase	36.49	6.1	2.43	35	11	19	gi|9949314
75	Citrate synthase	48.0	6.2					
113	ATPase associated with various cellular activities, AAA_5	33.34	5.9	2.43	32	9	7	gi|48729699
117	isocitrate dehydrogenase, NADP-dependent, prokaryotic type	46.11	5.4	2.18	27	16	8	gi|48729767
	Amino acid Metabolism							
22	Ketol-acid reductoisomerase	37.19	5.5	2.43	34	13	6	gi|48728466
38	histidinol-phosphate aminotransferase HisH	39.99	4.9	1.65	19	5	9	gi|13475919
58	arginine deiminase	46.69	5.6	2.33	38	21	7	gi|48730780
74	Aspartyl-tRNA synthetase	66.2	5.3	2.43				
104	2-isopropylmalate synthase (Alpha-isopropylmalate synthase) [Amino acid transport and	62.758	5.23	2.43	23	8	24	gi|38257977

Spot No.	Protein Description	Theoretical MW [kDa]	Theoretical pI	Score	Sequence coverage %	Peptides matched	Peptides not-matched	NCBInr accession No.
	metabolism]							
118	Ornithine carbamoyltransferase [Amino acid Metabolism]	38.24	6.1	2.28	56	22	5	gi|48730781
119	Argininosuccinate synthase [Amino acid Metabolism]	45.5	5.4	1.72	32	10	11	gi|48730315
	Cell division and replication							
3	chromosomal replication initiator protein DnaA	54.24	8.30	2.43	14	7	7	gi|28262837
18	DNA-directed RNA polymerase, alpha subunit	37.33	4.90	2.43	36	14	18	gi|28851115
21	DNA polymerase III, delta prime subunit	36.946	6.33	1.80	26	9	7	gi|42735025
26	cell division protein FtsA	44.7	5.2	1.65	54	22	7	gi|68346679
	Transcriptional regulators							
44	Transcriptional Regulator, LysR family	33.643	7.21	1.75	49	12	8	gi|78696079
86	Cyclic nucleotide-binding:Bacterial regulatory protein, Crp	26.618	9.85	1.78	40	9	8	gi|77691852
124	transcriptional regulator OmpR	27.78	5.80	1.66	42	11	5	gi|28896928
	Non- clasified proteins							
33	Porphobilinogen deaminase	34.338	6.06	2.43	36	12	10	gi|19714161
40	L0015-like protein (Transposase IS66 family)	31.30	9.5	1.70	16	3	12	gi|18265862
41	conserved hypothetical protein	34.31	10.5	2.43	42	11	13	gi|33592722
49	response regulator CorR	22.11	6.5	2.43	38	8	57	gi|15282020
70	electron transfer flavoprotein beta-subunit	27.73	5.8	2.43	38	10	9	gi|33592118
78	hypothetical protein Pflu02003553 (putative signal peptide)	50.74	8.9	1.72	29	15	23	gi|48730134

Spot No.	Protein Description	Theoretical MW [kDa]	Theoretical pI	Score	Sequence coverage %	Peptides matched	Peptides not-matched	NCBInr accession No.
79	hypothetical protein (high homology with Phage integrase [Pseudomonas fluorescens PfO-1] GI:77456973)	36.61	9.5	1.71	36	9	5	gi|24985122
80	hypothetical protein (high homology with Phage integrase [Pseudomonas fluorescens PfO-1] GI:77456973)	36.61	9.5	1.71	36	9	19	gi|24985122
85	Uncharacterized conserved protein	39.41	8.8	2.43	21	8	6	gi|23467370
91	repressor of phase I flagellin	20.01	7.9	1.89	52	11	7	gi|46395288
96	transposase	47.37	10.1	2.33	9	5	36	gi|21554219
97	hypothetical protein Pflu02003553	52.00	8.9	1.66	19	7	17	gi|48730134
98	Transposase	20.95	9.6	2.43	28	6	50	gi|29896025
100	flagellar protein FliS	15.22	4.80	1.73	68	7	23	gi|24113301
102	Septum formation inhibitor-activating ATPase	30.46	5.5	1.70	40	9	13	gi|48731998
108	twitching motility protein PilT	38.983	6.33	1.83	46	15	2	gi|53757925
110	delta-aminolevulinic acid dehydratase	37.00	5.4	1.73	18	4	32	gi|21110452
112	TraN-like (conserved hypothetical TraN-like protein found in conjugate transposon)	42.52	5.9	1.65	16	5	9	gi|29611516
115	conserved hypothetical protein (predicted kinase)	48.35	5.6	1.70	13	5	12	gi|16265283
116	Protease subunit of ATP-dependent Clp proteases	23.95	5.40	2.07	23	8	24	gi|38257977
120	Signal recognition particle GTPase	23.34	8.9	1.72	33	8	13	gi|23008862
123	repeat protein K	31.21	6.2	2.43	41	10	9	gi|34369789
125	putative transaldolase-like protein	25.02	5.50	2.43	36	8	3	gi|19746931
131	hypothetical protein	28.0	6.1	1.79	35	8	4	gi|49658854

Table ap-1b. Identification and/or confirmation of proteins in *Pseudomonas* sp. strain MT1 by *ab initio* sequencing and sequence homology search

Spot No.	Protein Description	Theor. MW [kDa]	Theor. pI	Peptide Sequence	Bit Score	Precursor Mass	NCBInr accession No.
5	Dihydrolipoamide dehydrogenase	49.765	5.92	MAAANDTGGFVK	32.5	1181.39	gi|1706442
6	Dihydrolipoamide dehydrogenase	49.765	5.92	LALGGTCLDVGAAMPSK	33.3	1660.79	gi|1706442
7	Dihydrolipoamide dehydrogenase	49.765	5.92	LDGAEVNVGTFPAFASGR	35.8	1807.79	gi|1706442
8	UDP-N-acetylmuramoylalanine-D-glutamate ligase	49.886	5.51	SSEFEERGEK	27.0	1197.39	gi|21204233
19	Branched-chain amino acid ABC transporter, periplasmic amino acid-binding protein	39.656	6.41	FSDEDPANVPSADAFK	31.5	1709.59	gi|70728680
22	Ketol-acid reductoisomerase	36.236	5.47	NVALSYAAGVGGGR	36.2	1291.59	gi|70732562
25	Salicylate hydroxylase	46.890	5.19	ALDGLGLGDAYR	29.9	1220.39	gi|82393825
24	3-oxoadipate:succinyl-CoA transferase, A subunit	30.892	5.75	TFPNNLYDQLLGAGGCAR	34.3	1909.79	gi|68342996
28	Catechol 1,2-dioxygenase	33.573	4.87	ENQLGLAGGTPR TLEGPLYVANAMQGEGQAR	30.2 35.9	1212.39 2004.79	gi|400768
29	Putative oxygenase	30.544	5.45	DYVAGYTCLADNSAR	34.1	1859.59	gi|33573503
30	Outer membrane porin F precursor	36.567	4.69	LYFTDNFMCR	27.6	1309.51	gi|130681
31	OprF [Fragment]	33.379	4.49	LAYDEVHNVR LYFTDNFYAR QVLTNQYGVESSR	31.7 35.6 39.4	1215.39 1309.39 1480.59	gi|37704670
35	Tricarboxylate transport protein TctC, putative	35.191	5.62	LAQSALVNEK	33.4	1072.39	gi|70728818
39	succinyl-CoA synthase, alpha subunit	30.688	8.19	AQVDHGEANAAHWVK	30.8	1632.79	gi|83746093
39	Succinyl-CoA synthetase, alpha subunit	29.944	6.08	FAALQDAGAR RSGTLTYCPVK PAVAATGATASVLYVPA	27.8 24.8 36.6	1019.39 1454.59 2108.79	gi|70729112

Spot No.	Protein Description	Theor. MW [kDa]	Theor. pI	Peptide Sequence	Bit Score	Precursor Mass	NCBInr accession No.
43	NmrA-like	26.812	5.15	YFGSVLDDQSLTAGK	37.1	1600.59	gi|77458502
46	Protocatechuate 3,4-dioxygenase, beta subunit	26.292	6.18	SLPSYALGYR DNDLGPPQGER	31.4 27.8	1126.39 1197.39	gi|70728700
51	Isochorismatase hydrolase	22.836	5.16	NNVLALG	24.0	1127.39	gi|77382197
53	(Acyl-carrier protein) phosphodiesterase	21.765	5.70	QLTQTFLSGAWK	27.4	1379.59	gi|77381662
54	Alkyl hydroperoxide reductase, C subunit	20.507	4.98	LVELNDGGVGR	32.6	1128.39	gi|26989162
55	Alkyl hydroperoxide reductase, C subunit	20.507	4.98	AEDATLAPSLDLVGLK	32.1	1612.79	gi|26989162
59	Superoxide dismutase [Fe]	22.122	5.58	ALTEAFGSVAK	28.8	1093.39	gi|2511749
60	Superoxide dismutase [Fe]	21.807	5.56	FVAEQFEGK	31.0	1054.39	gi|24982333
61	YceI precursor	22.386	7.83	AGFEGTTTLK	29.7	1024.39	gi|77385508
62	Outer membrane protein H1 [Precursor]	21.255	7.88	LFGGVTAGLTK EDADFASLTFGASGTDK YYATYDNVSGSHDGLK	29.9 26.2 44.7	1105.59 1773.59 1831.59	gi|77460462
64	Probable electron transfer flavoprotein	26.581	7.65	ADGSGVDLANAR	31.8	1145.39	gi|17427935
65	extracellular solute-binding protein, family 3	34.640	6.47	LGAAAVFGDATK	32.0	1120.39	gi|77381203
66	BpoC (high homology with arylesterase, POSSIBLE NON-HAEM PEROXIDASE))	30.164	6.63	TDDNPDGPLTEK	30.3	1301.39	gi|41409635
67	Senescence marker protein-30	34.297	5.52	TENGSVYPVRAGGEASGR	31.4	1806.79	gi|91786097
68	UDP-N-acetylenolpyruvoylglucosamine reductase	38.474	9.68	WEALLQYLDLGSLEEEK	27.6	2035.79	gi|30316005
107	3-oxoadipate enol-lactonase	27.974	5.39	WFTPDFSEANPAAAK	32.1	1651.59	gi|70728704
130	Xenobiotic reductase B	37.397	5.53	ALETAELADLVDAYR	42.6	1649.59	gi|70728715
132	Succinate dehydrogenase, iron-sulfur protein	26.135	6.58	LASLDDPFSVFR	40.9	1366.59	gi|28852641
133	porin D	48.46	5.48	LLPEVATGTLLTSNELK	47.3	1798.79	gi|70732098
134	Catechol 1,2-dioxygenase	33.573	4.87	DQQLGLAGGTPR	30.4	1212.59	gi|77458554
135	Electron transfer flavoprotein, alpha	31.261	5.13	TPAPATLNTVAAAAK	40.1	1396.59	gi|63256120

Spot No.	Protein Description	Theor. MW [kDa]	Theor. pI	Peptide Sequence	Bit Score	Precursor Mass	NCBInr accession No.
	subunit						

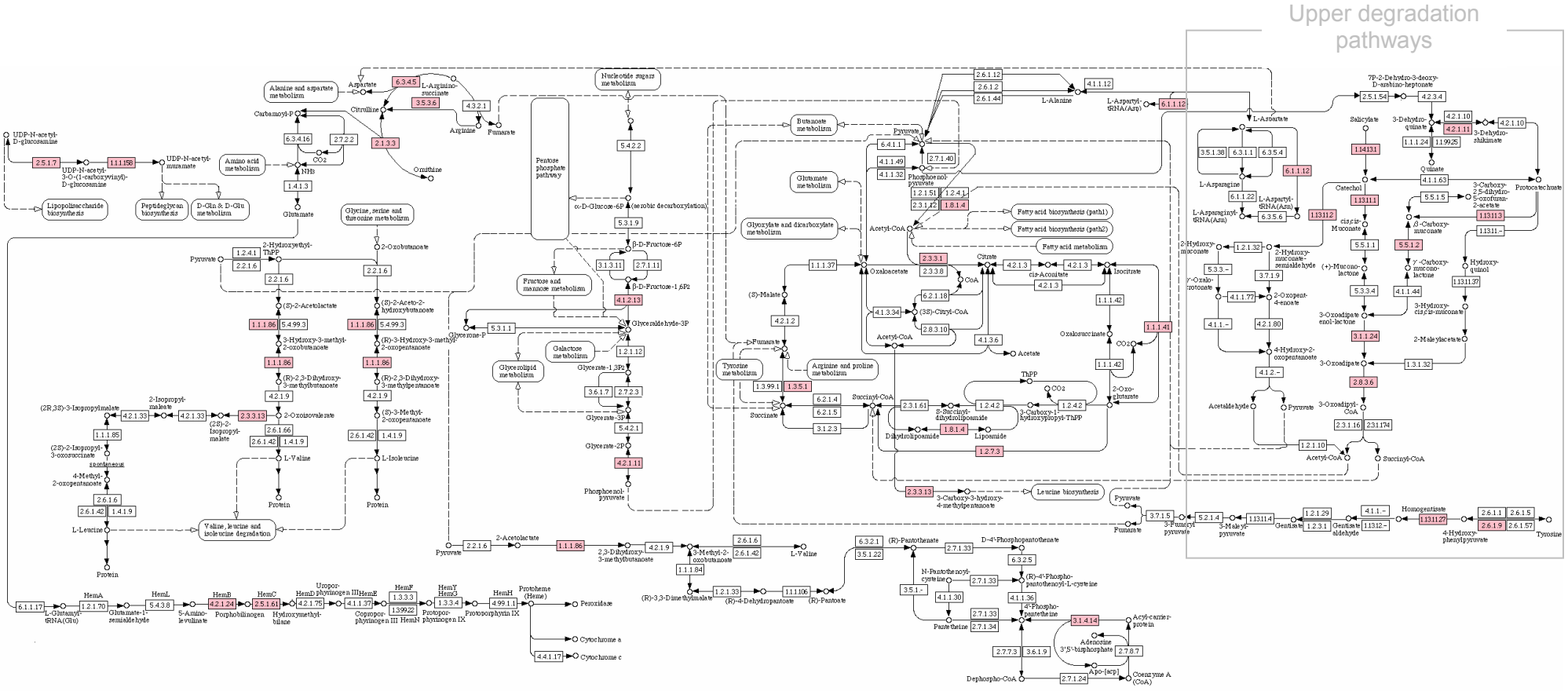

Figure 38. Simplified metabolic map localization of metabolic enzymes identified in *Pseudomonas* sp. MT1 proteome (highlighted in red). Source: KEGG Release 39.0, 2006. Kyoto Encyclopedia of Genes and Genome (KEGG), Kanehisa Laboratory, Bioinformatics Center, Institute for Chemical Research, Kyoto University, Japan.

Table ap-2a. Protein differential expression (DE) comparison of *Pseudomonas* sp. MT1 cultures at D = 0.1 and 0.4 d^{-1} (D = 0.2 d^{-1} as reference for DE = 1.0)

Spot No.	Protein Description	MT1 D=0.1 d^{-1} DE	MT1 D=0.4 d-1 DE
	Aromatic degradation enzymes		
9	3-carboxy-cis,cis-muconate cycloisomerase	0.35 ± 0.01	0.75 ± 0.27
23	2,3-dihydroxybiphenyl 1,2-dioxygenase	0.30 ± 0.07	2.69 ± 0.11
24	3-oxoadipate:succinyl-CoA transferase, A subunit	0.71 ± 0.03	2.30 ± 0.64
25	salicylate hydroxylase	0.22 ± 0.09	2.34 ± 0.54
28	Catechol 1,2-dioxygenase	0.09 ± 0.02	1.11 ± 0.34
29	Putative oxygenase	0.76 ± 0.10	1.48 ± 0.85
37	3-oxoadipate:succinyl-CoA transferase, B subunit	1.61 ± 0.60	0.67 ± 0.07
46	Protocatechuate 3,4-dioxygenase, beta subunit	0.68 ± 0.45	1.32 ± 0.45
57	Protocatechuate 3,4-dioxygenase alpha subunit	2.16 ± 0.10	8.59 ± 3.33
72	hydroxyphenylpyruvate dioxygenase	0.70 ± 0.28	8.29 ± 0.06
81	biphenyl dioxygenase	1.06 ± 0.33	1.36 ± 0.34
82	2-keto-4-pentenoate hydratase/2-oxohepta-3-ene-1,7-dioic acid hydratase (catechol pathway)	0.32 ± 0.15	2.90 ± 1.90
87	catechol 2,3-dioxygenase	1.10 ± 0.26	4.19 ± 1.69
90	3-oxoadipate:succinyl-CoA transferase, B subunit	1.01 ± 0.04	0.73 ± 0.62
107	3-oxoadipate enol-lactonase	0.88 ± 0.45	1.24 ± 0.02
114	3-oxoadipate:succinyl-CoA transferase, alpha subunit	n.d.	1.85 ± 1.06
130	xenobiotic reductase B	0.91 ± 0.08	2.47 ± 0.23
134	Catechol 1,2-dioxygenase	0.24 ± 0.21	1.35 ± 0.05
	Periplasmic, outer membrane proteins and transporters		
19	Branched-chain amino acid ABC transporter, periplasmic amino acid-binding protein	0.36 ± 0.03	1.83 ± 1.26

27	Uncharacterized protein conserved in bacteria (hypothetical membrane associated protein)	0.39 ± 0.28	1.25 ± 0.12
30	Outer membrane porin F precursor	11.10 ± 3.29	0.49 ± 0.10
31	OprF (Outer membrane protein and related peptidoglycan-associated (lipo)proteins)	n.d.	n.d.
35	Tricarboxylate transport protein TctC, putative	1.47 ± 0.04	n.d.
42	ABC-type amino acid transport/signal transduction systems, periplasmic component/domain (extracellular solute-binding protein, family 3)	0.28 ± 0.25	2.66 ± 0.41
47	Membrane protease subunits, stomatin/prohibitin homologs (HflC-like protein)	n.d.	5.74 ± 1.89
48	ABC-type amino acid transport/signal transduction systems, periplasmic component/domain	4.52 ± 1.50	1.22 ± 0.03
52	ABC-type amino acid transport/signal transduction systems, periplasmic component/domain (extracellular solute-binding protein, family 3)	0.79 ± 0.45	5.81 ± 2.25
61	YceI precursor	0.72 ± 0.05	1.31 ± 0.18
62	Outer membrane protein H1 [Precursor]; Starvation-inducible outer membrane lipoprotein	n.d.	3.00 ± 0.47
63	yojA (periplasmic ferredoxin-type protein, subunit of nitrate reductase)	0.52	14.89 ± 15.74
65	extracellular solute-binding protein, family 3	0.39 ± 0.28	1.25 ± 0.12
88	Starvation-inducible outer membrane lipoprotein		30.78 32.68
93	ABC-type amino acid transport/signal transduction systems, periplasmic component/domain	2.33 ± 0.04	1.85 ± 0.35
103	ABC-type amino acid transport/signal transduction systems, periplasmic component/domain (extracellular solute-binding protein, family 3)	2.73 ± 0.20	4.80
109	ABC-type Fe3+-hydroxamate transport system, periplasmic component	0.28 ± 0.13	0.45 ± 0.12
111	outer membrane porin (OprD homolog)	0.50 ± 0.40	1.02 ± 0.63
126	ABC-type amino acid transport/signal transduction systems, periplasmic component/domain (extracellular solute-binding protein, family 3)	1.15 ± 0.73	34.47 ± 20.05
133	porin D	1.39 ± 0.40	0.35 ± 0.02
	Cell envelope biogenesis		
5	Dihydrolipoamide dehydrogenase	1.77 ± 0.17	n.d.
6	Dihydrolipoamide dehydrogenase	1.12 ± 0.45	n.d.

7	Dihydrolipoamide dehydrogenase	0.81 ± 0.23	n.d.
8	UDP-N-acetylmuramoylalanine-D-glutamate ligase	1.38 ± 0.47	0.99 ± 0.18
43	NmrA-like [Cell envelope biogenesis, outer membrane]	0.73 ± 0.37	0.73
45	Enoyl-[acyl-carrier-protein] reductase (NADH)	0.69 ± 0.26	1.51 ± 0.25
53	(Acyl-carrier protein) phosphodiesterase	n.d.	n.d.
68	UDP-N-acetylenolpyruvoylglucosamine reductase	0.38 ± 0.02	0.86 ± 0.02
95	Glycosyltransferases involved in cell wall biogenesis	0.80 ± 0.14	0.36 ± 0.02
105	UDP-N-acetylglucosamine enolpyruvyl transferase	1.13 ± 0.62	1.13 ± 0.95
122	(3R)-hydroxymyristoyl-[acyl carrier protein] dehydratase ((3R)-hydroxymyristoyl ACP dehydrase)	0.89 ± 0.44	n.d.
	Stress Response		
1	penicillin acylase	0.90 ± 0.07	0.60 ± 0.02
2	Transcription termination factor NusA	n.d.	0.69
11	D-alanyl-D-alanine carboxypeptidase, fraction A; penicillin-binding protein 5	n.d.	n.d.
16	Translation elongation factor TU	1.80 ± 0.13	0.96 ± 0.24
34	Translation elongation factor Ts	0.40 ± 0.09	1.61 ± 0.04
54	Alkyl hydroperoxide reductase, subunit C	0.79 ± 0.02	1.44 ± 0.21
55	Alkyl hydroperoxide reductase, subunit C	0.30 ± 0.06	1.24 ± 0.22
59	Superoxide dismutase [Fe]	3.84 ± 0.88	0.93 ± 0.12
60	Superoxide dismutase [Fe]	0.90 ± 0.09	1.39 ± 0.05
66	BpoC (high homology with arylesterase, POSSIBLE NON-HAEM PEROXIDASE))	1.85 ± 0.18	0.94 ± 0.09
77	CagA (cytotoxin associated protein A)	n.d.	1.03 ± 0.03
92	Universal stress protein UspA	0.70 ± 0.71	0.21 ± 0.10
94	NTP pyrophosphohydrolases including oxidative damage repair enzymes	2.31 ± 0.43	0.37
99	Chaperonin GroEL	0.97 ± 0.28	2.69 ± 0.63
101	beta-lactamase	8.65 ± 4.81	24.67
106	Chaperonin Cpn10	n.d. n.d.	7.06 ± 1.19

121	Hydrogen peroxide-inducible genes activator	0.75 ± 0.37	1.91 ± 0.82
	Central Metabolism		
4	glutamine synthetase, type I	0.58 ± 0.19	1.19 ± 0.43
10	FKBP-type peptidyl-prolyl cis-trans isomerase (trigger factor)	0.30 ± 0.13	1.11 ± 0.05
12	F0F1-type ATP synthase, beta subunit	n.d.	n.d.
13	F0F1-type ATP synthase, beta subunit	0.61 ± 0.16	1.66 ± 0.33
14	ATP synthase F1, alpha subunit	2.37 ± 0.38	0.83 ± 0.05
128	ATP synthase F1, alpha subunit	1.46 ± 0.41	0.73 ± 0.27
129	F0F1-type ATP synthase, alpha subunit	0.84 ± 0.35	1.35 ± 0.50
15	FKBP-type peptidyl-prolyl cis-trans isomerase (trigger factor)	n.d.	n.d.
17	Enolase	3.75 ± 0.49	1.40 ± 0.07
20	succinyl-CoA synthase, beta subunit	0.34 ± 0.34	2.12 ± 1.20
32	Fructose-1,6-bisphosphate aldolase	5.96 ± 6.63	1.17 ± 0.01
39	Succinyl-CoA synthetase, alpha subunit	0.28 ± 0.42	1.08 ± 0.19
89	succinyl-CoA synthase, alpha subunit	0.62 ± 0.07	1.81 ± 0.06
56	Acetoacetyl-CoA reductase protein	0.57 ± 0.44	1.73
71	Succinyl-CoA synthetase, beta subunit	0.37 ± 0.32	2.59 ± 0.08
73	glyceraldehyde 3-phosphate dehydrogenase	0.89 ± 0.92	8.29 ± 0.06
75	Citrate synthase	0.90 ± 0.67	0.72 ± 0.54
113	ATPase associated with various cellular activities, AAA_5	1.65	n.d.
117	isocitrate dehydrogenase, NADP-dependent, prokaryotic type	0.26 ± 0.03	2.52 ± 1.01
132	Succinate dehydrogenase, iron-sulfur protein	0.38 ± 0.02	0.96 ± 0.26
	Amino acid Metabolism		
22	Ketol-acid reductoisomerase (KARI)	0.43	0.71 ± 0.30
38	histidinol-phosphate aminotransferase HisH	0.46 ± 0.16	0.91 ± 0.27
58	arginine deiminase	0.25 ± 0.00	0.63 ± 0.03
74	Aspartyl-tRNA synthetase	1.05 ± 0.36	1.01 ± 0.42

104	2-isopropylmalate synthase (Alpha-isopropylmalate synthase) [Amino acid transport and metabolism]	0.56 ± 0.50	1.89 ± 0.33
118	Ornithine carbamoyltransferase [Amino acid Metabolism]	1.22 ± 0.20	2.64
119	Argininosuccinate synthase [Amino acid Metabolism]	0.52 ± 0.28	0.71 ± 0.61
	Cell division and replication		
3	chromosomal replication initiator protein DnaA	1.16 ± 0.61	0.55 ± 0.63
18	DNA-directed RNA polymerase, alpha subunit	1.02 ± 0.79	0.80 ± 0.13
21	DNA polymerase III, delta prime subunit	0.92 ± 0.96	6.43 ± 6.75
26	cell division protein FtsA	1.67 ± 0.76	13.75 ± 7.31
69	RNA-directed DNA polymerase	1.29 ± 0.60	0.31 ± 0.17
	Transcriptional regulators		
44	Transcriptional Regulator, LysR family	0.19 ± 0.23	0.77 ± 0.26
76	putative transcriptional regulator	n.d.	0.86 ± 0.65
86	Cyclic nucleotide-binding:Bacterial regulatory protein, Crp	2.04 ± 1.11	4.74
124	transcriptional regulator OmpR	0.77 ± 0.42	0.51 ± 0.60
	Non- clasified proteins		
33	Porphobilinogen deaminase	3.41 ± 1.71	2.78 ± 0.23
40	L0015-like protein (Transposase IS66 family)	0.78 ± 0.26	0.88 ± 0.14
41	conserved hypothetical protein	0.30 ± 0.15	1.22 ± 0.28
49	response regulator CorR	n.d.	3.72
51	Isochorismatase hydrolase	1.66 ± 0.40	0.89 ± 0.41
64	Probable electron transfer flavoprotein	0.97 ± 0.67	9.71 ± 0.12
67	Senescence marker protein-30	0.06 ± 0.01	0.77 ± 0.26
70	electron transfer flavoprotein beta-subunit	1.16 ± 0.20	8.85 ± 5.29
78	hypothetical protein Pflu02003553 (putative signal peptide)	0.76 ± 0.31	1.04 ± 0.30
79	hypothetical protein (high homology with Phage integrase [Pseudomonas fluorescens PfO-1] GI:77456973)	0.82 ± 0.27	1.12 ± 0.28
80	hypothetical protein (high homology with Phage integrase [Pseudomonas fluorescens PfO-1] GI:77456973)	1.64 ± 1.27	1.07 ± 0.13

85	Uncharacterized conserved protein	1.15 ± 1.12	6.29 ± 0.82
91	repressor of phase I flagellin	1.08 ± 0.31	5.81 ± 4.80
96	transposase	0.67 ± 0.14	2.03 ± 0.48
97	hypothetical protein Pflu02003553	0.78 ± 0.01	0.99 ± 0.52
98	Transposase	0.92 ± 0.12	1.58 ± 0.60
100	flagellar protein FliS	n.d.	1.54 ± 0.03
102	Septum formation inhibitor-activating ATPase	2.98	19.52 ± 2.60
108	twitching motility protein PilT	1.55 ± 0.22	5.69 ± 0.50
110	delta-aminolevulinic acid dehydratase	1.15 ± 0.73	1.74 ± 0.40
112	TraN-like (conserved hypothetical TraN-like protein found in conjugate transposon)	n.d.	n.d.
115	conserved hypothetical protein (predicted kinase)	0.76 ± 0.77	1.02 ± 0.20
116	Protease subunit of ATP-dependent Clp proteases	n.d.	n.d.
120	Signal recognition particle GTPase	n.d.	n.d.
123	repeat protein K	n.d.	n.d.
125	putative transaldolase-like protein	0.62 ± 0.27	1.76 ± 0.06
131	hypothetical protein	n.d.	n.d.

n.d. = not determined

Table ap-2b. Protein differential expression (DE) comparison of community cultures (*Pseudomonas* sp. MT1 and *A. xylosoxidans* MT3) at D = 0.1 d^{-1} (D = 0.2 d^{-1} as reference for DE = 1.0)

Spot No.	Protein Description	MT1 +MT3 D= 0.1 d^{-1} DE
	Aromatic degradation enzymes	
9	3-carboxy-cis,cis-muconate cycloisomerase	0.20 ± 0.11
23	2,3-dihydroxybiphenyl 1,2-dioxygenase	0.87 ± 0.66
24	3-oxoadipate:succinyl-CoA transferase, A subunit	0.75 ± 0.09
25	salicylate hydroxylase	0.37 ± 0.03
28	Catechol 1,2-dioxygenase	0.86 ± 0.01
29	Putative oxygenase	1.47 ± 1.19
37	3-oxoadipate:succinyl-CoA transferase, B subunit	0.60 ± 0.30
46	Protocatechuate 3,4-dioxygenase, beta subunit	1.46 ± 0.12
57	Protocatechuate 3,4-dioxygenase alpha subunit	1.76 ± 1.10
72	hydroxyphenylpyruvate dioxygenase	0.52 ± 0.02
81	biphenyl dioxygenase	1.42 ± 0.67
82	2-keto-4-pentenoate hydratase/2-oxohepta-3-ene-1,7-dioic acid hydratase (catechol pathway) HpaG	17.93 ± 2.76
84	reductase component of salicylate 5-hydroxylase	n.d.
87	catechol 2,3-dioxygenase	0.88 ± 0.24
90	3-oxoadipate:succinyl-CoA transferase, B subunit	0.70 ± 0.19
107	3-oxoadipate enol-lactonase	1.39 ± 1.08
114	3-oxoadipate:succinyl-CoA transferase, alpha subunit	n.d.
130	xenobiotic reductase B	0.79 ± 0.15
134	Catechol 1,2-dioxygenase	0.23 ± 0.05
	Periplasmic, outer membrane proteins and transporters	
19	Branched-chain amino acid ABC transporter, periplasmic amino acid-binding protein	0.34
27	Uncharacterized protein conserved in bacteria (hypothetical membrane associated protein)	0.60 ± 0.36
30	Outer membrane porin F precursor	5.79 ± 1.68
31	OprF (Outer membrane protein and related peptidoglycan-associated (lipo)proteins)	n.d.
35	Tricarboxylate transport protein TctC, putative	0.58 ± 0.36
42	ABC-type amino acid transport/signal transduction systems, periplasmic component/domain (extracellular solute-binding protein, family 3)	0.46 ± 0.31
47	Membrane protease subunits, stomatin/prohibitin homologs (HflC-like protein)	2.18 ± 2.01
48	ABC-type amino acid transport/signal transduction systems, periplasmic component/domain	2.44 ± 0.11

52	ABC-type amino acid transport/signal transduction systems, periplasmic component/domain (extracellular solute-binding protein, family 3)	2.26 ± 0.38
61	YceI precursor	1.38 ± 0.37
62	Outer membrane protein H1 [Precursor]; Starvation-inducible outer membrane lipoprotein	n.d.
63	yojA (periplasmic ferredoxin-type protein, subunit of nitrate reductase)	0.70 ± 0.02
65	extracellular solute-binding protein, family 3	0.40 ± 0.14
88	Starvation-inducible outer membrane lipoprotein	1.13 ± 0.26
93	ABC-type amino acid transport/signal transduction systems, periplasmic component/domain	1.45 ± 0.54
103	ABC-type amino acid transport/signal transduction systems, periplasmic component/domain (extracellular solute-binding protein, family 3)	1.06 ± 0.90
109	ABC-type Fe3+-hydroxamate transport system, periplasmic component	4.58 ± 5.02
111	outer membrane porin (OprD homolog)	0.75 ± 0.02
126	ABC-type amino acid transport/signal transduction systems, periplasmic component/domain (extracellular solute-binding protein, family 3)	1.58 ± 0.08
133	porin D	1.33 ± 1.06
	Cell envelope biogenesis	
5	Dihydrolipoamide dehydrogenase	1.20 ± 0.28
6	Dihydrolipoamide dehydrogenase	1.12 ± 0.13
7	Dihydrolipoamide dehydrogenase	0.65 ± 0.04
8	UDP-N-acetylmuramoylalanine-D-glutamate ligase	0.64 ± 0.07
43	NmrA-like [Cell envelope biogenesis, outer membrane]	0.72 ± 0.15
45	Enoyl-[acyl-carrier-protein] reductase (NADH)	0.35 ± 0.17
53	(Acyl-carrier protein) phosphodiesterase	0.29 ± 0.11
68	UDP-N-acetylenolpyruvoylglucosamine reductase	1.62 ± 0.03
95	Glycosyltransferases involved in cell wall biogenesis	0.90 ± 0.20
105	UDP-N-acetylglucosamine enolpyruvyl transferase	0.72 ± 0.27
122	(3R)-hydroxymyristoyl-[acyl carrier protein] dehydratase ((3R)-hydroxymyristoyl ACP dehydrase)	0.94 ± 0.31
	Stress Response	
1	penicillin acylase	0.77 ± 0.42
2	Transcription termination factor NusA	n.d.
11	D-alanyl-D-alanine carboxypeptidase, fraction A; penicillin-binding protein 5	n.d.
16	Translation elongation factor TU	2.47 ± 0.36
34	Translation elongation factor Ts	0.48 ± 0.05
54	Alkyl hydroperoxide reductase, subunit C	1.34 ± 0.65
55	Alkyl hydroperoxide reductase, subunit C	0.60 ± 0.31
59	Superoxide dismutase [Fe]	5.40 ± 0.08
60	Superoxide dismutase [Fe]	1.81 ± 0.77

66	BpoC (high homology with arylesterase, POSSIBLE NON-HAEM PEROXIDASE))	1.25 ± 0.24
77	CagA (cytotoxin associated protein A)	0.91 ± 0.17
92	Universal stress protein UspA	0.54 ± 0.15
94	NTP pyrophosphohydrolases including oxidative damage repair enzymes	1.02 ± 0.27
99	Chaperonin GroEL	1.68 ± 0.57
101	beta-lactamase	1.52 ± 1.91
106	Chaperonin Cpn10	0.63
121	Hydrogen peroxide-inducible genes activator	1.85 ± 0.99
	Central Metabolism	
4	glutamine synthetase, type I	0.72 ± 0.18
10	FKBP-type peptidyl-prolyl cis-trans isomerase (trigger factor)	0.23 ± 0.20
12	F0F1-type ATP synthase, beta subunit	0.54 ± 0.46
13	F0F1-type ATP synthase, beta subunit	0.47 ± 0.15
14	ATP synthase F1, alpha subunit	0.16 ± 0.10
128	ATP synthase F1, alpha subunit	0.34 ± 0.08
129	F0F1-type ATP synthase, alpha subunit	0.29 ± 0.07
15	FKBP-type peptidyl-prolyl cis-trans isomerase (trigger factor)	n.d.
17	Enolase	0.44 ± 0.22
20	succinyl-CoA synthase, beta subunit	0.33 ± 0.11
32	Fructose-1,6-bisphosphate aldolase	n.d.
39	Succinyl-CoA synthetase, alpha subunit	0.46 ± 0.46
89	succinyl-CoA synthase, alpha subunit	0.98 ± 0.84
56	Acetoacetyl-CoA reductase protein	1.34 ± 1.25
71	Succinyl-CoA synthetase, beta subunit	0.63 ± 0.02
73	glyceraldehyde 3-phosphate dehydrogenase	0.98 ± 1.15
75	Citrate synthase	1.13 ± 0.25
113	ATPase associated with various cellular activities, AAA_5	n.d.
117	isocitrate dehydrogenase, NADP-dependent, prokaryotic type	1.48 ± 0.29
132	Succinate dehydrogenase, iron-sulfur protein	0.97 ± 0.07
	Amino acid Metabolism	
22	Ketol-acid reductoisomerase	1.41
38	histidinol-phosphate aminotransferase HisH	1.40 ± 0.98
58	arginine deiminase	0.19 ± 0.04
74	Aspartyl-tRNA synthetase	1.01 ± 0.47
104	2-isopropylmalate synthase (Alpha-isopropylmalate synthase) [Amino acid transport and metabolism]	0.76 ± 0.06
118	Ornithine carbamoyltransferase [Amino acid Metabolism]	n.d.
119	Argininosuccinate synthase [Amino acid Metabolism]	0.19 ± 0.16
	Cell division and replication	
3	chromosomal replication initiator protein DnaA	1.33 ± 0.71
18	DNA-directed RNA polymerase, alpha subunit	1.23 ± 0.54

21	DNA polymerase III, delta prime subunit	1.60 ± 1.18
26	cell division protein FtsA	1.20 ± 0.32
69	RNA-directed DNA polymerase	0.39 ± 0.09
	Transcriptional regulators	
44	Transcriptional Regulator, LysR family	0.45 ± 0.34
76	putative transcriptional regulator	n.d.
86	Cyclic nucleotide-binding:Bacterial regulatory protein, Crp	1.66 ± 0.48
124	transcriptional regulator OmpR	0.98 ± 0.66
	Non- clasified proteins	
33	Porphobilinogen deaminase (HemC)	2.10 ± 1.36
40	L0015-like protein (Transposase IS66 family)	2.18 ± 2.01
41	conserved hypothetical protein	1.41 ± 1.72
49	response regulator CorR	1.36
51	Isochorismatase hydrolase	1.58 ± 0.25
64	Probable electron transfer flavoprotein	0.69 ± 0.04
67	Senescence marker protein-30	0.47 ± 0.31
70	electron transfer flavoprotein beta-subunit	1.22 ± 0.27
78	hypothetical protein Pflu02003553 (putative signal peptide)	0.54 ± 0.28
79	hypothetical protein (high homology with Phage integrase [Pseudomonas fluorescens PfO-1] GI:77456973)	5.82 ± 2.25
80	hypothetical protein (high homology with Phage integrase [Pseudomonas fluorescens PfO-1] GI:77456973)	0.88 ± 0.17
85	Uncharacterized conserved protein	0.37 ± 0.10
91	repressor of phase I flagellin	0.91 ± 0.07
96	transposase	1.39 ± 0.34
97	hypothetical protein Pflu02003553	1.28 ± 0.24
98	Transposase	1.62 ± 0.67
100	flagellar protein FliS	0.40 ± 0.34
102	Septum formation inhibitor-activating ATPase	1.49 ± 0.21
108	twitching motility protein PilT	1.19 ± 0.36
110	delta-aminolevulinic acid dehydratase	0.81 ± 0.07
112	TraN-like (conserved hypothetical TraN-like protein found in conjugate transposon)	n.d.
115	conserved hypothetical protein (predicted kinase)	1.17 ± 0.03
116	Protease subunit of ATP-dependent Clp proteases	n.d.
120	Signal recognition particle GTPase	1.76 ± 0.06
123	repeat protein K	n.d.
125	putative transaldolase-like protein	1.44 ± 0.76
131	hypothetical protein	n.d.

Table ap-2c. Protein differential expression (DE) comparison of *Pseudomonas* sp. MT1 and community (*Pseudomonas* sp. MT1 and *A. xylosoxidans* MT3) cultures at D = 0.1 d^{-1} (*Pseudomonas* sp. MT1 D = 0.1 d^{-1} as reference for DE = 1.0)

Spot No.	Protein Description	MT1 +MT3 D = 0.1 d^{-1} DE
	Aromatic degradation enzymes	
9	3-carboxy-cis,cis-muconate cycloisomerase	0.30 ± 0.05
23	2,3-dihydroxybiphenyl 1,2-dioxygenase	0.87 ± 0.09
24	3-oxoadipate:succinyl-CoA transferase, A subunit	1.33 ± 0.51
25	salicylate hydroxylase	0.23 ± 0.05
28	Catechol 1,2-dioxygenase	1.67 ± 0.14
29	Putative oxygenase	0.61 ± 0.44
37	3-oxoadipate:succinyl-CoA transferase, B subunit	n.d.
46	Protocatechuate 3,4-dioxygenase, beta subunit	0.78 ± 0.10
57	Protocatechuate 3,4-dioxygenase alpha subunit	0.14 ± 0.05
72	hydroxyphenylpyruvate dioxygenase	2.89 ± 0.77
81	biphenyl dioxygenase	n.d.
82	2-keto-4-pentenoate hydratase/2-oxohepta-3-ene-1,7-dioic acid hydratase (catechol pathway)	3.73 ± 0.66
84	reductase component of salicylate 5-hydroxylase	2.33 ± 0.70
87	catechol 2,3-dioxygenase	0.73 ± 0.04
90	3-oxoadipate:succinyl-CoA transferase, B subunit	1.48 ± 0.65
107	3-oxoadipate enol-lactonase	0.67 ± 0.50
114	3-oxoadipate:succinyl-CoA transferase, alpha subunit	n.d.
130	xenobiotic reductase B	2.64 ± 0.90
134	Catechol 1,2-dioxygenase	2.18 ± 0.07
	Periplasmic, outer membrane proteins and transporters	
19	Branched-chain amino acid ABC transporter, periplasmic amino acid-binding protein	0.90 ± 1.07
27	Uncharacterized protein conserved in bacteria (hypothetical membrane associated protein)	0.74 ± 0.58
30	Outer membrane porin F precursor	0.18 ± 0.15
31	OprF (Outer membrane protein and related peptidoglycan-associated (lipo)proteins)	n.d.
35	Tricarboxylate transport protein TctC, putative	n.d.
36	glr2336 (high homology with probable RND efflux membrane fusion protein precursor [Pseudomonas aeruginosa PAO1] gi|9949671)	n.d.
42	ABC-type amino acid transport/signal transduction systems, periplasmic component/domain (extracellular solute-binding protein, family 3)	0.52 ± 0.07
47	Membrane protease subunits, stomatin/prohibitin homologs (HflC-like protein)	n.d.
48	ABC-type amino acid transport/signal transduction systems, periplasmic component/domain	1.84 ± 0.01

52	ABC-type amino acid transport/signal transduction systems, periplasmic component/domain (extracellular solute-binding protein, family 3)	0.18 ± 0.03
61	YceI precursor	0.69 ± 0.11
62	Outer membrane protein H1 [Precursor]; Starvation-inducible outer membrane lipoprotein	1.79 ± 1.26
63	yojA (periplasmic ferredoxin-type protein, subunit of nitrate reductase)	0.46 ± 0.06
65	extracellular solute-binding protein, family 3	0.40 ± 0.00
88	Starvation-inducible outer membrane lipoprotein	0.91 ± 0.17
93	ABC-type amino acid transport/signal transduction systems, periplasmic component/domain	0.72 ± 0.09
103	ABC-type amino acid transport/signal transduction systems, periplasmic component/domain (extracellular solute-binding protein, family 3)	1.81 ± 0.53
109	ABC-type Fe3+-hydroxamate transport system, periplasmic component	1.47 ± 1.08
111	outer membrane porin (OprD homolog)	0.41 ± 0.19
126	ABC-type amino acid transport/signal transduction systems, periplasmic component/domain (extracellular solute-binding protein, family 3)	1.05 ± 0.47
133	porin D	0.30 ± 0.20
	Cell envelope biogenesis	
5	Dihydrolipoamide dehydrogenase	0.76 ± 0.33
6	Dihydrolipoamide dehydrogenase	0.58 ± 0.19
7	Dihydrolipoamide dehydrogenase	0.37 ± 0.03
8	UDP-N-acetylmuramoylalanine-D-glutamate ligase	1.42 ± 0.48
43	NmrA-like [Cell envelope biogenesis, outer membrane]	0.71
45	Enoyl-[acyl-carrier-protein] reductase (NADH)	0.30 ± 0.09
53	(Acyl-carrier protein) phosphodiesterase	n.d.
68	UDP-N-acetylenolpyruvoylglucosamine reductase	0.64 ± 0.02
95	Glycosyltransferases involved in cell wall biogenesis	1.55
105	UDP-N-acetylglucosamine enolpyruvyl transferase	0.93 ± 0.68
122	(3R)-hydroxymyristoyl-[acyl carrier protein] dehydratase ((3R)-hydroxymyristoyl ACP dehydrase)	n.d.
	Stress Response	
1	penicillin acylase	0.52 ± 0.05
2	Transcription termination factor NusA	1.62 ± 0.40
11	D-alanyl-D-alanine carboxypeptidase, fraction A; penicillin-binding protein 5	n.d.
16	Translation elongation factor TU	1.85 ± 1.39
34	Translation elongation factor Ts	0.32 ± 0.02
54	Alkyl hydroperoxide reductase, subunit C	1.63 ± 0.74
55	Alkyl hydroperoxide reductase, subunit C	1.17 ± 0.29
59	Superoxide dismutase [Fe]	1.11 ± 0.41
60	Superoxide dismutase [Fe]	1.03 ± 0.75
66	BpoC (high homology with arylesterase, POSSIBLE NON-HAEM PEROXIDASE))	1.05 ± 0.55
77	CagA (cytotoxin associated protein A)	n.d.

92	Universal stress protein UspA	0.51 ± 0.01
94	NTP pyrophosphohydrolases including oxidative damage repair enzymes	1.59 ± 1.33
99	Chaperonin GroEL	0.59 ± 0.09
101	beta-lactamase	0.45 ± 0.34
106	Chaperonin Cpn10	n.d.
121	Hydrogen peroxide-inducible genes activator	1.05 ± 0.48
	Central Metabolism	
4	glutamine synthetase, type I	1.02 ± 0.11
10	FKBP-type peptidyl-prolyl cis-trans isomerase (trigger factor)	0.52 ± 0.35
12	F0F1-type ATP synthase, beta subunit	0.82 ± 0.80
13	F0F1-type ATP synthase, beta subunit	0.36 ± 0.00
14	ATP synthase F1, alpha subunit	0.68 ± 0.45
128	ATP synthase F1, alpha subunit	0.95 ± 0.14
129	F0F1-type ATP synthase, alpha subunit	1.23 ± 1.22
15	FKBP-type peptidyl-prolyl cis-trans isomerase (trigger factor)	n.d.
17	Enolase	1.19 ± 0.81
20	succinyl-CoA synthase, beta subunit	1.38 ± 0.80
32	Fructose-1,6-bisphosphate aldolase	0.99 ± 0.47
39	Succinyl-CoA synthetase, alpha subunit	1.07 ± 0.84
89	succinyl-CoA synthase, alpha subunit	0.40 ± 0.40
56	Acetoacetyl-CoA reductase protein	1.25 ± 1.32
71	Succinyl-CoA synthetase, beta subunit	0.21 ± 0.12
73	glyceraldehyde 3-phosphate dehydrogenase	3.88 ± 0.82
75	Citrate synthase	1.90 ± 1.44
113	ATPase associated with various cellular activities, AAA_5	n.d.
117	isocitrate dehydrogenase, NADP-dependent, prokaryotic type	0.28 ± 0.07
132	Succinate dehydrogenase, iron-sulfur protein	0.63 ± 0.15
	Amino acid Metabolism	
22	Ketol-acid reductoisomerase	1.47 ± 0.20
38	histidinol-phosphate aminotransferase HisH	1.45 ± 0.22
58	arginine deiminase	0.67 ± 0.12
74	Aspartyl-tRNA synthetase	0.79 ± 0.09
104	2-isopropylmalate synthase (Alpha-isopropylmalate synthase) [Amino acid transport and metabolism]	1.02 ± 0.24
118	Ornithine carbamoyltransferase [Amino acid Metabolism]	0.81 ± 0.64
119	Argininosuccinate synthase [Amino acid Metabolism]	0.13 ± 0.03
	Cell division and replication	
3	chromosomal replication initiator protein DnaA	0.81 ± 0.15
18	DNA-directed RNA polymerase, alpha subunit	0.74 ± 0.32
21	DNA polymerase III, delta prime subunit	2.27 ± 0.58
26	cell division protein FtsA	2.78 ± 0.78
69	RNA-directed DNA polymerase	0.26 ± 0.03
	Transcriptional regulators	
44	Transcriptional Regulator, LysR family	n.d.

76	putative transcriptional regulator	0.76 ± 0.22
86	Cyclic nucleotide-binding:Bacterial regulatory protein, Crp	0.74 ± 0.10
124	transcriptional regulator OmpR	0.80
	Non- clasified proteins	
33	Porphobilinogen deaminase	0.75 ± 0.37
40	L0015-like protein (Transposase IS66 family)	n.d.
41	conserved hypothetical protein	1.66 ± 2.49
49	response regulator CorR	n.d.
51	Isochorismatase hydrolase	1.65 ± 1.75
64	Probable electron transfer flavoprotein	1.82 ± 0.01
67	Senescence marker protein-30	n.d.
70	electron transfer flavoprotein beta-subunit	1.60 ± 0.29
78	hypothetical protein Pflu02003553 (putative signal peptide)	1.19 ± 0.10
79	hypothetical protein (high homology with Phage integrase [Pseudomonas fluorescens PfO-1] GI:77456973)	1.69 ± 0.19
80	hypothetical protein (high homology with Phage integrase [Pseudomonas fluorescens PfO-1] GI:77456973)	0.88 ± 0.11
83	hypothetical protein HP1454	n.d.
85	Uncharacterized conserved protein	0.74 ± 0.19
91	repressor of phase I flagellin	1.66 ± 2.08
96	transposase	n.d.
97	hypothetical protein Pflu02003553	1.41 ± 0.02
98	Transposase	0.81 ± 0.02
100	flagellar protein FliS	15.51
102	Septum formation inhibitor-activating ATPase	0.99 ± 0.11
108	twitching motility protein PilT	1.37 ± 0.10
110	delta-aminolevulinic acid dehydratase	1.19 ± 0.60
112	TraN-like (conserved hypothetical TraN-like protein found in conjugate transposon)	n.d.
115	conserved hypothetical protein (predicted kinase)	1.13 ± 0.75
116	Protease subunit of ATP-dependent Clp proteases	2.50 ± 0.26
120	Signal recognition particle GTPase	n.d.
123	repeat protein K, TprK (Major Outer Sheath Protein)	n.d.
125	putative transaldolase-like protein	1.05 ± 0.67
131	hypothetical protein	n.d.

Table ap-2d. Protein differential expression comparison of *Pseudomonas* sp. MT1 and community (*Pseudomonas* sp. MT1 and *A. xylosoxidans* MT3) cultures at D = 0.2 d^{-1} (*Pseudomonas* sp. MT1 D = 0.2 d^{-1} as reference for DE = 1.0)

Spot No.	Protein Description	MT1 +MT3 D= 0.2 d^{-1} DE
	Aromatic degradation enzymes	
9	3-carboxy-cis,cis-muconate cycloisomerase	0.69 ± 0.18
23	2,3-dihydroxybiphenyl 1,2-dioxygenase	1.21 ± 0.33
24	3-oxoadipate:succinyl-CoA transferase, A subunit (CatJ alpha)	1.84 ± 0.13
25	salicylate hydroxylase	1.56 ± 0.21
28	Catechol 1,2-dioxygenase	0.53 ± 0.21
29	Putative oxygenase	0.68 ± 0.05
37	3-oxoadipate:succinyl-CoA transferase, B subunit	0.83 ± 0.99
46	Protocatechuate 3,4-dioxygenase, beta subunit	0.85 ± 0.01
57	Protocatechuate 3,4-dioxygenase alpha subunit	2.84 ± 2.93
72	hydroxyphenylpyruvate dioxygenase	1.83 ± 1.83
81	biphenyl dioxygenase	2.90
82	2-keto-4-pentenoate hydratase/2-oxohepta-3-ene-1,7-dioic acid hydratase (catechol pathway)	0.48 ± 0.09
84	reductase component of salicylate 5-hydroxylase	1.01
87	catechol 2,3-dioxygenase	1.79
90	3-oxoadipate:succinyl-CoA transferase, B subunit (CatJ beta)	0.32 ± 0.15
107	3-oxoadipate enol-lactonase (CatD)	2.41 ± 0.05
114	3-oxoadipate:succinyl-CoA transferase, alpha subunit	n.d.
130	xenobiotic reductase B	1.28 ± 0.25
134	Catechol 1,2-dioxygenase	0.80
	Periplasmic, outer membrane proteins and transporters	
19	Branched-chain amino acid ABC transporter, periplasmic amino acid-binding protein	1.10 ± 0.63
27	Uncharacterized protein conserved in bacteria (hypothetical membrane associated protein)	0.90 ± 0.42
30	Outer membrane porin F precursor	0.47 ± 0.07
42	ABC-type amino acid transport/signal transduction systems, periplasmic component/domain (extracellular solute-binding protein, family 3)	1.29 ± 0.91
47	Membrane protease subunits, stomatin/prohibitin homologs (HflC-like protein)	1.33 ± 0.51
48	ABC-type amino acid transport/signal transduction systems, periplasmic component/domain	0.41 ± 0.03
52	ABC-type amino acid transport/signal transduction systems, periplasmic component/domain (extracellular solute-binding protein, family 3)	0.80
61	YceI precursor	0.56 ± 0.30
62	Outer membrane protein H1 [Precursor]; Starvation-inducible outer membrane lipoprotein	1.66 ± 0.67

Spot No.	Protein Description	MT1 +MT3 D= 0.2 d^{-1} DE
63	yojA (periplasmic ferredoxin-type protein, subunit of nitrate reductase)	0.89 ± 0.04
65	extracellular solute-binding protein, family 3	0.90 ± 0.42
88	Starvation-inducible outer membrane lipoprotein	3.85 ± 2.64
93	ABC-type amino acid transport/signal transduction systems, periplasmic component/domain	1.94 ± 0.12
103	ABC-type amino acid transport/signal transduction systems, periplasmic component/domain (extracellular solute-binding protein, family 3)	3.86 ± 1.80
109	ABC-type Fe3+-hydroxamate transport system, periplasmic component	0.35 ± 0.31
111	outer membrane porin (OprD homolog)	1.32 ± 0.94
126	ABC-type amino acid transport/signal transduction systems, periplasmic component/domain (extracellular solute-binding protein, family 3)	1.80 ± 0.05
133	porin D	2.43
	Cell envelope biogenesis	
5	Dihydrolipoamide dehydrogenase	1.20 ± 0.21
6	Dihydrolipoamide dehydrogenase	1.05 ± 0.03
7	Dihydrolipoamide dehydrogenase	0.81 ± 0.24
8	UDP-N-acetylmuramoylalanine-D-glutamate ligase	1.16 ± 0.01
43	NmrA-like [Cell envelope biogenesis, outer membrane]	0.80 ± 0.21
45	Enoyl-[acyl-carrier-protein] reductase (NADH)	1.16 ± 0.19
53	(Acyl-carrier protein) phosphodiesterase	n.d.
68	UDP-N-acetylenolpyruvoylglucosamine reductase	0.56 ± 0.18
95	Glycosyltransferases involved in cell wall biogenesis	0.85 ± 0.07
105	UDP-N-acetylglucosamine enolpyruvyl transferase	0.95 ± 0.33
122	(3R)-hydroxymyristoyl-[acyl carrier protein] dehydratase ((3R)-hydroxymyristoyl ACP dehydrase)	n.d.
	Stress Response	
1	penicillin acylase	1.27 ± 0.82
2	Transcription termination factor NusA	1.57 ± 0.45
11	D-alanyl-D-alanine carboxypeptidase, fraction A; penicillin-binding protein 5	n.d.
16	Translation elongation factor TU	0.47 ± 0.33
34	Translation elongation factor Ts	1.04 ± 0.11
54	Alkyl hydroperoxide reductase, subunit C	1.01 ± 0.37
55	Alkyl hydroperoxide reductase, subunit C	1.23 ± 0.72
59	Superoxide dismutase [Fe]	0.60 ± 0.11
60	Superoxide dismutase [Fe]	0.69 ± 0.27
66	BpoC (high homology with arylesterase, POSSIBLE NON-HAEM PEROXIDASE))	0.52 ± 0.00
77	CagA (cytotoxin associated protein A)	0.72 ± 0.28
92	Universal stress protein UspA	1.16 ± 0.40

Spot No.	Protein Description	MT1 +MT3 D= 0.2 d^{-1} DE
94	NTP pyrophosphohydrolases including oxidative damage repair enzymes	1.36 ± 1.02
99	Chaperonin GroEL	0.76 ± 0.11
101	beta-lactamase	5.42 ± 5.11
106	Chaperonin Cpn10	2.73 ± 0.79
121	Hydrogen peroxide-inducible genes activator	1.18 ± 0.02
	Central Metabolism	
4	glutamine synthetase, type I	1.33 ± 0.55
10	FKBP-type peptidyl-prolyl cis-trans isomerase (trigger factor)	0.76 ± 0.07
12	F0F1-type ATP synthase, beta subunit	1.40 ± 0.88
13	F0F1-type ATP synthase, beta subunit	n.d.
14	ATP synthase F1, alpha subunit	1.37 ± 0.27
128	ATP synthase F1, alpha subunit	1.33 ± 0.08
129	F0F1-type ATP synthase, alpha subunit	1.13 ± 0.14
15	FKBP-type peptidyl-prolyl cis-trans isomerase (trigger factor)	n.d.
17	Enolase	1.31 ± 0.32
20	succinyl-CoA synthase, beta subunit	1.01 ± 0.01
32	Fructose-1,6-bisphosphate aldolase	n.d.
39	Succinyl-CoA synthetase, alpha subunit	1.14 ± 0.03
89	succinyl-CoA synthase, alpha subunit	0.56 ± 0.46
56	Acetoacetyl-CoA reductase protein	1.16
71	Succinyl-CoA synthetase, beta subunit	3.32 ± 2.77
73	glyceraldehyde 3-phosphate dehydrogenase	1.13 ± 0.32
75	Citrate synthase	0.20 ± 0.04
113	ATPase associated with various cellular activities, AAA_5	n.d.
117	isocitrate dehydrogenase, NADP-dependent, prokaryotic type	1.10 ± 1.20
132	Succinate dehydrogenase, iron-sulfur protein	0.05 ± 0.01
	Amino acid Metabolism	
22	Ketol-acid reductoisomerase	0.42 ± 0.14
38	histidinol-phosphate aminotransferase HisH	0.71 ± 0.24
58	arginine deiminase	0.24 ± 0.10
74	Aspartyl-tRNA synthetase	0.95 ± 0.41
104	2-isopropylmalate synthase (Alpha-isopropylmalate synthase) [Amino acid transport and metabolism]	0.66 ± 0.35
118	Ornithine carbamoyltransferase [Amino acid Metabolism]	3.35 ± 2.73
119	Argininosuccinate synthase [Amino acid Metabolism]	1.17 ± 0.10
	Cell division and replication	
3	chromosomal replication initiator protein DnaA	1.31 ± 0.31
18	DNA-directed RNA polymerase, alpha subunit	1.43 ± 0.74
21	DNA polymerase III, delta prime subunit	1.69 ± 0.03
26	cell division protein FtsA	3.58 ± 0.04

Spot No.	Protein Description	MT1 +MT3 D= 0.2 d^{-1} DE
69	RNA-directed DNA polymerase	0.85 ± 0.20
	Transcriptional regulators	
44	Transcriptional Regulator, LysR family	0.64 ± 0.30
76	putative transcriptional regulator	n.d.
86	Cyclic nucleotide-binding:Bacterial regulatory protein, Crp	1.25 ± 0.64
124	transcriptional regulator OmpR	0.61 ± 0.39
	Non- clasified proteins	
33	Porphobilinogen deaminase	2.13 ± 0.20
40	L0015-like protein (Transposase IS66 family)	1.07 ± 0.33
41	conserved hypothetical protein	0.34 ± 0.14
49	response regulator CorR	0.72
51	Isochorismatase hydrolase	0.95 ± 0.33
64	Probable electron transfer flavoprotein	2.85 ± 1.04
67	Senescence marker protein-30	0.65 ± 0.43
70	electron transfer flavoprotein beta-subunit	n.d.
78	hypothetical protein Pflu02003553 (putative signal peptide)	1.26 ± 0.74
79	hypothetical protein (high homology with Phage integrase [Pseudomonas fluorescens PfO-1] GI:77456973)	0.59 ± 0.08
80	hypothetical protein (high homology with Phage integrase [Pseudomonas fluorescens PfO-1] GI:77456973)	6.71 ± 8.31
83	hypothetical protein HP1454	n.d.
85	Uncharacterized conserved protein	6.37 ± 1.99
91	repressor of phase I flagellin	3.85 ± 2.64
96	transposase	0.93 ± 0.33
97	hypothetical protein Pflu02003553	0.67 ± 0.14
98	Transposase	0.97 ± 0.03
100	flagellar protein FliS	1.60 ± 0.20
102	Septum formation inhibitor-activating ATPase	5.05 ± 6.45
108	twitching motility protein PilT	1.41 ± 0.28
110	delta-aminolevulinic acid dehydratase	1.02 ± 0.25
112	TraN-like (conserved hypothetical TraN-like protein found in conjugate transposon)	n.d.
115	conserved hypothetical protein (predicted kinase)	1.62
116	Protease subunit of ATP-dependent Clp proteases	n.d.
120	Signal recognition particle GTPase	n.d.
123	repeat protein K	n.d.
125	putative transaldolase-like protein	0.84 ± 0.33
131	hypothetical protein	n.d.

n.d.: not determined

Table ap-2e. Protein differential expression (DE) comparison of *Pseudomonas* sp. MT1 during 2 mM 4-chlorosalicylate shock load stress (*Pseudomonas* sp. MT1 D = 0.2 d^{-1} before the shock load as reference for DE = 1.0)

Spot No.	Protein Description	MT1 2h DE	MT1 5h DE	MT1 7h DE
	Aromatic degradation enzymes			
9	3-carboxy-cis,cis-muconate cycloisomerase	0.81 ± 0.25	0.42 ± 0.03	1.34 ± 0.06
23	2,3-dihydroxybiphenyl 1,2-dioxygenase	1.74 ± 0.22	0.83 ± 0.16	1.29 ± 0.01
24	3-oxoadipate:succinyl-CoA transferase, A subunit	3.02 ± 0.21	2.12 ± 0.23	2.76 ± 0.29
25	salicylate hydroxylase	1.84 ± 0.17	0.88 ± 0.10	1.19 ± 0.77
28	Catechol 1,2-dioxygenase	0.50 ± 0.09	0.63 ± 0.10	0.32 ± 0.18
29	Putative oxygenase	1.53 ± 0.03	1.03 ± 0.05	1.35 ± 0.10
37	3-oxoadipate:succinyl-CoA transferase, B subunit	1.31 ± 0.22	0.43 ± 0.28	0.42 ± 0.48
46	Protocatechuate 3,4-dioxygenase, beta subunit	1.89 ± 0.28	1.34 ± 0.15	2.51 ± 0.24
57	Protocatechuate 3,4-dioxygenase alpha subunit	4.52 ± 1.51	0.66 ± 0.04	1.15 ± 0.38
72	hydroxyphenylpyruvate dioxygenase	1.04 ± 0.34	1.95 ± 0.32	1.10 ± 0.48
81	biphenyl dioxygenase	1.08 ± 0.06	1.30 ± 0.33	1.05 ± 0.03
82	2-keto-4-pentenoate hydratase/2-oxohepta-3-ene-1,7-dioic acid hydratase (catechol pathway)	0.84 ± 0.01	1.27 ± 0.19	0.72 ± 0.22
84	reductase component of salicylate 5-hydroxylase	1.67 ± 0.36	0.87 ± 0.13	0.95 ± 0.40
87	catechol 2,3-dioxygenase	1.23 ± 0.05	1.85 ± 0.26	1.50 ± 0.86
90	3-oxoadipate:succinyl-CoA transferase, B subunit	0.72 ± 0.18	0.74 ± 0.08	0.77 ± 0.23
107	3-oxoadipate enol-lactonase	1.42 ± 0.04	1.06 ± 0.18	0.99 ± 0.17
114	3-oxoadipate:succinyl-CoA transferase, alpha subunit	3.49 ± 0.33	0.87 ± 0.01	1.37 ± 0.12
130	xenobiotic reductase B	2.53 ± 0.77	3.01 ± 0.30	4.67 ± 0.88
134	Catechol 1,2-dioxygenase	0.46 ± 0.09	0.95 ± 0.00	0.25 ± 0.15
	Periplasmic, outer membrane proteins and transporters			

19	Branched-chain amino acid ABC transporter, periplasmic amino acid-binding protein	1.90 ± 0.53	0.82 ± 0.14	1.57 ± 0.38
27	Uncharacterized protein conserved in bacteria (hypothetical membrane associated protein)	0.92 ± 0.38	0.61 ± 0.05	0.58 ± 0.25
30	Outer membrane porin F precursor	3.04 ± 0.62	5.77 ± 0.50	0.10 ± 0.03
31	OprF (Outer membrane protein and related peptidoglycan-associated (lipo)proteins)	n.d.	n.d.	n.d.
35	Tricarboxylate transport protein TctC, putative	n.d.	n.d.	n.d.
36	glr2336 (high homology with probable RND efflux membrane fusion protein precursor [Pseudomonas aeruginosa PAO1] gi|9949671)	n.d.	n.d.	n.d.
42	ABC-type amino acid transport/signal transduction systems, periplasmic component/domain (extracellular solute-binding protein, family 3)	1.54 ± 0.23	0.52 ± 0.00	0.85 ± 0.60
47	Membrane protease subunits, stomatin/prohibitin homologs (HflC-like protein)	3.04 ± 0.75	n.d.	8.72 ± 8.96
48	ABC-type amino acid transport/signal transduction systems, periplasmic component/domain	0.53 ± 0.11	1.50 ± 0.51	1.41 ± 0.80
52	ABC-type amino acid transport/signal transduction systems, periplasmic component/domain (extracellular solute-binding protein, family 3)	0.42 ± 0.13	0.45 ± 0.09	0.26 ± 0.07
61	YceI precursor	2.90 ± 0.35	4.84 ± 0.63	4.80 ± 0.44
62	Outer membrane protein H1 [Precursor]; Starvation-inducible outer membrane lipoprotein	2.72 ± 0.48	0.71 ± 0.21	0.67 ± 0.07
63	yojA (periplasmic ferredoxin-type protein, subunit of nitrate reductase)	1.07 ± 0.20	3.34 ± 0.61	1.09 ± 0.23
65	extracellular solute-binding protein, family 3	0.71 ± 0.09	0.75 ± 0.24	0.44 ± 0.06
88	Starvation-inducible outer membrane lipoprotein	0.92 ± 0.05	1.14 ± 0.16	1.36 ± 0.12
93	ABC-type amino acid transport/signal transduction systems, periplasmic component/domain	0.75 ± 0.18	0.59 ± 0.13	0.58 ± 0.48
103	ABC-type amino acid transport/signal transduction systems, periplasmic component/domain (extracellular solute-binding protein, family 3)	11.49 ± 2.31	3.81 ± 2.94	5.31 ± 3.12
109	ABC-type Fe3+-hydroxamate transport system,	n.d.	0.32 ± 0.13	0.85 ± 0.16

	periplasmic component			
111	outer membrane porin (OprD homolog)	1.01 ± 0.12	1.18 ± 0.29	1.13 ± 0.37
126	ABC-type amino acid transport/signal transduction systems, periplasmic component/domain (extracellular solute-binding protein, family 3)	12.15 ± 4.28	5.30 ± 0.94	0.96 ± 0.49
133	porin D	0.17 ± 0.14	0.84 ± 0.08	0.17 ± 0.14
	Cell envelope biogenesis			
5	Dihydrolipoamide dehydrogenase	0.95 ± 0.13	0.97 ± 0.09	0.91 ± 0.09
6	Dihydrolipoamide dehydrogenase	1.12 ± 0.02	0.96 ± 0.09	0.91 ± 0.10
7	Dihydrolipoamide dehydrogenase	1.49 ± 0.17	1.01 ± 0.21	1.33 ± 0.35
8	UDP-N-acetylmuramoylalanine-D-glutamate ligase	0.99 ± 0.12	1.49 ± 0.53	0.66 ± 0.09
43	NmrA-like [Cell envelope biogenesis, outer membrane]	0.55 ± 0.45	1.52 ± 0.34	0.25 ± 0.02
45	Enoyl-[acyl-carrier-protein] reductase (NADH)	3.55 ± 0.83	3.59 ± 0.12	4.81 ± 1.19
53	(Acyl-carrier protein) phosphodiesterase	n.d.	n.d.	68.25 ± 26.82
68	UDP-N-acetylenolpyruvoylglucosamine reductase	0.92 ± 0.38	0.75 ± 0.24	1.00 ± 0.19
95	Glycosyltransferases involved in cell wall biogenesis	0.37 ± 0.13	0.58 ± 0.33	0.26 ± 0.04
105	UDP-N-acetylglucosamine enolpyruvyl transferase	1.93 ± 0.10	1.24 ± 0.07	2.07 ± 0.66
122	(3R)-hydroxymyristoyl-[acyl carrier protein] dehydratase ((3R)-hydroxymyristoyl ACP dehydrase)	12.06 ± 0.83	1.63 ± 0.10	2.63 ± 0.31
	Stress Response			
1	penicillin acylase	1.18 ± 0.24	1.26 ± 0.08	1.11 ± 0.81
2	Transcription termination factor NusA	0.97 ± 0.16	2.04 ± 0.02	0.60 ± 0.20
11	D-alanyl-D-alanine carboxypeptidase, fraction A; penicillin-binding protein 5	n.d.	n.d.	n.d.
16	Translation elongation factor TU	4.49 ± 0.90	5.60 ± 1.30	3.06 ± 0.64
34	Translation elongation factor Ts	1.12 ± 0.13	0.75 ± 0.15	1.35 ± 0.56
54	Alkyl hydroperoxide reductase, subunit C	3.38 ± 0.88	10.43 ± 1.09	6.11 ± 1.24
55	Alkyl hydroperoxide reductase, subunit C	1.23 ± 0.38	5.69 ± 1.20	5.68 ± 0.57
59	Superoxide dismutase [Fe]	0.91 ± 0.06	1.42 ± 0.46	1.25 ± 0.29

60	Superoxide dismutase [Fe]	1.36 ± 0.29	0.92 ± 0.09	1.37 ± 0.27
66	BpoC (high homology with arylesterase, POSSIBLE NON-HAEM PEROXIDASE))	0.62 ± 0.02	0.44 ± 0.04	0.49 ± 0.13
77	CagA (cytotoxin associated protein A)	1.54 ± 0.38	1.06 ± 0.26	3.32 ± 0.32
92	Universal stress protein UspA	0.58 ± 0.17	0.35 ± 0.18	0.23 ± 0.06
94	NTP pyrophosphohydrolases including oxidative damage repair enzymes	1.56 ± 0.40	1.66 ± 0.57	0.62 ± 0.09
99	Chaperonin GroEL	1.63 ± 0.34	1.51 ± 0.26	0.88 ± 0.16
101	beta-lactamase	1.00 ± 0.14	10.91 ± 8.33	2.18 ± 1.66
106	Chaperonin Cpn10	4.31 ± 0.41	0.86 ± 0.08	3.83 ± 4.09
121	Hydrogen peroxide-inducible genes activator	10.88 ± 3.18	2.83 ± 0.16	12.57 ± 1.68
	Central Metabolism			
4	glutamine synthetase, type I	1.05 ± 0.07	0.95 ± 0.05	0.58 ± 0.01
10	FKBP-type peptidyl-prolyl cis-trans isomerase (trigger factor)	0.98 ± 0.09	1.09 ± 0.03	1.17 ± 0.16
12	F0F1-type ATP synthase, beta subunit	1.34 ± 0.16	1.07 ± 0.19	1.74 ± 0.52
13	F0F1-type ATP synthase, beta subunit	n.d.	n.d.	n.d.
14	ATP synthase F1, alpha subunit	n.d.	n.d.	n.d.
128	ATP synthase F1, alpha subunit	1.11 ± 0.11	1.30 ± 0.30	0.86 ± 0.06
129	F0F1-type ATP synthase, alpha subunit	2.50 ± 0.23	1.56 ± 0.29	1.52 ± 0.48
15	FKBP-type peptidyl-prolyl cis-trans isomerase (trigger factor)	n.d.	n.d.	n.d.
17	Enolase	0.38 ± 0.04	7.91 ± 1.39	2.23 ± 2.13
20	succinyl-CoA synthase, beta subunit	1.41 ± 0.18	0.92 ± 0.16	1.18 ± 0.21
32	Fructose-1,6-bisphosphate aldolase	1.52 ± 0.14	1.68 ± 0.06	3.17 ± 0.47
39	Succinyl-CoA synthetase, alpha subunit	1.43 ± 0.28	0.60 ± 0.09	0.69 ± 0.07
89	succinyl-CoA synthase, alpha subunit	0.97 ± 0.03	0.23 ± 0.07	1.05 ± 1.18
56	Acetoacetyl-CoA reductase protein	0.37 ± 0.07	0.17 ± 0.15	0.29 ± 0.18
71	Succinyl-CoA synthetase, beta subunit	1.45 ± 0.40	1.00 ± 0.07	1.90 ± 0.12
73	glyceraldehyde 3-phosphate dehydrogenase	0.46 ± 0.12	1.49 ± 0.83	0.73 ± 0.23

75	Citrate synthase	0.41 ± 0.21	0.31 ± 0.06	0.26 ± 0.09
113	ATPase associated with various cellular activities, AAA_5	n.d.	n.d.	10.15 ± 7.48
117	isocitrate dehydrogenase, NADP-dependent, prokaryotic type	1.84 ± 0.17	0.88 ± 0.10	1.19 ± 0.77
132	Succinate dehydrogenase, iron-sulfur protein	n.d.	n.d.	n.d.
	Amino acid Metabolism			
22	Ketol-acid reductoisomerase	0.80 ± 0.21	1.18 ± 0.10	0.32 ± 0.06
38	histidinol-phosphate aminotransferase HisH	0.87 ± 0.10	0.69 ± 0.11	0.45 ± 0.05
58	arginine deiminase	1.17 ± 0.25	0.58 ± 0.09	0.14 ± 0.03
74	Aspartyl-tRNA synthetase	1.77 ± 0.12	2.39 ± 0.06	0.73 ± 0.29
104	2-isopropylmalate synthase (Alpha-isopropylmalate synthase) [Amino acid transport and metabolism]	1.03 ± 0.41	1.00 ± 0.84	1.53 ± 0.36
118	Ornithine carbamoyltransferase [Amino acid Metabolism]	1.49 ± 0.47	1.87 ± 0.22	1.28 ± 0.23
119	Argininosuccinate synthase [Amino acid Metabolism]	1.58 ± 0.41	0.51 ± 0.06	0.96 ± 0.12
	Cell division and replication			
3	chromosomal replication initiator protein DnaA	1.11 ± 0.23	1.38 ± 0.21	0.61 ± 0.11
18	DNA-directed RNA polymerase, alpha subunit	0.66 ± 0.20	1.07 ± 0.43	0.73 ± 0.02
21	DNA polymerase III, delta prime subunit	0.51 ± 0.31	1.36 ± 0.63	0.65 ± 0.07
26	cell division protein FtsA	1.11 ± 0.26	1.39 ± 0.99	2.71 ± 0.34
69	RNA-directed DNA polymerase	1.12 ± 0.24	1.17 ± 0.81	0.63 ± 0.03
	Transcriptional regulators			
44	Transcriptional Regulator, LysR family	0.63 ± 0.01	1.01 ± 0.41	0.64 ± 0.06
76	putative transcriptional regulator	0.17 ± 0.09	0.44 ± 0.05	n.d.
86	Cyclic nucleotide-binding:Bacterial regulatory protein, Crp	1.06 ± 0.08	0.50 ± 0.17	2.49 ± 0.56
124	transcriptional regulator OmpR	0.67 ± 0.14	0.91 ± 0.21	0.78 ± 0.08
	Non- clasified proteins			
33	Porphobilinogen deaminase	1.02 ± 0.14	1.25 ± 0.35	0.73 ± 0.03

40	L0015-like protein (Transposase IS66 family)	0.67 ± 0.18	n.d.	1.67 ± 0.16
41	conserved hypothetical protein	0.53 ± 0.10	0.36 ± 0.11	0.30 ± 0.05
49	response regulator CorR	0.96 ± 0.27	1.26 ± 0.17	1.25 ± 0.60
51	Isochorismatase hydrolase	1.93 ± 0.10	1.60 ± 1.87	1.04 ± 0.31
64	Probable electron transfer flavoprotein	2.41 ± 1.58	0.97 ± 0.02	5.41 ± 0.77
67	Senescence marker protein-30	0.26 ± 0.00	0.46 ± 0.13	0.18 ± 0.06
70	electron transfer flavoprotein beta-subunit	3.06 ± 0.57	1.38 ± 0.05	1.18 ± 0.02
78	hypothetical protein Pflu02003553 (putative signal peptide)	2.42 ± 1.64	4.27 ± 0.43	3.99 ± 1.70
79	hypothetical protein (high homology with Phage integrase [Pseudomonas fluorescens PfO-1] GI:77456973)	0.78 ± 0.15	5.93 ± 0.63	0.58 ± 0.02
80	hypothetical protein (high homology with Phage integrase [Pseudomonas fluorescens PfO-1] GI:77456973)	0.72 ± 0.09	0.82 ± 0.41	0.68 ± 0.03
83	hypothetical protein HP1454	n.d.	n.d.	n.d.
85	Uncharacterized conserved protein	3.47 ± 1.49	1.80 ± 0.39	2.47 ± 0.78
91	repressor of phase I flagellin	3.31 ± 0.54	1.36 ± 0.12	4.09 ± 2.29
96	transposase	1.24 ± 0.12	1.03 ± 0.40	4.16 ± 2.09
97	hypothetical protein Pflu02003553	4.68 ± 0.07	1.53 ± 0.34	1.62 ± 0.66
98	Transposase	0.55 ± 0.04	1.27 ± 0.21	2.50 ± 0.13
100	flagellar protein FliS	2.24 ± 0.93	0.92 ± 0.22	4.72 ± 0.05
102	Septum formation inhibitor-activating ATPase	7.06 ± 2.95	3.85 ± 2.39	5.41 ± 0.77
108	twitching motility protein PilT	2.38 ± 0.55	4.97 ± 0.08	4.15 ± 0.29
110	delta-aminolevulinic acid dehydratase	0.83 ± 0.00	0.59 ± 0.21	0.54 ± 0.10
112	TraN-like (conserved hypothetical TraN-like protein found in conjugate transposon)	n.d.	n.d.	n.d.
115	conserved hypothetical protein (predicted kinase)	1.30 ± 0.26	0.70 ± 0.26	1.35 ± 0.52
116	Protease subunit of ATP-dependent Clp proteases	n.d.	n.d.	n.d.
120	Signal recognition particle GTPase	n.d.	n.d.	2.50 ± 0.13

123	repeat protein K	n.d.	n.d.	n.d.
125	putative transaldolase-like protein	0.51 ± 0.17	0.32 ± 0.01	0.31 ± 0.03
131	hypothetical protein	0.89 ± 0.12	0.39 ± 0.20	0.98 ± 0.62

n.d. = not determined

Table ap-2f. Protein differential expression (DE) comparison of community (*Pseudomonas* sp. MT1 and A.xylosoxidans MT3) culture during 2 mM 4-chlorosalicylate shock load stress (Community *at D* = 0.2 d^{-1} before the shock load as reference for DE = 1.0)

Spot No.	Protein Description	MT1 +MT3 5h DE
	Aromatic degradation enzymes	
9	3-carboxy-cis,cis-muconate cycloisomerase	0.84 ± 0.39
23	2,3-dihydroxybiphenyl 1,2-dioxygenase	0.86 ± 0.10
24	3-oxoadipate:succinyl-CoA transferase, A subunit	1.43 ± 0.11
25	salicylate hydroxylase	1.50 ± 0.06
28	Catechol 1,2-dioxygenase	1.20 ± 0.41
29	Putative oxygenase	1.48 ± 0.02
37	3-oxoadipate:succinyl-CoA transferase, B subunit	1.07 ± 0.11
46	Protocatechuate 3,4-dioxygenase, beta subunit	1.27 ± 0.26
57	Protocatechuate 3,4-dioxygenase alpha subunit	1.32 ± 0.27
72	hydroxyphenylpyruvate dioxygenase	0.18 ± 0.11
81	biphenyl dioxygenase	0.99 ± 0.69
82	2-keto-4-pentenoate hydratase/2-oxohepta-3-ene-1,7-dioic acid hydratase (catechol pathway)	0.99 ± 0.32
84	reductase component of salicylate 5-hydroxylase	0.43 ± 0.05
87	catechol 2,3-dioxygenase	0.21 ± 0.02
90	3-oxoadipate:succinyl-CoA transferase, B subunit	1.37 ± 0.67
107	3-oxoadipate enol-lactonase	1.08 ± 0.06
114	3-oxoadipate:succinyl-CoA transferase, alpha subunit	n.d.
130	xenobiotic reductase B	1.61 ± 0.07
134	Catechol 1,2-dioxygenase	1.18 ± 0.05
	Periplasmic, outer membrane proteins and transporters	
19	Branched-chain amino acid ABC transporter, periplasmic amino acid-binding protein	1.22 ± 0.22
27	Uncharacterized protein conserved in bacteria (hypothetical membrane associated protein)	1.49 ± 0.18
30	Outer membrane porin F precursor	0.97 ± 0.55
31	OprF (Outer membrane protein and related peptidoglycan-associated (lipo)proteins)	n.d.
35	Tricarboxylate transport protein TctC, putative	1.46 ± 0.07
36	glr2336 (high homology with probable RND efflux membrane fusion protein precursor [Pseudomonas aeruginosa PAO1] gi|9949671)	n.d.
42	ABC-type amino acid transport/signal transduction systems, periplasmic component/domain (extracellular solute-binding protein, family 3)	1.26 ± 0.23
47	Membrane protease subunits, stomatin/prohibitin homologs (HflC-like protein)	0.73 ± 0.27
48	ABC-type amino acid transport/signal transduction systems, periplasmic component/domain	2.21 ± 0.97

52	ABC-type amino acid transport/signal transduction systems, periplasmic component/domain (extracellular solute-binding protein, family 3)	2.93 ± 0.63
61	YceI precursor	1.14 ± 0.58
62	Outer membrane protein H1 [Precursor]; Starvation-inducible outer membrane lipoprotein	1.33 ± 0.53
63	yojA (periplasmic ferredoxin-type protein, subunit of nitrate reductase)	0.66 ± 0.33
65	extracellular solute-binding protein, family 3	1.49 ± 0.18
88	Starvation-inducible outer membrane lipoprotein	n.d.
93	ABC-type amino acid transport/signal transduction systems, periplasmic component/domain	1.06 ± 0.19
103	ABC-type amino acid transport/signal transduction systems, periplasmic component/domain (extracellular solute-binding protein, family 3)	0.66 ± 0.28
109	ABC-type Fe3+-hydroxamate transport system, periplasmic component	0.69 ± 0.12
111	outer membrane porin (OprD homolog)	0.90 ± 0.07
126	ABC-type amino acid transport/signal transduction systems, periplasmic component/domain (extracellular solute-binding protein, family 3)	1.03 ± 0.27
133	porin D	4.80 ± 2.33
	Cell envelope biogenesis	
5	Dihydrolipoamide dehydrogenase	0.93 ± 0.09
6	Dihydrolipoamide dehydrogenase	1.25 ± 0.10
7	Dihydrolipoamide dehydrogenase	1.45 ± 0.06
8	UDP-N-acetylmuramoylalanine-D-glutamate ligase	1.29 ± 0.92
43	NmrA-like [Cell envelope biogenesis, outer membrane]	0.20 ± 0.00
45	Enoyl-[acyl-carrier-protein] reductase (NADH)	1.45 ± 0.04
53	(Acyl-carrier protein) phosphodiesterase (AcpH)	2.62 ± 0.92
68	UDP-N-acetylenolpyruvoylglucosamine reductase	1.10 ± 0.24
95	Glycosyltransferases involved in cell wall biogenesis	0.32 ± 0.08
105	UDP-N-acetylglucosamine enolpyruvyl transferase	1.19 ± 0.03
122	(3R)-hydroxymyristoyl-[acyl carrier protein] dehydratase ((3R)-hydroxymyristoyl ACP dehydrase)	n.d.
	Stress Response	
1	penicillin acylase	0.86 ± 0.11
2	Transcription termination factor NusA	n.d.
11	D-alanyl-D-alanine carboxypeptidase, fraction A; penicillin-binding protein 5	1.51 ± 0.41
16	Translation elongation factor TU (EF-Tu)	1.10 ± 0.23
34	Translation elongation factor Ts (EF-Ts)	1.43 ± 0.27
54	Alkyl hydroperoxide reductase, subunit C (AhpC2)	1.65 ± 1.29
55	Alkyl hydroperoxide reductase, subunit C (AhpC1)	2.14 ± 0.11
59	Superoxide dismutase [Fe] (SOD1)	1.28 ± 0.96
60	Superoxide dismutase [Fe] (SOD2)	1.70 ± 0.07

66	BpoC (high homology with arylesterase, POSSIBLE NON-HAEM PEROXIDASE))	1.33 ± 0.57
77	CagA (cytotoxin associated protein A)	0.84 ± 0.31
92	Universal stress protein UspA	0.34 ± 0.02
94	NTP pyrophosphohydrolases including oxidative damage repair enzymes	0.68 ± 0.27
99	Chaperonin GroEL	1.20 ± 0.05
101	beta-lactamase	0.33 ± 0.09
106	Chaperonin Cpn10	1.10 ± 0.26
121	Hydrogen peroxide-inducible genes activator	0.93 ± 0.35
	Central Metabolism	
4	glutamine synthetase, type I	0.44 ± 0.04
10	FKBP-type peptidyl-prolyl cis-trans isomerase (trigger factor)	1.31 ± 0.23
12	F0F1-type ATP synthase, beta subunit	0.74 ± 0.07
13	F0F1-type ATP synthase, beta subunit	1.24 ± 0.03
14	ATP synthase F1, alpha subunit	1.04 ± 0.21
128	ATP synthase F1, alpha subunit	0.90 ± 0.07
129	F0F1-type ATP synthase, alpha subunit	1.16 ± 0.17
15	FKBP-type peptidyl-prolyl cis-trans isomerase (trigger factor)	n.d.
17	Enolase	0.73 ± 0.16
20	succinyl-CoA synthase, beta subunit	0.89 ± 0.30
32	Fructose-1,6-bisphosphate aldolase	1.96
39	Succinyl-CoA synthetase, alpha subunit	1.50 ± 0.13
89	succinyl-CoA synthase, alpha subunit	1.34 ± 0.49
56	Acetoacetyl-CoA reductase protein	1.13 ± 0.49
71	Succinyl-CoA synthetase, beta subunit	0.99 ± 0.19
73	glyceraldehyde 3-phosphate dehydrogenase	0.44 ± 0.06
75	Citrate synthase	0.47 ± 0.05
113	ATPase associated with various cellular activities, AAA_5	0.79 ± 0.22
117	isocitrate dehydrogenase, NADP-dependent, prokaryotic type	1.50 ± 0.06
132	Succinate dehydrogenase, iron-sulfur protein	1.06 ± 0.14
	Amino acid Metabolism	
22	Ketol-acid reductoisomerase	1.75 ± 0.34
38	histidinol-phosphate aminotransferase HisH	1.41 ± 0.37
58	arginine deiminase (ADI)	3.95 ± 0.38
74	Aspartyl-tRNA synthetase	1.49 ± 0.35
104	2-isopropylmalate synthase (Alpha-isopropylmalate synthase) [Amino acid transport and metabolism]	1.63 ± 0.05
118	Ornithine carbamoyltransferase [Amino acid Metabolism]	n.d.
119	Argininosuccinate synthase [Amino acid Metabolism] (Assyn)	0.34 ± 0.12
	Cell division and replication	
3	chromosomal replication initiator protein DnaA	0.77 ± 0.35
18	DNA-directed RNA polymerase, alpha subunit	0.59 ± 0.08

21	DNA polymerase III, delta prime subunit	0.56 ± 0.29
26	cell division protein FtsA	2.83 ± 0.48
69	RNA-directed DNA polymerase	0.89 ± 0.01
	Transcriptional regulators	
44	Transcriptional Regulator, LysR family	1.42 ± 0.02
76	putative transcriptional regulator	1.25 ± 0.40
86	Cyclic nucleotide-binding:Bacterial regulatory protein, Crp	n.d.
124	transcriptional regulator OmpR	0.82 ± 0.16
	Non- clasified proteins	
33	Porphobilinogen deaminase	0.49 ± 0.06
40	L0015-like protein (Transposase IS66 family)	1.20 ± 0.54
41	conserved hypothetical protein	1.42 ± 0.10
49	response regulator CorR	1.56 ± 0.20
51	Isochorismatase hydrolase	1.32 ± 0.31
64	Probable electron transfer flavoprotein	0.88 ± 0.45
67	Senescence marker protein-30	1.41 ± 0.04
70	electron transfer flavoprotein beta-subunit	0.57 ± 0.00
78	hypothetical protein Pflu02003553 (putative signal peptide)	0.70 ± 0.13
79	hypothetical protein (high homology with Phage integrase [Pseudomonas fluorescens PfO-1] GI:77456973)	0.56 ± 0.29
80	hypothetical protein (high homology with Phage integrase [Pseudomonas fluorescens PfO-1] GI:77456973)	0.66 ± 0.00
83	hypothetical protein HP1454	n.d.
85	Uncharacterized conserved protein	0.91 ± 0.04
91	repressor of phase I flagellin	1.19 ± 0.44
96	transposase	1.42 ± 0.48
97	hypothetical protein Pflu02003553	0.78 ± 0.24
98	Transposase	1.11 ± 0.24
100	flagellar protein FliS	0.41 ± 0.10
102	Septum formation inhibitor-activating ATPase	0.45 ± 0.04
108	twitching motility protein PilT	1.09 ± 0.35
110	delta-aminolevulinic acid dehydratase	1.22 ± 0.08
112	TraN-like (conserved hypothetical TraN-like protein found in conjugate transposon)	2.77 ± 0.11
115	conserved hypothetical protein (predicted kinase)	0.34 ± 0.12
116	Protease subunit of ATP-dependent Clp proteases	1.57 ± 0.43
120	Signal recognition particle GTPase	n.d.
123	repeat protein K	n.d.
125	putative transaldolase-like protein	0.63 ± 0.10
131	hypothetical protein	0.76 ± 0.36

n.d. = not determined